ADVANCED ENERGY MATERIALS
www.advenergymat.de

Device Performance of Emerging Photovoltaic Materials (Version 5)

Osbel Almora, Guillermo C. Bazan, Carlos I. Cabrera, Luigi A. Castriotta, Sule Erten-Ela, Karen Forberich, Kenjiro Fukuda, Fei Guo, Jens Hauch, Anita W.Y. Ho-Baillie, T. Jesper Jacobsson, Rene A.J. Janssen, Thomas Kirchartz, Richard R. Lunt, Xavier Mathew, David B. Mitzi, Mohammad K. Nazeeruddin, Jenny Nelson, Ana F. Nogueira, Ulrich. W. Paetzold, Barry P. Rand, Uwe Rau, Takao Someya, Christian Sprau, Lídice Vaillant-Roca, and Christoph J. Brabec**

This 5th annual "*Emerging PV Report*" highlights the latest advancements in the performance of emerging photovoltaic (e-PV) devices across various e-PV research areas, as documented in peer-reviewed articles published since August 2023. Updated graphs, tables, and analyses are provided, showcasing several key performance parameters, including the power conversion efficiency, open-circuit voltage, short-circuit current, fill factor, light utilization efficiency, and stability test energy yield. These parameters are presented as functions of the photovoltaic bandgap energy and average visible transmittance for each technology and application and are contextualized using benchmarks such as the detailed balance efficiency limit.

1. Introduction

Emerging photovoltaic (e-PV) devices (see **Table 1**)[1–4] hold great promise for providing cheaper, cleaner, and more versatile scalable electricity generation, serving as an alternative and/or complement to traditional photovoltaics (PVs) such as silicon devices. Among e-PV devices, the heterostructure architecture has emerged as the most successful approach, utilizing absorber materials such as metal halide perovskites, polymers, dyes, kesterites, or matildites. However,

O. Almora
Universitat Rovira i Virgili
Tarragona 43007, Spain
E-mail: osbel.almora@urv.cat

O. Almora, C. J. Brabec
Erlangen Graduate School of Advanced Optical Technologies (SAOT)
91052 Erlangen, Germany
E-mail: christoph.brabec@fau.de

G. C. Bazan
Departments of Chemistry and Chemical Engineering
National University of Singapore
Singapore 117543, Singapore

C. I. Cabrera
Unidad Académica de Ciencia y Tecnología de la Luz y la Materia
Universidad Autónoma de Zacatecas
Zacatecas 98160, Mexico

L. A. Castriotta
Department of Electronic Engineering
CHOSE (Centre for Hybrid and Organic Solar Energy)
Tor Vergata University of Rome
Via del Politecnico 1, Rome 00133, Italy

The ORCID identification number(s) for the author(s) of this article can be found under https://doi.org/10.1002/aenm.202404386

DOI: 10.1002/aenm.202404386

S. Erten-Ela
Ege University
Solar Energy Institute
Bornova, Izmir 35100, Turkey

K. Forberich, J. Hauch, C. J. Brabec
Forschungszentrum Jülich GmbH
Helmholtz
Institut Erlangen
Nürnberg for Renewable Energy (HI ERN)
91058 Erlangen, Germany

K. Fukuda, T. Someya
Thin-Film Device Laboratory & Center for Emergent Matter Science
RIKEN
Saitama 351-0198, Japan

F. Guo
Institute of New Energy Technology
College of Physics & Optoelectronic Engineering
Jinan University
Guangzhou 510632, China

A. W. Y. Ho-Baillie
School of Physics and The University of Sydney Nano Institute
The University of Sydney
NSW 2006, Australia

T. J. Jacobsson
Department of Physics
Chemistry and Biology (IFM)
Linköping University
Linköping 58339, Sweden

optimizing these devices for higher power conversion efficiency (*PCE*) values, larger surface areas and enhanced performance durability has been challenging, primarily due to the complexity of the device interfaces and the intrinsic properties of e-PV materials.

Versatility is a key attribute of e-PV, as increasing the *PCE* for large-scale grid-connected electricity production is not the only research focus. Over the last decade, there has been growing research interest in potential applications such as flexible, transparent, and integrated PVs. This trend is evident in the increasing percentage of annual publications addressing these topics. However, unlike the *PCE* results, which can be certified by several international institutions, the standardized quantitative evaluation and certification of other critical aspects of e-PV devices, essential for proper validation and comparison, remain a work in progress. In this context, the emerging PV initiative,[5] along with its accompanying website and database, aims to establish an international framework and benchmarking system for the systematic collection, presentation, and analysis of data, serving as a reference for best practices and state-of-the-art reports.

The state-of-the-art achievements in e-PV devices, as reflected in academic publications detailing top-performing cells, have been systematically parameterized and reported since 2020 through the annual emerging PV reports (e-PVr),[1–4] of which this is the fifth edition. This report compiles the performance data of the best e-PV devices into comprehensible tables (e.g., see Green et al.).[6] Additionally, the PCE values are put into perspective by comparing the devices with respect to the bandgap energy of the absorber material, number of device junctions, application class, and performance stability. Notably, we present performance parameters for each technology and compare the experimental data to the corresponding theoretical limit in the detailed balance (DB)[7–9] model.

In this review article, we present updated graphs and tables of the best-performing research photovoltaic cells, incorporating the latest reports since August 2023. This includes over 170 new research articles listed in Tables 3–26, in agreement with our inclusion criteria (see Section 1.1), from over 340 new entries to the emerging-pv.org database during the last year. In the plot representations (Sections 2–5), older and newer values are distinguished by lighter and darker symbols, respectively. Similarly, in the tables (Section 7), the new entries are emphasized in bold. The following sections not only describe the updated plots and tables collected in our database but also highlight and discuss the most relevant and recent achievements in each section.

R. A. J. Janssen
Molecular Materials and Nanosystems & Institute for Complex Molecular Systems
Eindhoven University of Technology
MB Eindhoven 5600, The Netherlands

R. A. J. Janssen
Dutch Institute for Fundamental Energy Research
De Zaale 20, Eindhoven 5612 AJ, The Netherlands

T. Kirchartz, U. Rau
IMD-3 Photovoltaics
Forschungszentrum Jülich
52425 Jülich, Germany

T. Kirchartz
Faculty of Engineering and CENIDE
University of Duisburg-Essen
47057 Duisburg, Germany

R. R. Lunt
Department of Chemical Engineering and Materials Science
Department of Physics and Astronomy
Michigan State University
East Lansing, MI 48824, USA

X. Mathew
Instituto de Energías Renovables
Universidad Nacional Autónoma de México
Temixco, Morelos 62580, México

D. B. Mitzi
Department of Mechanical Engineering and Materials Science &
Department of Chemistry
Duke University
North Carolina, Durham 27708, USA

M. K. Nazeeruddin
Group for Molecular Engineering and Functional Materials
Ecole Polytechnique Fédérale de Lausanne
Institut des Sciences et Ingénierie Chimiques
Sion CH-1951, Switzerland

J. Nelson
Department of Physics
Imperial College London
London SW7 2BZ, UK

A. F. Nogueira
Institute of Chemistry
University of Campinas (UNICAMP)
Campinas, São Paulo 13083–970, Brazil

U. W. Paetzold
Institute of Microstructure Technology (IMT)
Karlsruhe Institute of Technology (KIT)
76344 Eggenstein-Leopoldshafen, Germany

U. W. Paetzold
Light Technology Institute (LTI)
Karlsruhe Institute of Technology (KIT)
76131 Karlsruhe, Germany

B. P. Rand
Department of Electrical and Computer Engineering and Andlinger Center for Energy and the Environment
Princeton University
Princeton, NJ 08544, USA

T. Someya
Electrical Engineering and Information Systems
The University of Tokyo
Tokyo 113–8656, Japan

C. Sprau
Light Technology Institute
Karlsruhe Institute of Technology (KIT)
Engesserstrasse 13, 76131 Karlsruhe, Germany

L. Vaillant-Roca
Photovoltaic Research Laboratory
Institute of Materials Science and Technology – Physics Faculty
University of Havana
Havana 10400, Cuba

C. J. Brabec
Zernike Institute for Advanced Materials University of Groningen
Groningen 9747, The Netherlands

C. J. Brabec
Department of Materials Science and Engineering
Institute of Materials for Electronics and Energy Technology (i-MEET)
Friedrich-Alexander-Universität Erlangen-Nürnberg
Martensstraße 7, 91058 Erlangen, Germany

Table 1. Abbreviations for PV technologies or material families (adapted from the e-PVr version 3).[3]

Abbreviation	Meaning and comments
Established photovoltaics	
a-Si:H	Amorphous silicon single junction photovoltaic cell (including a-SiGe:H devices).
CdTe	Cadmium telluride single junction photovoltaic cell
CIGS	$CuIn_xGa_{1-x}Se_2$-based single junction photovoltaic cell
GaAs	Gallium arsenide single junction photovoltaic cell
Si	Monocrystalline or polycrystalline silicon single junction photovoltaic cell, including homo- or heterojunction structures.
Emerging photovoltaics	
AgBiS	$AgBiS_2$-based single junction photovoltaic cells, the so-called matildite solar cells.
CIGS/DSSC	Monolithic/2-terminal tandem photovoltaic cell: $CuIn_xGa_{1-x}Se_2$-based bottom subcell and dye-sensitized top subcell
CIGS/perovskite	Monolithic/2-terminal tandem photovoltaic cell: $CuIn_xGa_{1-x}Se_2$-based bottom subcell and perovskite-based top subcell
CIGS/AlGaAs/GaInP	Monolithic/2-terminal triple junction photovoltaic cell: $CuIn_xGa_{1-x}Se_2$-based bottom subcell, AlGaAs-based middle subcell, and GaInP-based top subcell
CZTS	$Cu_2ZnSn(S,Se)_4$-based single junction photovoltaic cell
DSSC	Dye-sensitized single junction photovoltaic cell
DSSC/perovskite	Monolithic/2-terminal tandem photovoltaic cell: dye-sensitized bottom subcell and perovskite-based top subcell
GaAs/GaInP	Monolithic/2-terminal tandem photovoltaic cell: GaAs-based bottom subcell and GaInP-based top subcell
GaAs/perovskite	Monolithic/2-terminal tandem photovoltaic cell: GaAs-based bottom subcell and perovskite-based top subcell
GaAs(In,Bi,Al,P)	Monolithic/2-terminal triple junction photovoltaic cell including GaAs and no other material family specified in this table. For example InGaAs- or GaAsBi-based bottom subcell, GaAs-based middle subcell, and GaInP- or AlGaAs-based top subcell
nc-Si/a-Si	Monolithic/2-terminal tandem photovoltaic cell: nanocrystalline or microcrystalline Si bottom subcell and amorphous Si top subcell
nc-Si/nc-Si/a-Si	Monolithic/2-terminal triple junction photovoltaic cell: nanocrystalline silicon-based bottom and middle subcells, and amorphous silicon-based top subcell
OPV	Organic photovoltaic material-based single junction photovoltaic cell
OPV/a-Si	Monolithic/2-terminal tandem photovoltaic cell: organic-based bottom subcell and amorphous silicon-based top subcell
OPV/perovskite	Monolithic/2-terminal tandem photovoltaic cell: the bottom and top subcells are organic- and perovskite-based, respectively, or vice versa.
PSC	Perovskite single junction photovoltaic cell
SbS	$Sb_2(S,Se)_3$-based single junction photovoltaic cell
Si/DSSC	Monolithic/2-terminal tandem photovoltaic cell: Si-based bottom subcell and dye-sensitized top subcell
Si/GaAsP	Monolithic/2-terminal tandem photovoltaic cell: Si-based bottom subcell and $GaAs_{1-x}P_x$ -based top subcell
Si/GaInAsP/InGaP	Monolithic/2-terminal triple junction photovoltaic cell: silicon-based bottom subcell, GaInAsP-based middle subcell, and GaInP-based top subcell
Si/perov/perov	Monolithic/2-terminal triple junction photovoltaic cell: Si-based bottom subcell and perovskite-based middle and top subcells
Si/perovskite	Monolithic/2-terminal tandem photovoltaic cell: Si-based bottom subcell and perovskite-based top subcell
TLSC	Transparent luminescent solar concentrator, including a lightguide, luminophore, and mounted solar cell(s).

Additionally, we provide a commentary on the general trends and progress in the field over the past year.

1.1. Data Inclusion Criteria, Definitions and Emerging-pv.Org

Consistent with previous e-PVr,[4] to be considered for these surveys, the data must meet a set of specific criteria. First, it should be published in a peer-reviewed article in an academic journal and the article should include a "methods" section that allows experimental replication. Second, the article should provide essential data and a clear description of self-consistency checks.

With respect to the *PCE* values, both the current density–voltage (*J*–*V*) curve measured under standard conditions and the external quantum efficiency (*EQE*) spectra should be presented and should be consistent, insofar that the short-circuit current density (J_{sc}) determined from both methods should not differ by more than 10% relative.[10] Reporting 5 min of maximum power point (MPP) tracking is encouraged, particularly for perovskite solar cells (PSCs) and perovskite-based multi-junction devices.

For flexible solar cells, data from bending tests, including the number of bending cycles, bending strain, and *PCE* values before and after the bending test are required.[11] For the bending strain, the estimation of the device thickness (including substrate and encapsulation, if appropriate) and bending radius are the minimum requirements in the single-layer strain model.

For transparent/semitransparent devices, the explicit transmittance (*T*) spectrum of the entire device (not the separated

Table 2. Equations and definitions (updated after e-PVr version 3).[4]

No.	Equation	Definitions and comments	Refs.
(1)	$PCE = \frac{P_{out}}{P_{in}} = \frac{V_{oc} \cdot J_{sc} \cdot FF}{P_{in}}$	*PCE*, power conversion efficiency; P_{out}, output power density, P_{in}, incoming power density; V_{oc}, open-circuit voltage; J_{sc}, short-circuit current density; *FF*, fill factor	[1]
(2)	$EQE = \frac{A_m}{\frac{(\lambda - \frac{hc}{E_g})}{1+\exp[\kappa \frac{}{\lambda_s}]}}$	Procedure to determine E_g from the $EQE(\lambda)$ spectrum: *EQE*, external quantum efficiency; λ, wavelength; A_m, maximum EQE value just above the bandgap absorption threshold; *h*, Planck's constant; *c*, speed of light; E_g, photovoltaic bandgap energy; λ_s, sigmoid wavelength width parameter (*EQE* onset quality wavelength), $\kappa = \ln[7+4\sqrt{3}] \approx 2.63$, dimensionless coefficient related to the second derivative of the sigmoid.	[12]
(3)	$J_{sc,EQE} = \frac{q}{h\,c} \int EQE(\lambda)\,\lambda\,\Gamma_{AM1.5G}(\lambda)\,d\lambda$	$J_{sc,EQE}$, short-circuit current density as integrated from the EQE for the standard 1 sun illumination intensity AM1.5G spectrum $\Gamma_{AM1.5G}$ (typically in units of W m^{-2} nm^{-1}); *q* is the elementary charge.	
(4)	$EDBL = \frac{PCE^{real}}{PCE^{ideal}} = \frac{J_{sc}^{real}}{J_{sc}^{ideal}} \frac{V_{oc}^{real}}{V_{oc}^{ideal}} \frac{FF^{real}}{FF^{ideal}}$	*EDBL*, experiment-to-detailed balance limit ratio, the "real" superscript refers to the experimental values; the "ideal" superscript refers to the theoretical limit of each performance parameter as in the detailed-balance models,[7,8,14] e.g., the highest efficiency for a single junction cell with absorber material of bandgap energy E_g at a temperature T_c under a spectral irradiance Γ. The proper application of a detailed- -balance performance limit model on an experiment implies $EDBL \leq 1$.	[15]
(5)	$AVT = \frac{\int T(\lambda)\,P(\lambda)\,\lambda\,\Gamma_{AM1.5G}(\lambda)d\lambda}{\int P(\lambda)\,\lambda\,\Gamma_{AM1.5G}(\lambda)d\lambda}$	*AVT*, average visible transmittance; *T*, transmittance; *P*, the photopic response of the human eye.	[16]
(6)	$LUE = AVT \cdot PCE$	*LUE*, light utilization efficiency	[17]
(7)	$PBCC = EQE(\lambda) + T(\lambda) + R(\lambda)$	The photon balance consistency check implies PBCC≤ 1	[16]
(8)	$E_{\Delta\tau} = \int_0^{\Delta\tau} P_{out}\,dt = \int_0^{\Delta\tau} P_{in}\,PCE\,dt$	$\Delta\tau$, operational stability test time; $E_{\Delta\tau}$, operational stability test energy yield (STEY) for a test of duration $\Delta\tau$; *t*, time; STEY is taken for 200 h and 1000 h of stability tests as E_{200h} and E_{1000h}, respectively.	[1]
(9)	$DR_{\Delta\tau} = \frac{PCE(\tau) - PCE(0)}{\Delta\tau}$	$DR_{\Delta\tau}$, effective overall degradation rate for an operational stability test of duration $\Delta\tau$; DR_{200h} and DR_{1000h} are taken as the overall degradation rates for 200 h and 1000 h of stability tests, respectively.	[1]

absorber layer) is required. This will allow the estimation of the average visible transmittance (*AVT*) and light utilization efficiency (*LUE*).

In the case of operational stability test results, the published manuscript should clearly state both the initial and final efficiencies before and after 200 h or 1000 h of operation under 1 sun illumination. This will allow the estimation of the stability test energy yields (*STEY*) and degradation rates (*DR*).

For multijunction devices, only two-terminal (monolithic) devices with up to three junctions have been considered in the current version of the reports. For those devices, the *J–V* curve and *EQE* spectra of the full device should be provided along with the *EQE* spectra of each subcell.

Articles lacking some of the mandatory requirements to be included in the e-PVr could still be considered, provided an extended or additional supporting information document is posted on the *emerging-pv.org* website.[5] A more in-depth discussion on the accuracy, performance parameters, exclusion criteria, and tiebreak rules can be found in previous e-PVr[1–4] and in sections S1.5 and S1.6 (Supporting Information). A discussion on the "emergence" labeling for PV devices and its relation with the PV technology generations and research can be found in version 4 of the e-PVr.[4]

The equations, definitions, and useful references already presented in the previous e-PVr[4] and updated in the current version are summarized in **Table 2**. Table S2 (Supporting Information) reviews the minimal details to be included in a research article to be considered in an e-PVr. Notably, we here emphasize the use of the definition of the photovoltaic bandgap energy as the inflection point of the absorption threshold of the *EQE* spectrum.[12,13] This definition not only characterizes the operational response of the entire device (rather than an independent absorber layer or a combination of sub-layers) but also provides a framework for comparing different emerging technologies, in particular where single optical bandgap energy is not directly defined,[1] such as in organic photovoltaics.

Following the previous e-PVr,[4] each section showcases the best-performing cells as reported in the literature, grouped by different technologies or material families. The corresponding abbreviations are listed in Table 1. Importantly, for multijunction PV cells, we define the top subcell as the one that receives the total incident photon flux and generally has absorber material with the highest value of bandgap energy ($E_{g,top}$) compared to the other subcell(s). Similarly, the bottom subcell receives the residual and smaller fraction of the filtered incident photon flux and generally has the absorber material with the lowest value of bandgap energy ($E_{g,bottom}$) in the stack. For two-junction cells or tandem devices, only the top and bottom subcells exist. This is in contrast to triple junction cells, where a middle subcell is sandwiched between the top and bottom subcells, and which typically has an

absorber material with a bandgap energy ($E_{g,mid}$) whose value is between those of $E_{g,bottom}$, and $E_{g,top}$.

The Emerging-PV website and database[5] have shown significant advancement during the last year, not only as the recommended data collection and visualization tool for the e-PV initiative but also as an implementation framework for the definitions in Table 2. The main progress since August 2023 includes the analysis of in situ operational stability tests with automatic calculation of the energy yield (Equation S8, Supporting Information, Table 2), degradation rates (Equation S9, Supporting Information, Table 2), and characteristic times for the 95% and 80% relative decrease of *PCE*, t_{95}, and t_{80} respectively.

2. Highest Efficiency Photovoltaic Cells

2.1. Single Junction Devices

The top efficiency single junction research cells are listed in **Tables 3–7** and plotted in **Figure 1** as a function of the PV bandgap. The experimental data is presented alongside the single junction detailed-balance theoretical efficiency limit,[7] assuming radiative emission from both the front and the rear side of the photovoltaic cell.[18] Overall, the most relevant new efficiency records relate to OPVs and PSCs with PCE values higher than 20% and 26%, with absorber materials whose photovoltaic bandgap continues[4] to be clustered in the ranges 1.37–1.47 eV and 1.51–1.57eV, respectively.

PSCs made the highest contribution to our database with over 70 new entries (see **Table 3**), while a 26.7% certified efficiency record was listed by Green et al.[6] for a cell with a designated area of 0.052 cm^2. Among the already published studies, we highlight the work by Chen et al.,[19] who fabricated inverted (FTO/SAMs/$Cs_{0.05}FA_{0.85}MA_{0.1}PbI_3$/$C_{60}$/$SnO_x$/Ag) solar cells with the highest *PCE* value of 26.5% and certified quasi–steady state values of 26.15% and 24.74% for 0.05 and 1.04 cm^2 illuminated areas, respectively. The authors attribute the performance improvement to a reduction in contact resistance, energetic mismatch, and surface defect density between the perovskite and the C_{60} through a 4-chlorobenzenesulfonate (4Cl-BZS) treatment, resulting in a *FF* of over 86%.

Over 30 new OPVs entries were counted in our database (see **Table 4**), with the new highest certified *PCE* value of 15.8% presented by Faisst et al.[20] from a cell with a designated area of 1.064 cm^2. In this study, the authors increased the photogenerated current through a fully magnetron-sputtered multilayer antireflection coating custom-designed for the absorption profile of the D18:Y6 photoactive layer. Remarkably, after the first publication of OPV efficiencies above 20% for small-area devices by Guan et al.,[21] three more articles by Jiang et al.,[22] Chen et al.[23] and Zhu et al.[24] have claimed similar results. Guan and coworkers conducted an interface optimization that resulted in *PCE* values of 20.17% (certified 19.79%) and 18.41% for OPV cells with areas of 0.05 and 1.05 cm^2, respectively. They introduced the molecule of 2-(9H-carbazol-9-yl) (2PACz) in a self-assembled interlayer (SAI) configuration for optimizing the transport in the structure ITO/2PACz-SAI/PBDB-TF:L8-BO:BTP-eC9/PDINN)/Ag, which improved both the fill factor and photovoltage compared to those from devices with other hole transport materials, such as PEDOT:PSS. In contrast, in the work from Jiang and co-workers an asymmetric non-fullerene acceptor (Z8) featuring tethered phenyl groups improved the film nanomorphology for an efficiency of 20.2% (certified 19.8%) in devices with the D18:Z8:L8-BO ternary blend. Similarly, Chen and coworkers, the report of 20.22% (certified 19.66%) efficiency for a device active area of 4.84 mm^2 is attributed to the development of a novel non-fullerene acceptor, SMA, and its integration into the ternary blend PM6:BTP-eC9:SMA. Furthermore, Zhu and coworkers reported a 20.8% efficiency using additive-assisted layer-by-layer deposition that created a wrinkle-pattern morphology due to Marangoni-Bénard instability and radial flow during spin-coating, enhancing light capture capability.

Dye-sensitized solar cells continue to show a decline in research activities with only two new relevant *PCE* reports (below the absolute record) during the last year (see **Table 5**). Interestingly, Song et al.[25] fabricated multicolored fiber devices (see also flexible applications in next section) and introduced an alumina/polyurethane film as a light diffusion layer on the outermost encapsulating tube, and a phosphors/TiO_2/poly(vinylidene fluoride-*co*-hexafluoropropylene) film as a light conversion layer on the inner counter electrode. These diffusion and conversion layers not only improved the charge carrier photogeneration of the dye (N719) for photon energies higher than that of the photovoltaic bandgap (1.75 eV) but also introduced parasitic extra sub-bandgap photogeneration. This explains the increased short-circuit current value, even higher than the corresponding DB efficiency limit, while low V_{oc} and *FF* remained (see Figure 1).[12]

Over 20 new studies on kesterite solar cells were reported during the last year (see **Table 6**), and a few more works were also published on $Sb_2(S,Se)_3$ solar cells, although no new absolute *PCE* record was reported for these emerging inorganic technologies. Notably, Wang et al.[26] reported $Cu_2ZnSn(S, Se)_4$-based solar cells with a *PCE* of 14.5% (certified 14.3%) owing to the reduction of vacancy defects at grain boundaries through a redox reaction strategy utilizing palladium (Pd) to suppress these defects.

A new record efficiency matildite solar cell was reported by Li et al.[27] with a *PCE* value of 10.2% from a device with an active area of 0.06 cm^2. They also fabricated a 1.0 cm^2-area cell that achieved an efficiency of 9.16%. In that work, a vapor-assisted solution process was proposed to fabricate high-crystallinity submicron-grain $AgBiS_2$ films in a planar ITO/SnO_2/$AgBiS_2$/PTAA/MoO_3/Au configuration. The authors point out that the process optimization led to increased photogeneration of charge carriers which primarily stems from the enhanced light absorption ability of the submicron grain $AgBiS_2$ film.

Among the established technologies (see **Table 7**), the latest record performance of crystalline Si and CdTe thin-film cells have been featured in the efficiency tables by Green et al.[6] with certified values of 27.3% and 22.6% with designated areas of 243 and 0.445 cm^2, respectively.

Figure 2a further compares the *PCE* data in Figure 1 with respect to the DB efficiency limit in terms of the experiment-to-detailed balance limit ratio (*EDBL*, Equation S4, Supporting Information, Table 2). Among PSCs, the highest *PCE* values reach 86% *EDBL* and most of the latest results are higher than 75%. Only lead-free tin-based PSCs with bandgap energies between

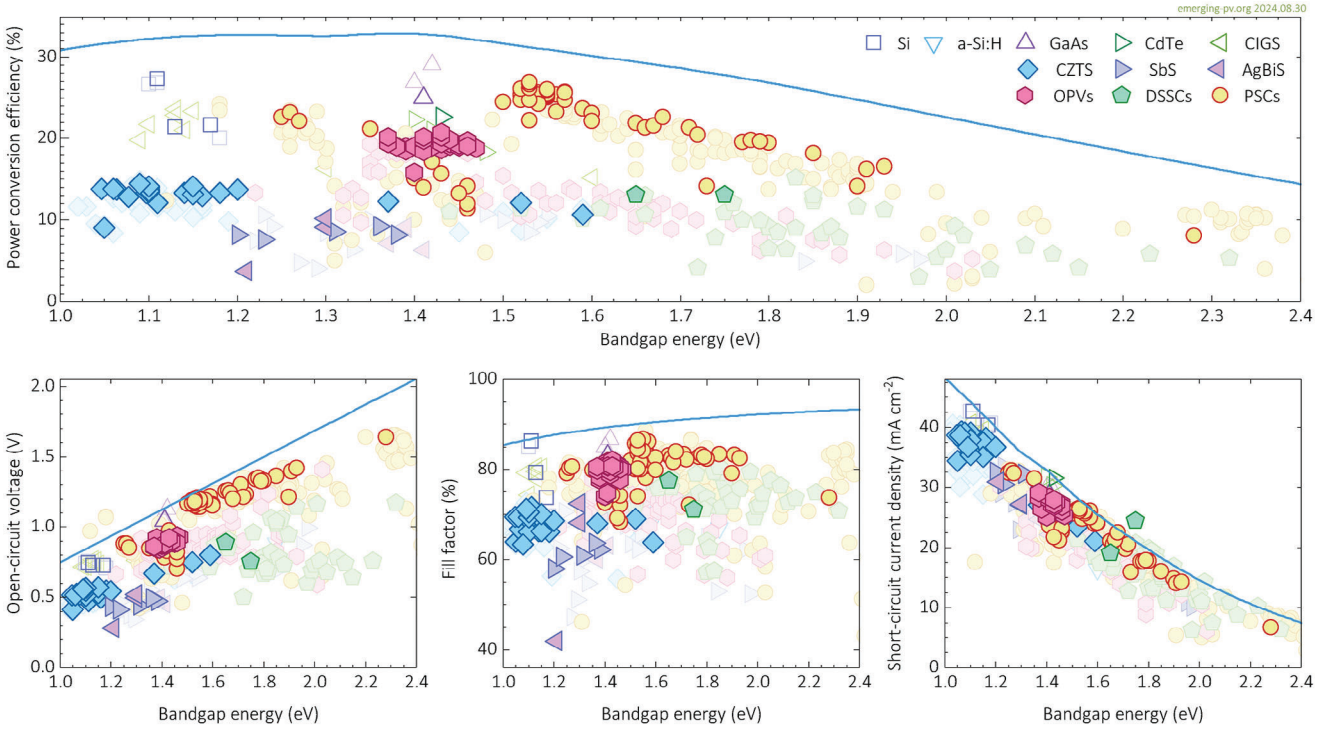

Figure 1. Highest efficiency single junction photovoltaic cells. Performance parameters as a function of effective absorber bandgap for different photovoltaic technologies: *PCE* (top) V_{oc} (bottom left), *FF* (bottom center), and J_{sc} (bottom right). Experimental data are summarized in Section 7.1, with the lighter and more opaque dots corresponding to reports before and after August 2023, respectively. The solid lines indicate the corresponding theoretical detailed-balance efficiency limit.[18]

1.40 and 1.46 eV have difficulties overcoming the 50% *EDBL*. OPV cells show even higher promise for optimization, because the highest reported *PCE* values are only 61% of the EBDL, and most of the latest efficiency reports show EBDL>55%. Moreover, last year's kesterite, matildite, and $Sb_2(S,Se)_3$ solar cells show even lower EDBL maximum values of 45%, 31%, and 28%, respectively. In addition, Figure 2b shows the updated logarithmic loss analysis[28] for the champion efficiency cells for each technology. The new matildite record shows a large photovoltage deficit as the main contributing factor to the energy loss. The main contribution to losses is likely associated with non-radiative recombination that lowers the open-circuit voltage. This feature is also reported for the new record cells on OPV, CdTe, and Si technologies. In the case of the latest efficiency record for OPV, photocurrent losses are the second most important limitation, possibly due to limited absorption. Remarkably, the latest records for CdTe and Si cells show nearly fully optimized values for the photocurrent and fill factor, which may correlate with negligible optical losses and parasitic ohmic resistance effects, respectively. Finally, the PSC showed an even distribution of losses between V_{oc}, J_{sc}, and *FF*.

The time evolution of the device performance presented in Figure 1 is shown in detail in Figure 2c, which also includes the data from NREL's "Best research-cell efficiency chart" (solid lines).[29] In this plot, we highlight the consistent and systematic reproduction of *PCE* values over 25%, 19%, and 13% for PSCs, OPVs, and kesterite devices, respectively. In contrast, a more discrete time evolution is found for DSSCs, $Sb_2(S,Se)_3$, and matildite solar cells.

The output power in milliwatts, corresponding to the data in Figure 1 is presented in Figure 2d as a function of the illuminated area of the reported laboratory cells. In this graph, the efficiency isolines (see dash-dot grey line) form diagonal-like contours. The closer they are to the top-right region of the graph, the higher the output power. Overall, studies on e-PV technologies continue to mostly report devices in the range between 0.05 and 0.1 cm^2, and it is only the latest Si solar cell record that demonstrates optimal performance for a cell area over 200 cm^2. The highest output power among PSCs was reported by Chen et al.[19] at 25.7 mW with the above-mentioned 1.04 cm^2 cell. Similarly, the top output power from OPV devices was as high as 19.3 mW, from a 1.05 cm^2-area cell in the aforementioned work by Guan et al.[21].

2.2. Multijunction Devices (Monolithic)

The performance parameters of monolithic/two-terminal multijunction photovoltaic research cells, with up to three junctions, are presented in **Figure 3** and listed in **Table 8–10**. These values are put into perspective by comparing them to the corresponding optimized bandgap DB efficiency limit, including radiative coupling. Remarkably, the improvement of perovskite multijunction cell performance continues and so is the number of entrants

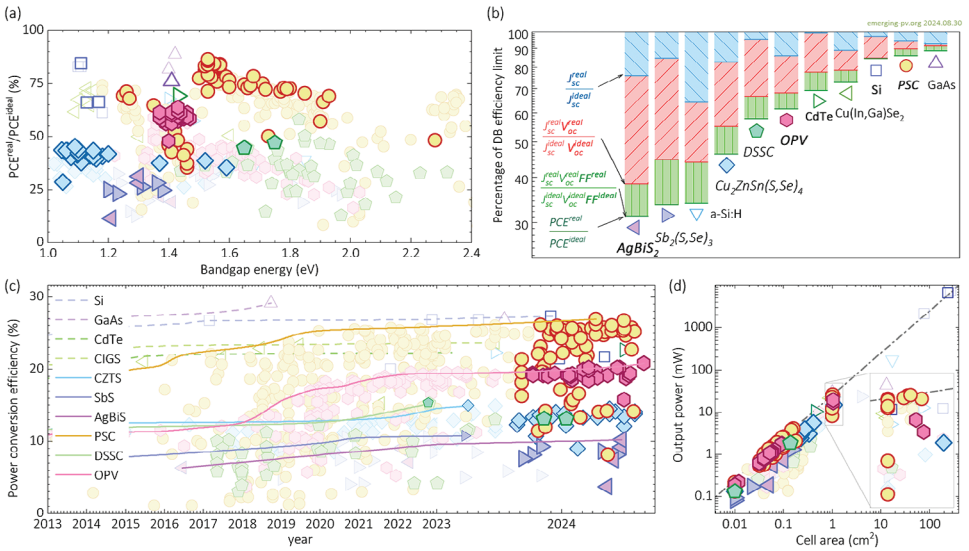

Figure 2. DB efficiency limit on the *PCE* data in Figure 1 shows a) the relative efficiencies with respect to the theoretical limit and b) the logarithmic loss analysis[28] for the top efficiency cell of each technology, as defined by Equation S4 (Supporting Information) in Table 2. c) The time evolution of *PCE* and d) output power with respect to the cell area. Opaque and light symbols indicate reports before and after August 2023, respectively. The solid lines in (c) contain the data from NREL's "Best research-cell efficiency chart."[29] The dash-dotted line in (d) is the efficiency isoline for *PCE* = 25%.

into this research area, including more than 30 start-up and established companies and ≈50 research institutions. Specifically, as of September 2024, there are three companies and seven research institutions reporting Si-perovskite tandem on 1cm^2-area devices with independently certified *PCE* values over 30% (see Table S3, Supporting Information).

A top-efficiency Si-perovskite tandem is listed by Green et al.[6] and credited to LONGI with a *PCE* value of 34.2% in a device with a designated area of 1.0044 cm^2. Among the research articles, the LONGI team (Liu et al.[30]) reported a certified PCE value of 33.89% in a tandem cell with an area of 1.004 cm^2. In that study, the authors propose a so-called "bilayer intertwined passivation strategy" where a nanoscale discretely distributed LiF ultrathin layer is followed by an additional deposition of diammonium diiodide molecules for optimization of the wide-bandgap perovskite/electron transport layer interface. As a result, not only the highest research article-published efficiency was obtained but also the *FF* and V_{oc} attained remarkable values as high as 83% and 1.97 V, respectively.

All-perovskite tandem solar cells still lag behind in terms of efficiency, since their higher photovoltage values do not compensate for the smaller photocurrent and fill factor when compared with Si-perovskite devices (see Figure 3). Specifically, Green et al.[6] listed a top efficiency of 30.1%, while the best performance for all-perovskite tandems among published articles was reported by Zhou et al.[31] with a *PCE* value of 28.24% (certified 27.35%) from a 0.1 cm^2 area cells. In this study, the authors introduced a functional N-(carboxyphenyl)guanidine hydrochloride (CPGCl) molecule for manipulating the crystallization and grain growth of tin-lead perovskites and to inhibit Sn^{2+} oxidation. The latter effect was attributed to the strong binding between CPGCl and tin (II) iodide, and the elevated energy barriers for oxidation. This optimization of the narrow-bandgap cell effectively increased the values of both, J_{sc} and V_{oc}, as compared with the control devices without the CPGCl additive. Triple-junction Si/perovskite/perovskite devices follow the all-perovskite cells (see Figure 3) with a new record *PCE* of 27.62% (certified 27.10%), as reported by Liu et al.[32]. The optimization of this new top-efficiency triple-junction e-PV device focused on the reduction of the V_{oc} losses in the top subcell. The authors introduced a pseudo-halide, cyanate (OCN^-), as a bromide substitute for the wide-bandgap perovskite and observed an enhancement in the uniformity of the perovskite film, which was also correlated with the higher formation energy of vacancy defects.

Organic-perovskite tandems, all-perovskite triple-junction devices, and CIGS-perovskite tandems are next in that order, with the highest *PCE* values of 25.82% (certified 25.06%),[33] 25.1% (certified 23.87%),[34] and 18.1%,[35] respectively. However, these cells are still unable to outperform high-efficiency single-junction PSCs with consolidated certified PCE values over 25% (see Figure 1 and Table 3). Moreover, new silicon-selenium tandem solar cells have been demonstrated by Nielsen et al.[36] with a first PCE value of 2.7%, due to relatively low values of J_{sc} and *FF*. Notably, the highest value of V_{oc} among all the multijunction cells peaks as high as 3.33 V for the all-perovskite triple-junction solar cells reported by Wang et al.[34]. In that work, the authors show that introducing propane-1,3-diammonium iodide during perovskite film fabrication improves the halide homogenization in the Br-rich perovskite of the top subcell. In contrast, the silicon-perovskite devices show the highest J_{sc} and *FF* values, as well as the highest output power. Purposely, we highlight the output power-cell area data in Figure 3, which clearly shows no cell reports among all-perovskite devices (tandem or triple junction) with area ≥ 0.2 cm^2, and no output power values over 100 mW for Si/perovskite tandems.[37]

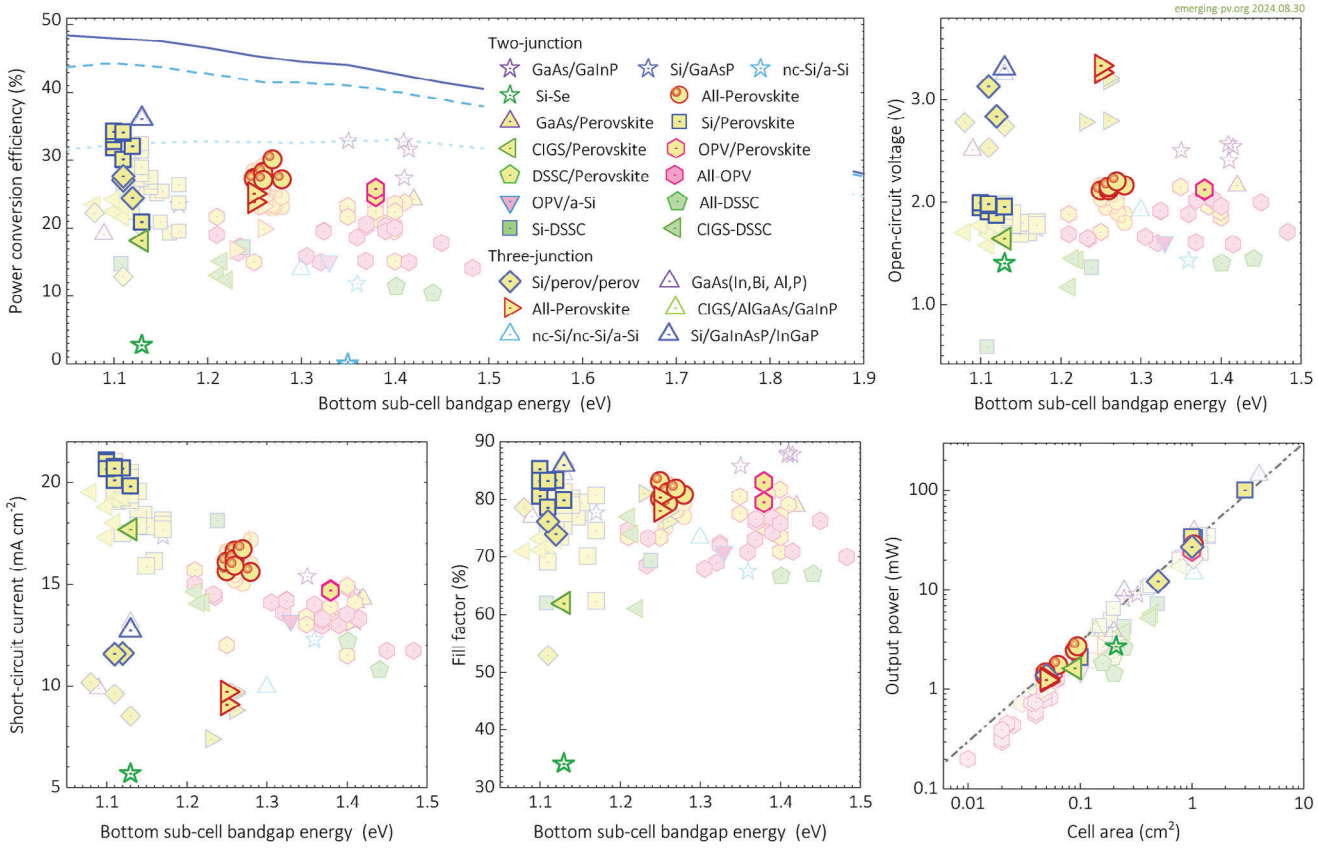

Figure 3. Highest efficiency values for monolithic/two-terminal multijunction photovoltaic research cells including up to three junctions. Performance parameters as a function of the absorber bandgap energy of the bottom subcell for various photovoltaic technologies: power conversion efficiency (top-left), open-circuit voltage (top-right), short-circuit current density (bottom-left), fill factor (bottom-center) as a function of bandgap energy and corresponding output power versus area (bottom-right). The dotted, dashed, and solid lines in the efficiency graph indicate the DB efficiency limits for one junction, double junction (top subcell optimized), and triple junction (top and middle subcell optimized) photovoltaic cells, respectively.[8,14] The dash-dot-dot line in the output power-area plot is the efficiency isoline for *PCE* = 30%. Light and opaque symbols indicate the reports published before and after August 2023, respectively.

3. Flexible Photovoltaic Cells

The performance parameters of relevant flexible solar cells are listed in **Tables 11–16** and presented in **Figure 4**, showing tremendous progress among perovskite-based devices and significant improvement shown among OPVs, emerging inorganics, and some established technologies. On the latter, impressive new record flexible silicon solar cells have been presented in the work by Li et al.,[38] reporting certified efficiencies from 26.81% with 125μm-thick wafers up to 26.06% with a thickness of 57μm, on an average area of 274.4cm^2 and an optimized power to weight ratio of 1.9W g^{-1}.

New records from emerging inorganic technologies (Table 15) include $Cu_2ZnSn(S,Se)_4$ and Sb_2Se_3 devices, showing maximum *PCE* values of 12.2% and 8.43% by Son et al.[39] and Liang et al.,[40] respectively. The new record kesterite cells consisted of a ≈1.4 μm-thick device deposited on a Mo foil, and the optimization results were correlated with grain boundary properties. For the Sb_2Se_3 new record device, a 50 μm-thick polyimide foil was used as the substrate, and the device optimization was attributed to the introduction of a PbSe transition layer toward the Mo contact. Other flexible kesterite and Sb_2Se_3 cells have also been reported with similar *PCE* and V_{oc} values within each technology, but differences in J_{sc} and *FF*, as shown in Figure 4.

Zhu et al.[41] showed a new application for dye-sensitized solar cells on fibers, with record-breaking *PCE* values up to 12.52% for flexible DSSCs. This was done by designing a porous hybrid counter electrode with high light reflectance that included a metal current collector fiber with an aligned carbon nanotube sheet and a porous titanium dioxide/poly(vinylidene fluoride-*co*-hexafluoropropylene) film. Notably, the *PCE* decreased by ≤ 10% after bending, twisting, or pressing for 1000 cycles. Compared to previous reports on flexible DSSCs in Figure 4, the fiber device presents similar V_{oc} values, which attributes the *PCE* increase to improved J_{sc} and *FF*.

For the first time, flexible OPVs exceeded efficiency values of 18% (see Table 12), as published by Zhang et al.,[42] who introduced a polymer-entangled spontaneous pseudo-planar heterojunction film with a crack onset strain of 11% for a device *PCE* value of 18.2%. Moreover, the mechanical stability of these cells was improved as well, maintaining 92% of the initial *PCE* after 1000 bending cycles with a 5 mm bending radius.

Flexible PSCs have shown unprecedented interest and work during the last year, with more than 20 new works listed in

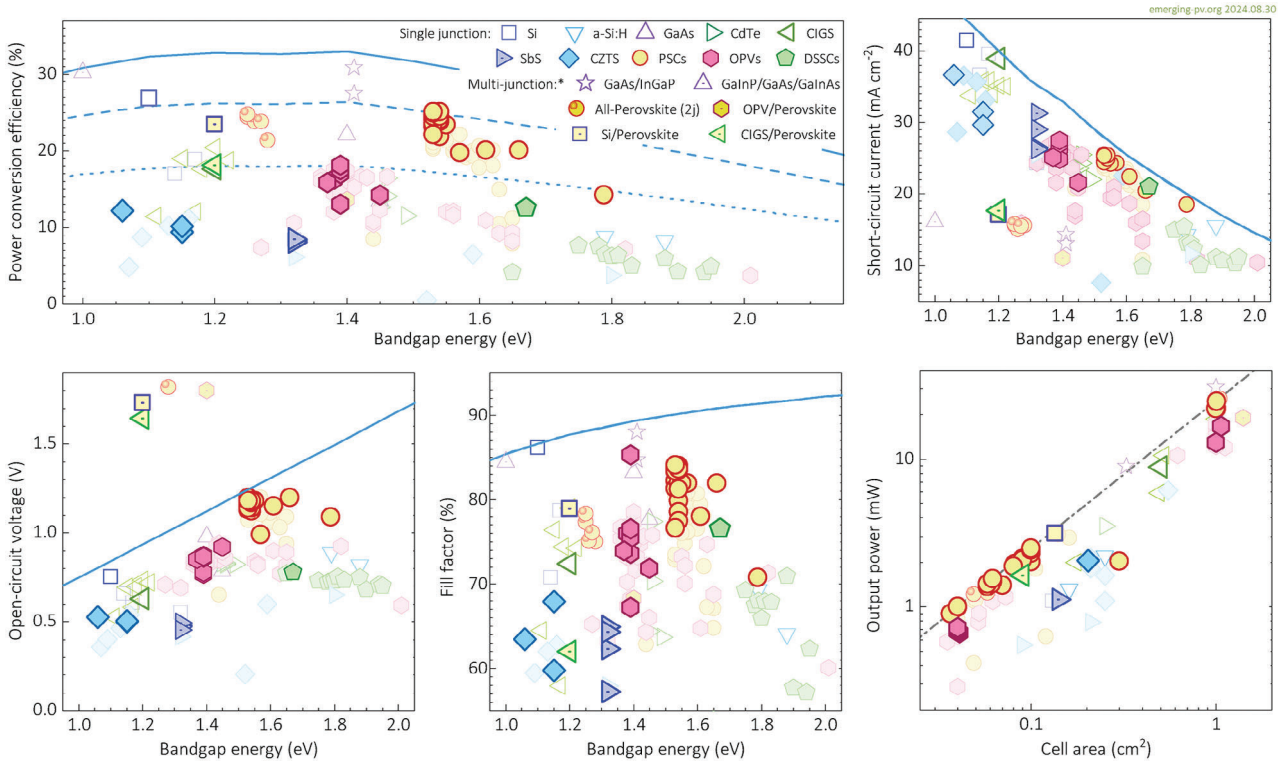

Figure 4. Flexible PVs and their performance parameters as a function of absorber (or bottom junction absorber in case of multijunction devices) bandgap energy for various photovoltaic technologies: power conversion efficiency (top-left), short-circuit current density (top-right), open-circuit voltage (bottom-left), fill factor (bottom-center) and output power versus area (bottom-right). Experimental data are summarized in Section 7.2 and the solid, dashed, and dotted lines indicate 100%, 80%, and 55% of the theoretical single junction DB efficiency limit,[18] respectively. The dash-dot line in the output power-area plot is the efficiency isoline for *PCE* = 25%. The lighter and opaque symbols are reports before and after August 2023, respectively.

Table 11, showing amazing improvements that now approach 80% of the single-junction DB efficiency limit (see dashed line in Figure 4). Specifically, PCE values up to 25.1% were independently reported by Tong et al.[43] and Ren et al.[44]. These studies mainly focused on improving the buried interface between the perovskite and transporting layers. The improvement has been achieved on both direct and inverted architectures, showing a technological maturity at this point, independently from the structure utilized. Certified efficiencies of 24.04%, 24.48%, and 24.90%, have also been reported by Wang et al.,[45] Wu et al.,[46] and Ren et al.,[44] respectively. Furthermore, Gong et al.[47] showed the best *PCE* value obtained for a 1.0 cm^2 area cell, with 24.45%, proposing a molecular encapsulation using glycerol monostearate as an effective approach to inhibit agglomeration and promoting uniform colloidal particle size in the perovskite precursor ink.[47] Hailegnaw et al.[48] increased the power per weight value (up to 44 W g^{-1}) using reduced substrate thicknesses and stable device materials/structures in flexible PSCs to power an energy-autonomous drone. Most of the aforementioned studies showed improved mechanical stability. Notably, Liu et al.[49] reported PSCs with 125 µm-thick ITO/PEN flexible substrates that withstood bending tests with more than 60 000 cycles at a curvature radius of 5.0 mm, retaining over 97% of its initial efficiency. In that study, the authors used a 0D additive for a full inorganic perovskite composition ($CsPbBr_{0.19}I_{2.81}$). Furthermore, the latest reports on high-efficiency flexible PSC show V_{oc} values higher than 95% of the corresponding DB limits (see solid lines in Figure 4), whereas J_{sc} and *FF* may require further optimization. Notably, the highest output energy among emerging flexible solar cells was reported by Gong et al.,[47] with 24.7 W from a 1.0 cm^2 cell.

New monolithic multijunction flexible solar cells have also been reported (see Table 14). Specifically, two new entries were registered for Si/perovskite and CIGS/perovskite by Wang et al.[50] and Zheng et al.,[35] with *PCE* values of 23.45% and 18.10%, respectively. For the Si/perovskite device, a remarkable silicon wafer thickness reduction was achieved for a ≈30 µm-tandem device with a certified stabilized efficiency of 22.8% and a power-to-weight ratio of 3.12 Wg^{-1}. Moreover, these flexible tandems maintained 98.2% of their initial performance after 3000 bending cycles at a bending radius of 1.0 cm. The CIGS/perovskite devices were fabricated on ≈50 µm thick conductive flexible stainless-steel substrates, leading to a deficient coverage of the CIGS subcell by the NiO_x transport layer deposited via solution-based methods. Instead, physical deposition methods were more successful, including the sputtered NiO_x hole-selective layer and the thermally evaporated C60/BCP electron-selective stack, while the perovskite layer was still spin-coated. Interestingly, Figure 4 illustrates how these two new flexible tandem cells present similar values of J_{sc} and V_{oc}, and the *PCE* difference relates to the much higher value of FF for the Si/perovskite solar cell, compared to that of the

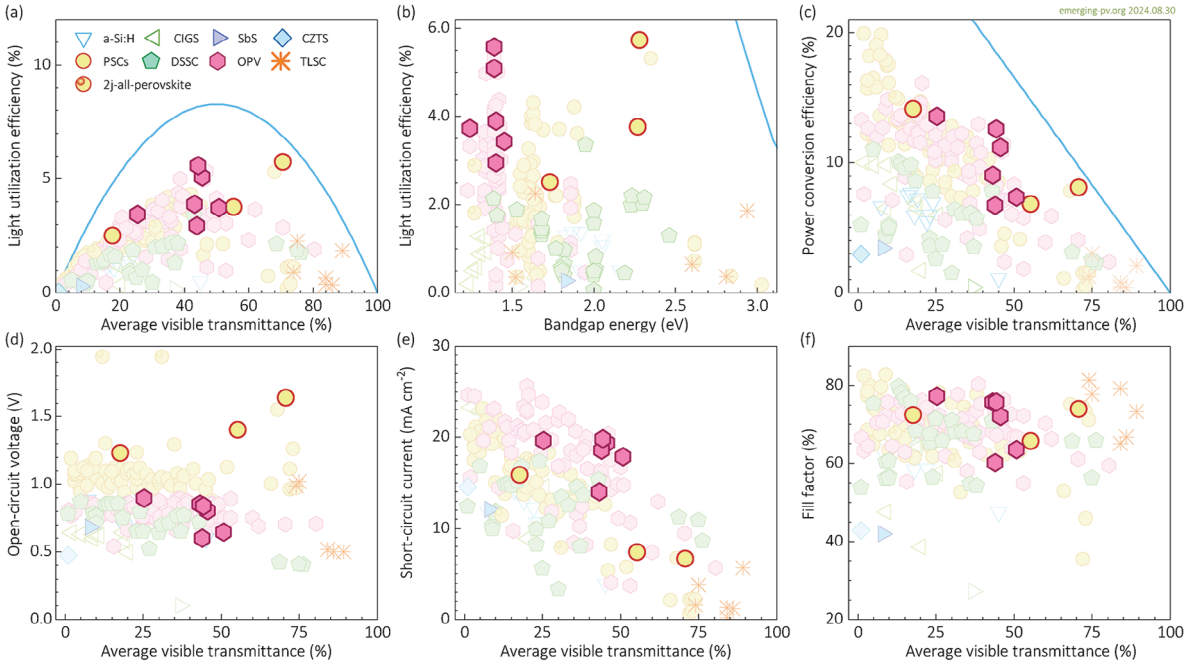

Figure 5. Best performing transparent and semitransparent PVs: *LUE* versus a) *AVT* and b) E_g; and c) *PCE*, d) V_{oc}, e) J_{sc}, and f) *FF* as a function of *AVT*. The experimental data are summarized in Section 7.3. The blue solid lines indicate the corresponding theoretical detailed balance efficiency limit for non-wavelength selective PVs. In (b), the multijunction cells are potted as a function of the bandgap energy of the absorber material in the bottom subcell. The lighter and more opaque symbols are reports before and after August 2023, respectively.

CIGS/perovskite device that may present higher series resistance losses.

4. Transparent and Semitransparent Photovoltaic Cells

Significant progress has been made over the last year in semitransparent PV devices, with new record-breaking values of light utilization efficiency (LUE, see Equation S6, Supporting Information) in Table 2) achieved by semitransparent and transparent OPV and transparent PSC devices, as shown in **Figure 5**. However, to the best of our knowledge, only nine published articles in the field meet the inclusion criteria and consistency checks of the emerging-pv.org database (see **Table 17–22**).

We emphasize the importance of consistently reporting the *EQE* and transmittance spectra of (semi-)transparent devices, rather than focusing solely on individual material films. Inconsistent reporting prevents accurate estimation of critical parameters such as the average visible transmittance (*AVT*, see Equation S5 in Table 2), the *LUE*, and the photon balance consistency check (*PBCC*, see Equation S7, Supporting Information in Table 2). These parameters are key for comparison and performance assessment in (semi-)transparent solar cells

Based on a wide bandgap $FAPbBr_3$ perovskite, Di Girolamo et al.[51] reported a 1.0 cm^2 large area device with an *AVT* over 70% together with a *PCE* of 8.1%, leading to a *LUE* value of 5.73%. This is the new record for the *LUE*, not only among PSCs (see Table 17) but also over the more general emerging-pv.org database. A high *PCE* was achieved via an interface passivation strategy, and a record single-junction device V_{oc} value as high as 1.73 V was also reported. Moreover, the transparency was optimized with an MgF_2 anti-reflective coating on the glass side and a nanoparticulate Al_2O_3 layer on the ITO back electrode, improving the *LUE* from 5.14% without bifacial light management to 5.73%. In another noteworthy example, $FAPbBr_3$ perovskite devices were fabricated on PET/ITO, combining semitransparency and flexibility in the same device in the study by Jafarzadeh et al.[52]. Without further optical engineering, *PCE* values of up to 6.8% and an *AVT* of over 55% led to *LUE* values of up to 3.76%. Although these results demonstrate that wide-bandgap perovskite solar cells can compete with, or even outcompete, OPV in terms of *LUE*, a high color rendering index (CRI)[16] remains a challenge, as high *AVT*s are typically achieved with materials whose absorption onset is close to the maximum of the photopic response of the human eye.

Among organic solar cells (see Table 18), low-bandgap absorber blends such as PTB7-Th:ATT-9 had already been shown in previous years to be one of the best compromise between selective semitransparency in the visible range and good *PCE* thanks to high near-infrared (NIR) distribution of the *EQE* spectra, even without optical modulation.[53] During this last year, Sun et al.[54] have replaced the typically evaporated thin Ag back electrode with AgNWs sandwiched in a modified hole-transport layer, achieving PTB7-Th:ATT-9 solar cells with more than 50% *AVT* at a *PCE* of 7.3%, leading to an *LUE* of 3.73%.

Similar *LUE* values can also be achieved with PM6 and Y-series non-fullerene acceptor (NFA) molecules that are less selectively transparent in the visible range, but lead to the highest *PCE* values in OPV devices. Yu et al.[55] fabricated semitransparent PM6:BTP-eC9:L8-BO solar cells and improved their transmissive properties with an optical resonator approach of TeO_2/Ag/TeO_2

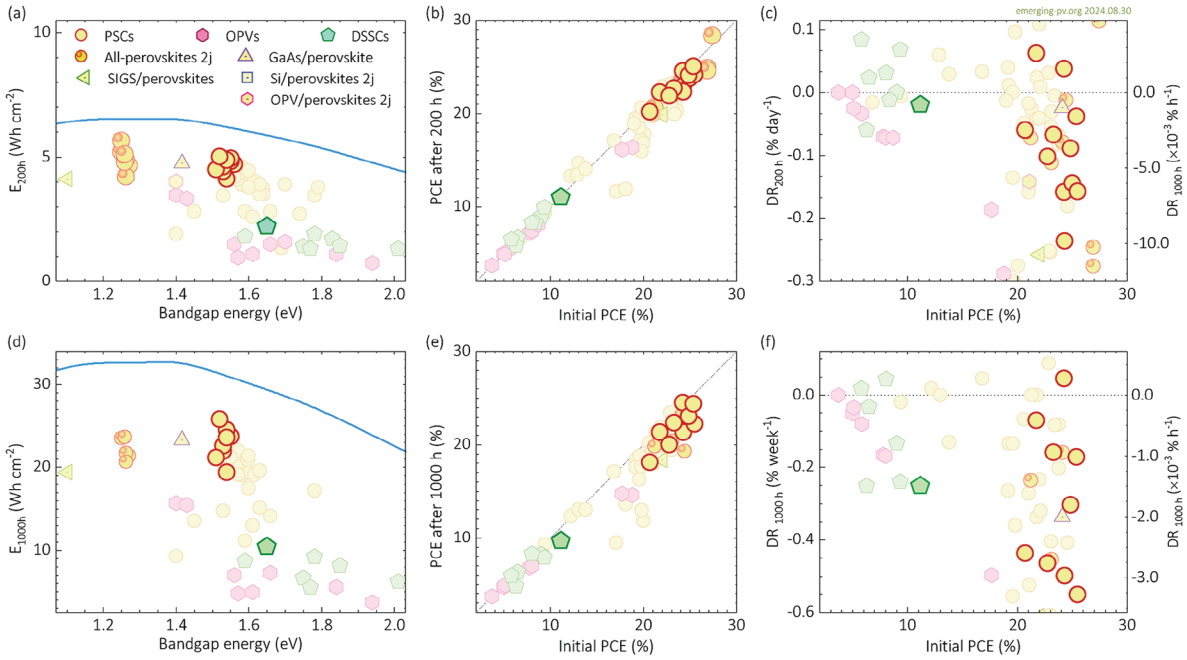

Figure 6. Operationally most stable emerging PVs for each technology during 200 h a–c) and 1000 h d–f) of testing: stability test energy yield (Equation S8, Supporting Information; Table 2) as a function of bandgap energy (a, d), final power conversion efficiency as a function of the initial value (b, e), and overall degradation rate (Equation S9, Supporting Information; Table 2) as a function of initial power conversion efficiency (c, f). The experimental data are summarized in Section 7.4 and the solid blue lines in the *STEY* panel (left) are the corresponding DB theoretical limits. The diagonal dot-dot-dashed lines in the middle panel indicate where the final efficiencies equal the initial values. The positive values above the horizontal dotted lines in the degradation rate panel (right) indicate that *PCE* increases with respect to the initial values.

on the thin Au/Ag back electrode. The highest *LUE* of 3.90% was achieved with an *AVT* of 43%, a *PCE* of 9.0%, and a remarkable CRI of 97%.

Semitransparent organic solar cells also clearly benefited from improvements in opaque single-junction PCEs, which now surpass 19% more regularly. For instance, in the work by Huang et al.,[56] the addition of a monomeric donor analog (DA) and an acceptor analog (Y5) improved the *PCE* values of quaternary opaque devices with PCE10-2F/Y6 and PM6:L8-BO up to 15.6% and 19.1%, respectively. Subsequently, when included in a rather simple semitransparent device architecture comprising a 15 nm thin Ag back electrode with a 35 nm layer of MoO_x on top, *AVT* values of 46% and 25% led to *LUE* values of 3.44% and 5.10%, for the DA:PCE10-2F/Y6:Y5 and DA:PM6:L8-BO:Y5 devices, respectively.

By combining a highly efficient absorber layer with sophisticated optical enhancement, a novel *LUE* record in OPV cells was achieved. Zhang et al.[57] investigated multi-stacked back electrodes of Ag, ZnS, and MgF_2 (and MoO_3 seed layers) to improve the back reflection of light beyond that of the human eye's response, while enhancing transmission in the visible region. Solar cells comprising a 60 nm thin PM6:BTP-eC9:L8-BO active layer, a back electrode of dielectric layers and one Ag layer, and an antireflective nanoimprinted moth-eye structure on the glass substrate achieved an *AVT* of 44% with an average *PCE* of 12.6%, resulting in an *LUE* value of 5.6%. This is a remarkable improvement over otherwise identical cells without an antireflective coating (4.1% *LUE*) and over those with only a simple ultrathin Ag electrode (2.6% *LUE*).

5. Operational Stability in Emerging Research Solar Cells

The stability of e-PVs is crucial for their potential industrial implementation and for ensuring the reproducibility and validation of reported research advancements. According to our inclusion criteria (see Section 1.1), **Figure 6** summarizes the latest reports from in situ stability tests conducted over 200 h and/or 1000 h under continuous 1-sun illumination, as listed in **Tables 23–26**. Overall, there is a consistent repetition of two trends, when compared with data from before August 2023. First, most of the new stability studies continue to focus on PSCs whose as-fabricated *PCE* (initial) are state-of-the-art values, which reproduce a cluster-like behavior for the energy yield with bandgap energies ≈1.52 eV (see Figure 6a,d). Remarkably, Liang et al.[58] reported a study following the ISOS L-1 protocol,[59] from which a stability test energy yield (STEY) value as high as 25.8 Wh cm^{-1} can be estimated. This is the highest STEY in our database for 1000 h of continuous operation under 1 sun illumination. Notably, in this work, the cells were kept in a nitrogen atmosphere and the stability of the device was attributed to the introduction of 1-(phenylsulfonyl)pyrrole to homogenize the distribution of the A-site cation composition in the $Cs_xFA_{1-x}PbI_3$ perovskite films.

The second reproduced trend relates to the faster degradation that occurs during the first 200 h of operational stability tests (Figure 6a–c), compared to that over a complete 1000 h experiment (Figure 6d–f). This is evident when comparing the final PCE (Figure 6b,e) and degradation rates (Figure 6c,f) after 200 h and 1000 h of operational stability testing as a function of the

initial PCE. In fact, an increase in the *PCE* value (positive degradation rate) over the first 200 h was observed for some devices, whereas a performance decrease (negative degradation rate) was reported after 1000 h. The only exception to this trend was reported by Xu et al.[60] whose stability test resulted in degradation rates of $+1.6 \times 10^{-3}\%h^{-1}$ and $+ 2.7 \times 10^{-4}\%h^{-1}$ for 200 and 1000 h of continuous operation under 1 sun illumination in a N_2 atmosphere, inside a glovebox. In this work, the authors optimized the hole transport layer by introducing a so-called interfacial molecular bridge between the perovskite and the PTAA. Specifically, they used quaternary ammonium Ph-$CH_2N^+(CH_3)_3$ cations, where the $-N^+(CH_3)_3$ groups preferentially insert into the perovskite frameworks, with a vertical downward orientation of the phenyl groups toward the perovskite-substrates, for improved charge carrier extraction and transport in both the in-plane and out-of-plane directions.

Notably, a new "most stable" DSSC was reported by Zhou et al.[61] with an STEY of 10.4 mWh cm^{-1} and a degradation rate of $-1.5 \times 10^{-3}\%h^{-1}$ (-0.25%/week) after 1000 h of operation under 1 sun illumination at room temperature and ambient air. This new achievement was attributed to introducing of 2-thiophenecarboxylic acid (THCA) as a post-interfacial surface-coating adsorbent for reduced recombination at the TiO_2 interface.

6. Conclusion

The comprehensive data trends presented in this fifth edition of the emerging photovoltaic reports highlight significant progress in emerging photovoltaic technologies, particularly in perovskite solar cells (PSCs) and organic photovoltaic (OPV) devices. These trends reveal increasing power conversion efficiencies (*PCE*) across multiple technologies, with perovskites reaching certified *PCE* values of over 26% and OPVs achieving more than 20%. Notably, these technologies continue to cluster around optimal bandgap ranges, specifically 1.37–1.57 eV.

The rapid advancement of perovskite-based devices dominates the newly reported efficiency records. These devices, especially in tandem and multijunction configurations, have significantly improved performance, and consistently yield certified efficiencies >30%, demonstrating high open-circuit voltages and fill factors. Flexible photovoltaic technologies have also shown remarkable progress, with flexible perovskite and OPV cells exceeding 24% and 18% *PCE*, respectively, along with enhanced mechanical stability and operational resilience.

In contrast, certain technologies such as dye-sensitized solar cells (DSSCs) have shown slower progress, with fewer record-breaking efficiency reports in the past year. Nevertheless, incremental improvements continue in stability and application-specific adaptations, such as flexible DSSCs.

Semitransparent e-PV devices have achieved significant progress over the last year, particularly in terms of light utilization efficiency (*LUE*), with new record-breaking values for both OPV and PSC devices. Wide-bandgap PSCs have demonstrated competitive *LUE* values, with records of up to 5.73%, while flexible semitransparent perovskite devices show promising *PCE* and transparency results. Similarly, OPV devices continue to advance, particularly through innovations in back-electrode design and optical enhancements, reaching *LUE* values as high as 5.6%.

We emphasize the growing importance of operational stability, as it is becoming a critical parameter for evaluating the long-term durability of photovoltaic devices. While recent reports indicate that PSCs have achieved exceptional *PCE* values, further advancements are needed to improve their stability under continuous operation. Unfortunately, a consistent lack of detail in the description of stability experiments remains a common issue in the literature. This gap hampers the accurate assessment of stability reports and limits the understanding of state-of-the-art achievements in the field.

We also underscore the importance of including not only the stability test conditions but also detailed information regarding the initial *PCE* value at the start of the experiment. This is crucial for estimating key parameters such as the stability test energy yield and degradation rates, which are vital for comparing the longevity of devices across studies.

Overall, the data trends indicate that while significant advances have been made in *PCE* and flexible applications, ongoing efforts to optimize stability, scalability, and mechanical robustness will be key to realizing the full potential of emerging photovoltaic technologies.

7. Tables

The tables below list the reports on the best achievements in most of the established and emerging PV technologies as a function of the device bandgap E_g. Unless otherwise noted, the E_g values were estimated by fitting the absorption threshold region of the corresponding *EQE* spectra to Equation S2 (Supporting Information) in Table 2. Note that, for some absorber materials this definition may result in a value slightly larger (typically on the order of the thermal energy) than that of the optical bandgap.[6] The new reports from articles published since August 2023 are highlighted in bold. The older reports from articles published before August 2023, which were already included in our previous surveys, are referenced to the corresponding e-PVr. In contrast, each older report that was missed in the corresponding previous e-PVr is now included with its corresponding individual citation. All citations, further data, and visualization tools can be found on the emerging-pv.org website. This website and database are the main and recommended data collection path for inclusion in the e-PVr and a useful instrument that complements the tables below.

In the case of *PCE* reports of PSCs showing hysteresis behavior in the *J–V* characteristic, while sweeping the voltage in different directions and/or scan rates, the lower *PCE* value has been considered in each case. This is discussed in detail in Section S1.1 (Supporting Information).

The *FF* values were automatically corrected to match the reported values of *PCE*, J_{sc}, and V_{oc} under standard 100 mW cm^{-2} illumination of the AM1.5G spectrum. Some reports show up to ± 0.5% discrepancies between the values in our tables and those reported in the original publications, owing to differences in the rounding digits and/or typos in the original manuscripts. Cells with mismatches of >0.5% may have been discarded (see Section S1.5, Supporting Information).

For transparent/semitransparent cells, note that the *AVT* values may differ from those reported in the original manuscripts when a definition different from that of Equation S5 (Supporting Information), in Table 2, is used in the original published article.

7.1. Highest Efficiency Research Solar Cells Tables

Table 3. Perovskite single-junction solar cells with the highest efficiency: Performance parameters as a function of device absorber bandgap energy (from the *EQE* spectrum).[12]

E_g [eV]	PCE [%]	V_{oc} [mV]	J_{sc} [mA cm^{-2}]	FF [%]	Absorber perovskite	Refs.
1.12	12.4	967	17.5	72.9	$MAPb_{0.5}Sn_{0.5}Br_3$:Bi^{3+}:$BA_2MA_4Sn_5I_{16}$	[3]
1.18	24.3	1070	29.1	78.0	$FA_{0.7}MA_{0.3}Pb_{0.7}Sn_{0.3}I_3$/BTBTI:PCBM	[3]
1.18	23.4	1067	28.9	75.8	$FA_{0.7}MA_{0.3}Pb_{0.7}Sn_{0.3}I_3$/BTBTI:PCBM	[3][a)]
1.25	22.6	880	32.4	79.1	$FA_{0.7}MA_{0.3}Sn_{0.5}Pb_{0.5}I_3$	[62]
1.25	20.7	843	30.6	80.2	$FA_{0.6}MA_{0.4}Pb_{0.4}Sn_{0.6}I_3$	[2]
1.25	22.2	841	33.0	80.0	$FA_{0.7}MA_{0.3}Pb_{0.5}Sn_{0.5}I_3$	[3]
1.26	23.4	871	33.0	81.4	$FA_{0.7}MA_{0.3}Pb_{0.5}Sn_{0.5}I_3$	[4]
1.26	23.2	880	32.8	80.1	$FA_{0.7}MA_{0.3}Pb_{0.5}Sn_{0.5}I_3$	[31]
1.26	21.0	850	31.5	79.11	$Cs_{0.1}FA_{0.6}MA_{0.3}Pb_{0.5}Sn_{0.5}I_3$	[4]
1.26	20.4	834	30.5	80.2	GuaSCN:$FA_{0.6}$ $MA_{0.4}Sn_{0.6}Pb_{0.4}I_3$	[2]
1.27	22.1	850	32.3	80.3	$FA_{0.7}MA_{0.3}Pb_{0.5}Sn_{0.5}I_3$	[63]
1.28	20.6	842	30.6	80.1	FSA: $FA_{0.7}MA_{0.3}Pb_{0.5}Sn_{0.5}I_3$	[2][a)]
1.28	21.7	850	31.6	80.8	FSA: $FA_{0.7}MA_{0.3}Pb_{0.5}Sn_{0.5}I_3$	[2]
1.28	21.2	820	32.5	79.3	$Cs_{0.2}FA_{0.8}Pb_{0.5}Sn_{0.5}I_3$	[4]
1.29	23.3	880	32.8	80.8	$Cs_{0.025}FA_{0.475}MA_{0.5}Pb_{0.5}Sn_{0.5}Br_{0.075}I_{2.925}$	[3]
1.29	20.3	842	31.6	76.3	$Cs_{0.17}FA_{0.83}Pb_{0.5}Sn_{0.5}I_3$	[4]
1.29	19.5	810	32.1	75.0	$Cs_{0.25}FA_{0.75}Pb_{0.5}Sn_{0.5}I_3$	[4]
1.30	18.8	820	29.6	77.3	$FA_{0.6}MA_{0.4}Pb_{0.4}Sn_{0.6}I_3$	[2]
1.30	17.1	840	27.9	73.0	$Cs_{0.05}FA_{0.8}MA_{0.15}Pb_{0.5}Sn_{0.5}I_3$	[2]
1.31	5.0	420	23.8	50.3	$CsSnI_3$	[2][b)]
1.31	7.1	486	22.9	64.0	$MASnI_3$	[2][b)]
1.31	14.1	740	26.7	71.4	$Cs_{0.25}FA_{0.75}Pb_{0.5}$ $Sn_{0.5}I_3$	[2]
1.32	11.6	720	23.4	68.9	$MAPb_{0.4}Sn_{0.6}$ $Br_{0.2}I_{2.8}$	[2]
1.33	7.5	450	24.9	67.0	$CsSnI_3$:MBAA	[2]
1.34	10.0	767	20.5	63.6	$MAPb_{0.4}Sn_{0.6}I_3$	[2]
1.34	12.1	780	20.7	75.1	$MAPb_{0.4}Sn_{0.6}Br_{0.4}I_{2.6}$	[2]
1.35	21.1	846	31.4	79.5	$FAPb_{0.5}Sn_{0.5}I_3$	[64]
1.35	16.3	780	26.5	79.0	$FAPb_{0.7}Sn_{0.3}I_3$	[2]
1.36	8.2	630	19.7	66.1	$CsSnI_3$	[2]
1.37	14.7	737	27.1	73.6	$FA_{0.3}MA_{0.7}Pb_{0.7}Sn_{0.3}I_3$	[2]
1.38	17.3	810	28.2	75.4	$FAPb_{0.75}Sn_{0.25}I_3$	[2]
1.38	15.2	800	26.2	72.5	$MAPb_{0.75}Sn_{0.25}I_3$	[2]
1.39	20.6	1020	26.6	76.0	$FA_{0.7}MA_{0.3}Pb_{0.7}Sn_{0.3}I_3$	[2]
1.40	15.4	856	24.8	72.4	$FA_{0.85}PEA_{0.15}SnI_3$	[65]
1.40	15.1	815	25.2	73.6	$FA_{0.85}PEA_{0.15}SnI_3$	[65][a)]
1.40	8.2	745	17.8	61.8	$MAPb_{0.6}Sn_{0.4}I_3$	[2]
1.40	10.1	655	22.1	69.6	$FASnI_3$ + DipI + $NaBH_4$	[3]
1.41	14.0	780	23.6	76.3	$FASnI_3$	[66]
1.42	17.1	830	26.9	76.7	$CsPb_{0.6}Sn_{0.4}I_3$	[67]
1.42	14.3	920	20.4	76.2	$FASnI_3$	[3]
1.42	14.4	820	22.4	78.0	$MAPb_{0.75}Sn_{0.25}I_3$	[2]
1.42	13.2	840	20.3	78.0	$EA_{0.098}EDA_{0.01}FA_{0.882}SnI_3$	[2]
1.43	15.7	974	21.7	74.1	$FASnI_3$	[68]
1.43	12.4	949	17.4	74.9	$FA_{0.85}PEA_{0.15}SnI_3$:NH_4SCN	[2][a)]
1.44	12.3	750	21.7	75.3	$EA_{0.098}EDA_{0.01}FA_{0.882}SnI_3$	[3]
1.44	10.1	642	22.2	70.8	$Cs_{0.2}FA_{0.8}SnI_3$	[2][a)]

(*Continued*)

Table 3. (Continued)

E_g [eV]	PCE [%]	V_{oc} [mV]	J_{sc} [mA cm^{-2}]	FF [%]	Absorber perovskite	Refs.
1.44	10.2	638	22.0	72.5	$FASnI_3$:FOEI	[2][a]
1.45	14.8	820	25.2	71.69	$FASnI_3$:FPEABr	[69]
1.45	14.0	828	24.0	69.3	$FASnI_3$:FPEABr	[3][a]
1.45	13.3	907	21.2	69.2	$FA_{0.75}MA_{0.25}SnBr_{0.25}I_{2.75}$	[70]
1.45	13.6	840	22.9	70.8	$FASnI_3$	[3]
1.45	12.8	869	19.6	74.5	$FARbSn(Br, Cl, I)_3$	[4]
1.46	14.2	821	23.3	74.1	$FASnI_3$	[71]
1.46	12.0	774	22.6	69.24	$FASnI_3$	[71][b]
1.46	11.4	700	22.6	72.3	$FASnI_3$	[72]
1.47	13.1	770	22.9	74.4	$Cs_{0.05}FA_{0.95}SnI_3$	[4]
1.48	6.0	460	23.9	53.9	$CsSnI_3$	[2]
1.49	22.3	1090	26.3	78.0	$FA_{0.6}MA_{0.4}PbI_3$ (sc)	[2]
1.50	24.5	1166	25.7	82.0	$FA_{0.95}Rb_{0.05}PbI_3$	[73]
1.51	25.6	1193	24.9	85.9	$Cs_{0.025}FA_{0.90}MA_{0.075}PbI_3$	[74]
1.51	25.0	1170	25.0	85.7	$Cs_{0.025}FA_{0.90}MA_{0.075}PbI_3$	[74]
1.52	26.1	1164	26.1	85.7	$Cs_{0.05}FA_{0.95}PbI_3$	[58]
1.52	25.4	1188	26.2	81.38	$FAPbI_3$	[75]
1.52	24.7	1175	26.3	80.1	$FAPbI_3$	[75][a]
1.52	25.3	1150	26.2	83.9	$Cs_{0.05}FA_{0.85}MA_{0.05}Rb_{0.05}PbBr_{0.15}I_{2.85}$	[3]
1.53	21.9	1142	25.5	75.2	$CsFAMARbPb(Cl, I)_3$	[4][b]
1.53	26.5	1180	26.4	86.2	$Cs_{0.05}FA_{0.85}MA_{0.1}PbI_3$	[19]
1.53	26.7	1193	26.5	84.5	[c]	[6][a]
1.53	26.2	1174	26.1	85.2	$Cs_{0.05}FA_{0.85}MA_{0.1}PbI_3$	[19][a]
1.53	24.7	1167	26.5	80.1	$Cs_{0.05}FA_{0.85}MA_{0.1}PbI_3$	[19][b]
1.53	25.6	1187	25.8	83.5	$FAPbI_3$	[76]
1.53	25.2	1181	25.7	82.9	$Cs_{0.05}FA_{0.95}PbI_3$	[77]
1.53	25.2	1180	26.2	81.5	$FAPbI_3$	[78]
1.53	25.1	1157	26.1	83.0	$Cs_{0.015}FA_{0.985}PbI_3$	[4]
1.53	25.4	1150	26.2	82.0	$Cs_{0.05}\ FA_{0.9}MA_{0.05}PbI_3$	[4]
1.53	25.2	1174	26.2	81.8	α-$FAPbI_3$	[2][a]
1.53	25.4	1174	26.4	81.9	$FAPbI_3$	[3]
1.53	25.5	1189	25.7	83.2	[c]	[2][a]
1.53	22.2	1153	26.0	74.5	$Cs_{0.04}FA_{0.9}MA_{0.06}PbI_3$	[79][a,b]
1.54	26.0	1190	26.0	84.0	[c]	[4][a]
1.54	26.0	1170	26.2	84.8	$Cs_{0.2}FA_{0.8}PbI_{1.9}Br_{1.1}$	[80]
1.54	25.3	1183	26.1	81.9	$Cs_{0.05}FA_{0.85}MA_{0.1}PbI_3$	[81][a]
1.54	25.6	1175	26.0	83.8	$FAPbI_3$	[82]
1.54	25.4	1207	25.1	84.0	$Cs_{0.05}FA_{0.931}MA_{0.019}PbBr_{0.06}I_{2.94}$	[83]
1.54	24.2	1197	24.8	81.5	$Cs_{0.05}FA_{0.931}MA_{0.019}PbBr_{0.06}I_{2.94}$	[83][a,b]
1.54	25.6	1182	26.2	82.6	$FAPbI_3$: $(PbI_2)_2RbCl$	[3][a]
1.54	25.2	1200	25.8	81.7	$FAPbI_3$	[84]
1.54	25.2	1138	26.1	84.9	$Cs_{0.05}FA_{0.9}MA_{0.05}PbI_3$	[4]
1.54	24.2	1173	25.8	79.8	$FAPbI_3$	[85][b]
1.54	25.7	1179	25.8	84.5	[c]	[3][a]
1.55	26.0	1171	25.6	86.5	$Cs_{0.05}FA_{0.931}MA_{0.019}PbI_3$	[86]
1.55	26.0	1193	26.0	84.0	$FA_{0.97}MA_{0.03}PbBr_{0.09}I_{2.91}$	[87]

(*Continued*)

Table 3. (Continued)

E_g [eV]	PCE [%]	V_{oc} [mV]	J_{sc} [mA cm^{-2}]	FF [%]	Absorber perovskite	Refs.
1.55	25.7	1184	25.7	84.2	$Cs_{0.05}FA_{0.931}MA_{0.019}PbBr_{0.06}I_{2.94}$	[88]
1.55	25.4	1182	25.4	84.9	$Cs_{0.05}FA_{0.931}MA_{0.019}PbI_3$	[86][a)]
1.55	25.2	1185	25.9	82.0	$FA_{0.97}MA_{0.03}PbBr_{0.09}I_{2.91}$	[87][a)]
1.55	25.7	1188	25.7	84.2	$Cs_{0.05}FA_{0.931}MA_{0.19}PbBr_{0.06}I_{2.948}$	[89][a)]
1.55	25.7	1170	25.7	85.3	$Cs_{0.1}FA_{0.9}PbI_3$	[90][a)]
1.55	25.2	1181	25.7	82.8	$FA_{0.96}MA_{0.04}PbBr_{0.04}I_{2.96}$	[91][a)]
1.55	25.2	1195	25.6	82.2	$Cs_{0.05}FA_{0.95}PbI_3$ (Cl)	[92][a)]
1.55	25.1	1140	26.0	84.4	$FAPbI_3$	[93][b)]
1.55	25.3	1182	25.8	82.9	$FAPbI_3$	[94]
1.55	25.1	1176	25.5	83.6	$FAPbI_3$	[95]
1.55	25.1	1123	25.7	86.9	$CsPbBr_3$:$FAPbI_3$	[4]
1.56	25.4	1185	25.4	84.6	$Cs_{0.01}FA_{0.9603}MA_{0.0297}PbBr_{0.09}I_{2.91}$	[96][a)]
1.56	23.3	1184	25.2	78.0	$Cs_{0.01}FA_{0.9603}MA_{0.0297}PbBr_{0.09}I_{2.91}$	[96][b)]
1.56	25.2	1201	24.8	84.5	$Cs_{0.05}FA_{0.9025}MA_{0.0475}PbBr_{0.15}I_{2.85}$	[4]
1.56	25.1	1209	24.7	83.9	$Cs_{0.05}FA_{0.9025}MA_{0.0475}PbBr_{0.15}I_{2.85}$	[4][a)]
1.56	25.1	1195	24.9	84.4	$FA_{0.995}MA_{0.005}PbBr_{0.015}I_{0.985}$	[3]
1.56	25.2	1180	24.1	84.8	[c)]	[2][a)]
1.56	25.2	1181	25.1	84.8	FAMAPb(I, Br, Cl)$_3$	[2][a)]
1.56	25.3	1193	25.1	84.6	FAMAPb(I, Br, Cl)$_3$	[2]
1.57	25.8	1194	25.5	84.9	$Cs_{0.05}FA_{0.9025}MA_{0.0475}PbBr_{0.15}I_{2.85}$	[97]
1.57	25.7	1190	26.0	83.2	$FAPbI_3$	[98]
1.57	25.6	1190	25.0	86.0	$Cs_{0.2}FA_{0.8}PbBr_{0.9}I_{2.1}$	[99]
1.57	24.7	1175	26.0	80.8	$FAPbI_3$	[98][a)]
1.57	24.4	1190	25.6	80.2	FAPb(I, Cl)$_3$	[4]
1.57	23.6	1179	24.3	82.4	FAPb(I, Cl)$_3$	[4][a)]
1.57	23.1	1170	23.8	82.7	$Cs_{0.05}FA_{0.9025}MA_{0.475}PbBr_{0.15}I_{2.85}$	[4]
1.57	23.0	1170	24.1	81.6	$Cs_{0.05}FA_{0.88}MA_{0.07}PbBr_{0.24}I_{2.76}$	[2]
1.57	23.0	1147	25.1	79.9	$FA_{0.95}MA_{0.05}PbBr_{0.15}I_{2.85}$	[3][a)]
1.57	23.4	1153	25.2	80.6	$Cs_{0.05}FA_{0.75}MA_{0.15}Rb_{0.05}PbBr_{0.15}I_{2.85}$	[3]
1.58	22.9	1173	23.4	80.0	$Cs_{0.05}FA_{0.9}MA_{0.05}PbBr_{0.26}I_{2.74}$	[3]
1.58	22.6	1186	24.2	78.6	$FA_{0.92}MA_{0.08}PbBr_{0.24}I_{2.76}$	[2][a)]
1.58	22.6	1178	22.73	84.4	[c)]	[2][a)]
1.59	23.7	1216	23.9	81.6	$Cs_{0.05}FA_{0.82}MA_{0.13}PbBr_{0.39}I_{2.61}$	[100]
1.59	21.0	1140	23.7	77.7	$FA_{0.85}MA_{0.15}PbBr_{0.45}I_{2.55}$	[2][a)]
1.60	23.1	1162	24.1	82.5	$Cs_{0.05}FA_{0.85}MA_{0.1}PbBr_{0.1}I_{0.9}$	[101]
1.60	22.1	1150	24.1	79.8	$Cs_{0.05}FA_{0.85}MA_{0.1}PbBr_{0.1}I_{0.9}$	[101][b)]
1.60	20.3	1130	23.2	77.4	MAPb(Cl, I)$_3$	[2][a)]
1.61	21.4	1120	23.1	82.9	$MAPbI_3$	[2][b)]
1.61	21.5	1192	21.6	83.6	$Cs_{0.05}FA_{0.88}MA_{0.07}PbBr_{0.44}I_{2.56}$	[2][a)]
1.61	23.2	1240	22.1	84.5	$Cs_{0.05}FA_{0.88}MA_{0.07}PbBr_{0.44}I_{2.56}$	[2]
1.61	22.6	1200	24.0	78.5	$Cs_{0.07}FA_{0.765}MA_{0.135}Rb_{0.03}PbBr_{0.45}I_{2.55}$	[2]
1.62	21.7	1180	22.5	81.7	$MAPbI_3$-DAP	[2]
1.63	20.3	1130	23.4	76.8	$Cs_{0.05}FA_{0.76}MA_{0.19}PbBr_{0.6}I_{2.4}$	[2]
1.64	22.4	1130	23.7	83.8	$Cs_{0.05}MA_{0.1425}FA_{0.8075}PbBr_{0.45}I_{2.55}$	[3]
1.64	20.4	1140	23.6	75.8	$Cs_{0.05}FA_{0.79}MA_{0.16}PbBr_{0.51}I_{2.49}$	[2]
1.65	21.9	1256	21.0	83.0	$Cs_{0.15}FA_{0.8}MA_{0.05}PbBr_{0.6}I_{2.4}$	[102]
1.65	21.8	1218	21.5	83.2	$Cs_{0.15}FA_{0.8}MA_{0.05}PbBr_{0.54}I_{2.46}$	[4]
1.65	18.6	1181	20.7	76.0	$Cs_{0.15}FA_{0.8}MA_{0.05}PbBr_{0.54}I_{2.46}$	[4][b)]
1.65	21.9	1230	21.2	84.0	$Cs_{0.1}FA_{0.2}MA_{0.7}PbBr_{0.45}I_{0.2.55}$	[3]
1.65	16.2	1109	19.6	74.2	MAPb(Br, I)$_3$	[2][a)]

(*Continued*)

Table 3. (Continued)

E_g [eV]	PCE [%]	V_{oc} [mV]	J_{sc} [mA cm^{-2}]	FF [%]	Absorber perovskite	Refs.
1.66	21.3	1260	20.5	82.6	$Cs_{0.15}FA_{0.65}MA_{0.2}PbBr_{0.6}I_{2.4}$	[103]
1.67	21.6	1240	21.3	81.8	$Cs_{0.213}FA_{0.757}MA_{0.03}PbBr_{0.437}Cl_{0.09}I_{2.473}$	[104]
1.68	22.7	1200	22.5	84.1	$Cs_{0.05}FA_{0.8}MA_{0.15}PbI_{2.25}Br_{0.75}$	[89][a)]
1.68	20.7	1220	21.3	79.7	$Cs_{0.05}$ $FA_{0.8}MA_{0.15}PbBr_{0.75}I_{2.25}$	[2]
1.69	20.7	1220	20.6	82.1	$CsPbI_3$	[4]
1.70	21.6	1220	21.7	81.5	$CsPbI_3$	[4]
1.70	18.8	1193	20.7	76.2	$CsPbI_3$	[4][b)]
1.70	21.2	1244	20.6	82.5	$CsPbI_3$	[4]
1.70	20.3	1230	20.3	81.5	$CsPbI_3$	[4]
1.70	20.2	1176	20.8	82.5	$CsPbI_3$	[3]
1.70	16.9	1170	20.2	71.5	$Cs_{0.2}FA_{0.8}PbBr_{0.75}I_{2.25}$	[2]
1.71	21.3	1300	19.7	83.4	$Cs_{0.1}FA_{0.8}MA_{0.1}PbBr_{0.9}I_{2.1}$	[105]
1.72	20.4	1210	20.5	82.0	$CsPbI_3$	[106]
1.72	18.6	1244	19.2	77.9	$Cs_{0.83}FA_{0.17}PbBr_{0.8}I_{2.2}$	[2]
1.72	18.3	1350	17.6	77.0	$MAPbBr_{0.6}I_{2.4}$	[2]
1.72	17.1	1200	19.4	73.5	$Cs_{0.17}FA_{0.83}PbBr_{1.2}I_{1.8}$	[2]
1.73	14.1	1230	15.9	72.7	$Cs_{0.1}FA_{0.9}PbBrI_2$	[107]
1.74	18.3	1269	18.9	76.3	$Cs_{0.095}MA_{0.1425}FA_{0.7125}Rb_{0.05}PbBrI_2$	[2]
1.74	20.0	1274	18.2	86.3	$Cs_{0.16}FA_{0.80}MA_{0.04}PbBr_{0.96}I_{2.04}$	[4]
1.74	20.2	1210	19.3	86.5	$Cs_{0.2}FA_{0.8}PbBr_{0.9}I_{2.1}$	[3]
1.75	19.8	1310	19.4	78.0	$Cs_{0.17}FA_{0.83}PbBr_{1.2}I_{1.8}$	[2]
1.76	18.5	1210	20.0	76.4	$Cs_{0.05}FA_{0.79}MA_{0.16}PbBr_{1.2}I_{1.8}$	[2]
1.77	19.5	1340	17.6	83	$Cs_{0.1}FA_{0.8}MA_{0.1}PbBr_{1.2}I_{1.8}$	[105]
1.78	19.8	1350	17.7	83.1	$Cs_{0.2}FA_{0.8}PbBr_{1.2}I_{1.8}$	[108]
1.79	19.6	1324	17.9	83.0	$Cs_{0.4}DMA_{0.1}FA_{0.5}PbBr_{0.72}Cl_{0.12}I_{2.16}$	[109]
1.79	19.3	1330	17.3	83.9	$Cs_{0.2}FA_{0.8}PbBr_{1.2}I_{1.8}$	[4][a)]
1.79	19.0	1250	19.0	80.0	$Cs_{0.12}FA_{0.83}MA_{0.05}PbBr_{1.2}I_{1.8}$	[2]
1.79	17.7	1255	17.4	81.1	$Cs_{0.4}DMA_{0.1}FA_{0.5}PbBr_{0.71}Cl_{0.15}I_{2.14}$	[3]
1.79	16.9	1270	16.2	82.3	$Cs_{0.15}FA_{0.85}PbBr_{1.2}I_{1.8}$	[4]
1.79	16.6	1175	18.0	78.4	$Cs_{0.2}FA_{0.8}PbBr_{1.2}I_{1.8}$	[4]
1.79	17.6	1230	18.0	79.5	$Cs_{0.3}FA_{0.7}PbBr_{1.2}I_{1.8}$	[4][a)]
1.80	19.5	1330	17.8	82.7	$Cs_{0.2}FA_{0.8}PbBr_{1.2}I_{1.8}$	[110]
1.80	19.1	1274	17.7	84.5	$Cs_{0.2}FA_{0.8}PbBr_{1.2}I_{1.8}$	[4]
1.81	16.3	1220	17.0	78.6	$Cs_{0.4}FA_{0.6}PbBr_{1.05}I_{1.95}$	[2]
1.82	17.2	1266	16.8	80.9	$Cs_{0.35}FA_{0.65}PbBr_{1.2}I_{1.8}$	[3]
1.83	16.9	1240	16.9	80.7	$FA_{0.6}MA_{0.4}PbBr_{1.2}I_{1.8}$	[3]
1.84	15.2	1260	15.6	77.3	$Cs_{0.2}FA_{0.8}PbBr_{1.2}I_{1.8}$-DAP	[2]
1.85	18.1	1360	16.0	83.0	$Cs_{0.1}FA_{0.8}MA_{0.1}PbBr_{1.5}I_{1.5}$	[105]
1.85	15.0	1296	15.6	74.2	$Cs_{0.17}FA_{0.83}PbBr_{1.5}I_{1.5}$	[2]
1.86	17.0	1340	15.9	79.8	$CsPbBr_{0.75}I_{2.25}$-0.5FAOAc	[2]
1.87	14.0	1280	14.0	78.1	$CsBa_{0.2}Pb_{0.8}BrI_2$	[2]
1.87	13.7	1220	14.6	76.8	$CsEu_{0.05}Pb_{0.95}BrI_2$	[2]
1.88	17.4	1420	15.0	81.4	$CsPbBrI_2$	[3]
1.88	15.9	1300	15.5	79.1	$CsPbBrI_2$	[2]
1.88	15.3	1250	15.4	79.0	$CsPbBrI_2$	[2]
1.89	16.0	1310	15.8	77.5	$CsPbBrI_2$	[2]
1.89	15.6	1300	15.3	78.3	$CsPbBr(Ac)_xI_{2-x}$	[2]
1.90	15.0	1240	16.0	75.6	$InCl_3$:$CsPbI_2Br$	[2][a)]
1.90	16.5	1242	16.3	81.3	$CsPbBrI_2$	[4]
1.90	16.1	1320	15.3	79.7	$CsPbBrI_2$	[2]

(*Continued*)

Table 3. (Continued)

E_g [eV]	PCE [%]	V_{oc} [mV]	J_{sc} [mA cm^{-2}]	FF [%]	Absorber perovskite	Refs.
1.90	14.5	1300	14.3	78.1	$CsPbBrI_2$	[4]
1.90	14.7	1302	14.2	79.6	$CsPbBrI_2$	[4]
1.90	14.2	1210	14.8	79.0	$CsPbBrI_2$	[111]
1.90	14.0	1269	14.9	73.8	$CsPbBrI_2$	[4]
1.91	16.2	1393	14.0	83.5	$Cs_{0.1}FA_{0.8}MA_{0.1}PbBr_{1.8}I_{1.2}$	[105]
1.91	14.5	1300	14.3	77.8	$CsPbBrI_2$	[4]
1.91	14.4	1312	15.6	70.1	$Cs_{0.83}FA_{0.17}PbBr_{1.8}I_{1.2}$	[2]
1.91	14.2	1160	15.7	77.9	$CsPbBrI_2$	[2]
1.91	2.0	620	5.4	60.8	$MA_3Sb_2I_9$+HI	[2][b]
1.93	16.6	1417	14.2	82.7	$Cs_{0.25}FA_{0.60}MA_{0.15}PbBr_{1.5}I_{1.35}OCN_{0.15}$	[32]
1.94	13.4	1240	14.2	76.0	$CsPbBr_{1.2}I_{1.8}$	[3]
1.98	8.3	1080	12.3	62.0	$CsPbBr_2I$	[2]
1.99	13.4	1312	13.4	76.3	$Cs_{0.85}Rb_{0.15}PbBr_{1.25}I_{1.75}$	[4]
2.00	9.6	1185	11.2	72.3	$Cs_{0.15}FA_{0.85}PbBr_{2.1}I_{0.9}$	[2]
2.03	2.8	836	6.4	52.7	$MAPbBr_{1.77}I_{1.23}$	[2]
2.04	10.3	1340	9.7	79.2	$MAPbBr_{2.1}I_{0.9}$	[2]
2.05	6.1	1450	5.4	77.1	$MAPbBr_2I$	[2]
2.09	10.2	1270	11.5	69.4	$CsPbBr_2I$	[2]
2.10	10.7	1261	11.8	72.0	$CsPbBr_2I$	[2]
2.11	9.2	1200	10.2	74.6	GAI-DEE-$CsPbBr_2I$	[2]
2.20	8.9	1639	7.7	70.6	$FAPbBr_3$	[3]
2.27	10.6	1552	8.9	76.5	$FAPbBr_3$	[2]
2.28	8.1	1640	6.7	74.0	$FAPbBr_3$	[51][b]
2.28	10.5	1520	8.3	83.0	$CsPbBr_3$	[3]
2.29	10.2	1650	8.7	71.1	$MAPbBr_3$	[3]
2.30	11.2	1574	8.5	83.7	$CsPbBr_3$	[4]
2.31	9.7	1458	8.1	81.9	$CsPbBr_3$	[2]
2.32	10.1	1653	7.7	79.1	$MAPbBr_3$	[2]
2.33	8.5	1580	6.6	82.0	$CsPbBr_3$	[2]
2.33	8.2	1470	7.3	76.1	$CsPbBr_3$	[2]
2.34	10.7	1635	7.8	84.1	$CsPbBr_3$	[3]
2.34	10.1	1602	7.9	80.0	$CsPbBr_3$	[2]
2.34	9.7	1584	7.4	82.8	$CsPbBr_3$	[2]
2.35	10.7	1622	7.9	83.5	$CsPbBr_3$	[2]
2.35	10.6	1610	7.8	84.4	$CsSnBr_3$	[2]
2.35	10.2	1611	7.8	81.0	$CsPbBr_3$	[3]
2.36	10.3	1570	8.2	79.6	$CsPb_{0.97}Tb_{0.03}Br_3$	[3]
2.36	4.0	1130	5.5	63.6	$CsPbBr_{2.9}I_{0.1}$	[2]
2.37	2.2	690	5.0	63.5	$MA_3Sb_2Cl_xI_{9-x}$	[2]
2.38	8.1	1490	6.9	78.8	$CsPbBr_3$	[2]
2.41	2.7	1020	5.2	51.2	$Cs_2AgBiBr_6$	[2]
2.42	1.1	870	2.9	43.0	$BdAPbI_4$	[2]
2.43	2.8	820	5.7	60.3	$CsPb_2Br_5$	[2]
2.44	2.4	1140	3.4	60.9	$FAPbBr_{2.1}Cl_{0.9}$	[2]
2.45	2.9	1010	4.1	70.9	$Cs_2AgBiBr_6$	[2]
2.46	1.7	1060	3.9	40.2	$Cs_2AgBiBr_6$	[2]
2.47	3.3	1278	3.3	77.5	$Cs_2AgBiBr_6$	[3]
2.48	1.4	1060	2.5	52.0	$FAPbBr_2Cl$	[2]

[a] Certified power conversion efficiency; [b] Notable exception included as a material and/or large-area highlight; [c] Notable exception included as a *PCE* highlight without the absorber information; [d] PCE from *J-V* with significant hysteresis and MPP tracking closer to the listed value; sc, single crystal.

Table 4. Organic single-junction solar cells with the highest efficiency: Performance parameters as a function of device absorber bandgap energy (from the *EQE* spectrum).[12]

E_g [eV]	PCE [%]	V_{oc} [mV]	J_{sc} [mA cm^{-2}]	FF [%]	Absorber blend	Refs.
1.22	13.4	663	30.0	67.1	PTB7-Th:ATT-9	[3]
1.32	13.0	916	20.2	70.1	BTR:Y6:bisPC_{71}BM	[3]
1.32	10.6	690	24.3	63.2	PTB7-Th:IEICO-4F	[2]
1.33	13.9	865	22.4	71.4	BTR:MeIC:Y11	[3]
1.34	12.8	712	27.3	65.9	PTB7-Th:IEICO-4F	[2]
1.35	19.3	870	28.6	77.9	PM6:BTP-eC9:L8-BO	[4]
1.35	17.0	804	27.2	76.4	PM6:mBzS-4F	[2]
1.35	15.9	820	26.3	73.4	PM6:Y6	[2]
1.36	15.9	846	25.4	74.1	PM6:Y11	[2][a)]
1.36	18.3	840	27.4	79.4	D18:NFAs	[4]
1.37	20.2	863	29.1	80.5	PM6:BTP-eC9:SMA	[23]
1.37	19.4	858	28.3	79.7	PM6:BTP-eC9:Y6-1O:PC_{71}BM	[112]
1.37	18.3	856	26.9	79.4	PM6:BTP-eC9:PC_{71}BM	[2]
1.38	19.1	869	28.3	77.5	PM6:BTP-eC9:L8-F	[113]
1.38	19.0	920	26.4	78.2	D18:L8-BO:L8-CBIC-Cl	[114]
1.38	18.9	880	26.9	79.8	PBDB-TCl:AITC:BTP-eC9	[4][a)]
1.38	19.1	880	26.9	80.7	PBDB-TCl:AITC:BTP-eC9	[4]
1.38	19.1	853	27.8	80.5	PM6:BTP-eC9	[4]
1.38	18.2	840	27.5	78.6	PM6:eC9	[4]
1.38	18.2	857	27.4	77.6	PM6:BTP-T-3Cl:BTP-4Cl-BO	[3]
1.38	18.8	861	27.5	79.4	PM6:BTP-eC9:BTP-S9	[3]
1.38	18.7	853	27.4	80.0	PM6:BTP-eC9:L8-BO-F	[3]
1.38	18.2	847	27.3	78.8	PM6:BTP-eC9:L8-BO-F	[3][a)]
1.38	18.7	862	27.4	79.3	PM6:BTP-eC9:BTP-S9	[3][a)]
1.39	19.0	846	27.9	80.5	PM6:BTP-eC9	[115]
1.39	18.5	841	27.8	79.1	PM6:BTP-eC9	[115][a)]
1.39	19.1	858	28.0	79.5	PM6:BTP-eC9:LA23	[4]
1.39	18.5	858	27.6	77.8	PM6-T:BTPeC9	[4]
1.39	18.1	848	27.5	77.5	PM6:Y6-1O:BO-4Cl	[3][a)]
1.39	18.2	859	27.7	76.6	D18:Y6	[2][a)]
1.39	18.2	863	27.1	77.9	PM6:BTP-eC9:ZY-4Cl	[3][a)]
1.39	18.5	855	27.5	78.9	PM6:Y6-1O:BO-4Cl	[3]
1.39	18.7	863	27.4	79.0	PM6:BTP-eC9:ZY-4Cl	[3]
1.40	19.9	860	28.8	80.4	PM6:BTP-eC9:o-BTP-eC9	[116]
1.40	15.8	851	25.1	73.9	[b,c)]	[6][a)]
1.40	19.1	869	27.8	78.9	DL1:Y6	[117]
1.40	19.3	861	27.9	80.4	PM6:BTP-eC9	[4]
1.40	18.9	859	27.9	79.2	PM6:BTP-eC9	[4][a)]
1.40	19.1	869	27.5	79.9	PBDB-TF:L8-BO:BTP-eC9	[3][a)]
1.40	19.4	863	27.6	81.2	PBDB-TF:L8-BO:BTP-eC9	[3]
1.40	14.0	880	24.4	65.3	PBNT-TzTz:Y6-BO	[4][b)]
1.41	20.2	880	28.4	80.9	PBDB-TF:L8-BO:BTP-eC9	[21]
1.41	19.8	880	27.9	80.7	PBDB-TF:L8-BO:BTP-eC9	[21][a)]
1.41	18.4	880	27.98	74.5	PBDB-TF:L8-BO:BTP-eC9	[21][b)]
1.41	19.7	884	27.2	81.8	PTQ10:m-BTP-PhC6	[118]
1.41	19.5	886	27.2	81.1	PBQx-TCl:PBDB-TF:eC9-2Cl	[4]
1.41	19.4	885	27.3	79.8	D18:BTP-eC9-4F:2TT	[119]

(*Continued*)

Table 4. (Continued)

E_g [eV]	PCE [%]	V_{oc} [mV]	J_{sc} [mA cm^{-2}]	FF [%]	Absorber blend	Refs.
1.41	19.2	879	27.2	80.3	PBQx-TF:eC9-2Cl	[4]
1.41	19.1	871	27.2	80.6	PM6:DY-P2EH:BTP-ec9	[120]
1.41	19.0	877	27.1	79.8	PBQx-TF:eC9-2Cl	[4][a)]
1.41	19.0	879	26.7	81.0	PBQx-TF:eC9-2Cl:F-BTA3	[3]
1.42	19.2	880	27.6	78.9	D18:L8-BO:BTP-eC9	[121]
1.42	19.0	881	27.1	79.6	PM6:L8-BO:T9SBO-F	[122]
1.42	15.6	838	25.0	74.4	[c)]	[2][a)]
1.43	20.9	923	27.9	80.8	D18-Cl:BTP-4F-P2EH	[24]
1.43	20.2	920	27.2	80.8	D18:Z8:L8-BO	[22]
1.43	19.8	900	27.0	81.0	D18:Z8:L8-BO	[22][a)]
1.43	19.4	883	26.8	81.8	PM6:L8-BO	[123]
1.43	19.1	870	27.2	80.4	PM6:Y6-HU	[124]
1.43	18.7	917	26.0	78.4	PM6:PY-V-γ: PffBQx-T	[125]
1.43	18.2	914	25.7	77.4	PM6:PY-1S1Se:PY-2Cl	[4][a)]
1.44	19.9	900	27.5	80.4	D18:PM6:L8-BO	[126]
1.44	19.4	901	26.5	81.0	D18:L8-BO	[127]
1.44	19.2	888	26.8	80.7	PM6:L8-BO:TQT	[128]
1.44	19.0	912	26.1	79.9	PBQx-TF:PM6/PY-IT (C5Ph)	[129]
1.44	19.2	914	26.6	79.0	[b,c)]	[4][a)]
1.44	18.2	883	26.1	79.0	PM6:L8-BO	[3][a)]
1.45	19.5	905	27.2	79.6	PBTz-F:PM6:L8-BO	[4]
1.45	19.6	896	26.7	81.9	PM6:D18:L8-BO	[3]
1.45	19.3	890	26.7	80.9	PM6:L8-BO	[130]
1.45	19.2	888	26.9	80.4	PM6:L8-BO	[131]
1.45	19.0	886	27.4	78.3	PM6:L8-BO	[131][a)]
1.45	19.1	918	26.9	77.3	D18:L8-BO	[3]
1.45	19.2	891	26.7	80.7	PM6:D18:L8-BO	[3][a)]
1.46	19.7	937	26.1	80.4	D18:AQx-2F	[132]
1.46	19.2	907	27.2	77.7	PMQ-Si605:PM6:BTP-H2	[133]
1.46	19.1	887	26.9	80.1	PM6:L8-BO:DICO	[134]
1.46	18.2	897	25.7	78.9	[c)]	[2][a)]
1.47	18.8	928	25.3	80.1	PM6:BO-EH-ACl	[135]
1.47	14.6	882	23.1	71.7	PBDB-T-2Cl:BP-4F:MF1	[2]
1.48	12.4	880	20.8	67.7	PBDB-T:IDT-EDOT:$PC_{71}BM$	[2]
1.50	15.4	920	22.6	74.1	PM6:DTTC-4Cl	[2]
1.51	13.3	780	22.9	75.0	PM6:SeTIC4Cl-DIO	[2]
1.52	10.4	850	18.0	68.0	PBDB-T:IDT-EDOT:$PC_{71}BM$	[2]
1.53	10.7	850	22.2	56.7	PM6:SeTIC4Cl	[2]
1.54	13.6	940	19.5	73.8	BTR:NITI:$PC_{71}BM$	[2]
1.55	12.0	840	19.5	73.3	PM6:IT-4F	[2]
1.56	12.1	826	20.9	70.1	PM6:IT-4F	[2]
1.58	13.9	950	21.7	67.4	PM6:DTTC-4F	[2]
1.58	13.5	880	20.6	74.53	PBDB-T-SF:IT-4F	[2]
1.61	13.4	940	20.2	70.5	PM6:DTC-4F	[2]
1.61	12.1	916	18.1	73.0	PBDB-T-2Cl:MF1	[2]
1.62	11.0	793	19.4	71.5	[c)]	[2][a)]
1.62	12.2	930	17.5	75.0	PTQ10:IDTPC	[2]
1.63	12.8	910	19.1	73.6	PTQ10:IDIC-2F	[2]
1.64	12.9	960	17.4	71.3	PTQ10:IDIC	[2]

(*Continued*)

Table 4. (Continued)

E_g [eV]	PCE [%]	V_{oc} [mV]	J_{sc} [mA cm^{-2}]	FF [%]	Absorber blend	Refs.
1.65	10.4	910	16.2	70.6	PBDB-T:ITIC	[4]
1.66	12.1	815	20.3	73.2	[c]	[2][a]
1.67	11.2	1080	16.3	63.6	PvBDTTAZ:O-IDTBR	[4]
1.67	11.5	791	19.7	73.7	[c]	[2][a]
1.68	12.0	1030	18.5	63.0	PBDTTT-EFT:EHIDTBR	[2]
1.69	8.9	878	13.9	72.9	PBT1-C:NFA	[2]
1.70	11.1	867	17.8	71.9	[c]	[2][a]
1.72	10.0	899	16.8	66.4	[c]	[2][a]
1.76	9.6	786	17.0	72.0	PPDT2FBT:$PC_{70}BM$	[2]
1.79	7.5	1140	10.6	62.1	BDT-ffBX-DT:PDI4	[2]
1.79	6.2	1230	8.9	56.6	BDT-ffBX-DT:SFPDI	[2]
1.85	9.0	900	13.8	72.9	BTR:$PC_{71}BM$	[2]
1.85	7.6	830	13.3	69.1	PBDB-T:$PC_{71}BM$	[2]
1.86	7.4	940	12.7	61.9	PBDB-T:NDP-Se-DIO	[2]
1.88	5.7	950	10.7	55.9	PBDB-T-2Cl:PC61BM	[2]
1.93	6.3	790	12.2	65.3	P3HT:TCBD14	[2]
2.01	3.7	592	10.4	59.2	P3HT:PCBM	[2]

[a] Certified power conversion efficiency; [b] Notable exception included as a large-area highlight; [c] Notable exception included as a *PCE* highlight without the absorber information.

Table 5. Dye-sensitized single-junction solar cells with the highest efficiency: Performance parameters as a function of device absorber bandgap energy (from the *EQE* spectrum).[12]

E_g [eV]	PCE [%]	V_{oc} [mV]	J_{sc} [mA cm^{-2}]	FF [%]	Sensitizing dye	Refs.
1.44	11.0	714	21.9	70.3	[b]	[2][a]
1.52	11.4	743	21.3	71.9	[b]	[2][a]
1.59	10.1	710	18.5	76.9	TF-tBu_C_3F_7	[2]
1.61	11.4	864	17.3	75.8	YS7	[136]
1.62	12.1	860	17.6	80.3	SGT-021	[137]
1.65	13.2	889	19.1	77.5	SGT-021/HC-A6+ThCA	[61]
1.66	13.0	910	18.1	78.0	SM315	[3]
1.66	10.7	849	16.6	75.9	BJS2	[2]
1.72	4.2	503	12.7	64.9	NP2	[4]
1.74	7.8	694	15.4	72.7	YD2	[2]
1.75	10.9	745	20.7	70.8	YKP-88/YKP-137 (6/4)	[2]
1.75	13.1	755	24.4	71.0	N719	[25]
1.76	12.0	960	15.9	79.0	SM371	[3]
1.77	10	740	18.1	74.7	N719	[2]
1.79	9.9	740	19.0	70.5	PI-COF:N719	[3]
1.80	9.1	744	19.0	64.0	N719	[2]
1.80	9.0	790	19.8	57.2	N719	[2]
1.80	6.5	663	13.3	74.5	SK7	[2]
1.81	8.5	700	19.4	62.6	N719	[3]
1.82	6.4	680	13.1	71.8	AN-11	[2]
1.83	15.2	1063	18.0	79.4	SL9 + SL10/BPHA	[3][a]
1.83	8.9	820	19.0	57.5	N719	[2]
1.85	12.3	1020	15.2	79.1	[b]	[2][a]

(*Continued*)

Table 5. (Continued)

E_g [eV]	PCE [%]	V_{oc} [mV]	J_{sc} [mA cm^{-2}]	FF [%]	Sensitizing dye	Refs.
1.85	13.4	1040	15.6	80.4	[b]	[4][a]
1.86	8.3	782	14.8	71.7	N719	[2]
1.87	9.1	1060	11.2	76.7	L351	[2]
1.88	7.8	730	14.3	74.7	TY4	[2]
1.90	11.6	0.946	16.9	72.9	ZL004	[4]
1.93	11.2	1140	13.0	75.6	L350	[2]
1.97	3.0	600	6.3	79.4	AN-14	[2]
1.99	5.4	689	11.3	69.5	SK6	[2]
2.00	6.3	732	12.0	71.7	CW10+SK6	[2]
2.01	9.2	1160	11	72.1	L349	[2]
2.02	8.1	760	14.3	75.0	TY6	[2]
2.05	3.9	680	7.4	77.5	AN-12	[2]
2.09	6.9	780	11.6	76.3	TY3	[2]
2.12	5.8	739	10.8	72.7	CW10	[2]
2.15	4.1	640	8.76	73.6	PS1	[3]
2.23	5.8	760	10.2	74.8	MS3	[2]
2.32	5.3	1170	6.4	70.8	L348	[2]

[a] Certified power conversion efficiency; [b] Notable exception included as a *PCE* highlight without the absorber information.

Table 6. Inorganic emerging single-junction solar cells with the highest efficiency: Performance parameters as a function of device photovoltaic absorber bandgap energy (from the *EQE* spectrum).[12]

E_g [eV]	PCE [%]	V_{oc} [mV]	J_{sc} [mA cm^{-2}]	FF [%]	Absorber material/technology	Refs.
0.98	11.2	430	39.2	66.8	$Cu_2ZnSn(Se, S)_4$	[2]
1.02	11.6	441	39.2	67.4	$Cu_2ZnSnSe_4$	[2]
1.03	11.6	423	40.6	67.3	$Cu_2ZnSnSe_4$	[2][a]
1.04	9.6	425	34.9	64.5	$Cu_2ZnSnSe_4$	[2]
1.05	9.4	457	32.5	63.3	$Cu_2ZnSnSe_4$	[2]
1.05	13.8	514	38.7	69.3	$Cu_2ZnSn(S, Se)_4$	[138][b,c]
1.05	9.0	410	34.3	64.0	$Cu_2ZnSn(S, Se)_4$	[139]
1.06	9.5	460	31.1	66.4	$Cu_2ZnSnSe_4$	[2]
1.06	13.8	526	39.3	66.5	$Cu_2ZnSn(S, Se)_4$	[140]
1.06	13.2	477	40.1	69.0	$Cu_2ZnSn(S, Se)_4$	[2]
1.06	12.7	461	40.4	68.3	$Cu_2ZnSn(S, Se)_4$	[2][a]
1.07	12.5	491	37.4	68.2	$Cu_2ZnSnSe_4$	[2][a]
1.07	12.1	538	35.3	63.7	$Cu_2ZnSn(S, Se)_4$	[4][a]
1.08	12.9	520	39.1	63.3	$Cu_2ZnSn(S, Se)_4$	[141]
1.08	12.4	522	33.3	71.3	$Cu_2ZnSn(S, Se)_4$	[2]
1.08	13.8	546	36.3	69.4	$Cu_2ZnSn(S, Se)_4$	[4][a]
1.08	14.1	551	35.7	71.8	$Cu_2ZnSn(S, Se)_4$	[4]
1.09	15.1	530	38.4	74.0	$Cu_2ZnSn(S, Se)_4$	[6][a]
1.09	14.5	555	36.7	71.2	$Cu_2ZnSn(S, Se)_4$	[26]
1.09	14.9	555	36.9	72.7	$Cu_2ZnSn(S, Se)_4$	[4][a]
1.10	13.5	511	37.9	69.5	$Cu_2ZnSn(S, Se)_4$	[6][a,d]
1.10	14.1	565	35.4	70.3	$(Ag, Cu)_2ZnSn(S, Se)_4$	[142]
1.10	14.0	542	39.1	66.0	$Cu_2ZnSn(S, Se)_4$	[143]
1.10	13.8	545	36.8	68.7	$(Ag, Cu)_2ZnSn(S,Se)_4$	[142][a]

(*Continued*)

Table 6. (Continued)

E_g [eV]	PCE [%]	V_{oc} [mV]	J_{sc} [mA cm^{-2}]	FF [%]	Absorber material/technology	Refs.
1.10	13.3	514	36.8	70.4	$(Ag,Cu)_2ZnSn(S,Se)_4$	[144]
1.10	13.6	546	35.9	69.4	$Cu_2ZnSn(S,Se)_4$	[145]
1.10	13.6	538	36.2	69.9	$Cu_2ZnSn(S,Se)_4$	[3]
1.11	13.9	550	35.8	71.0	$Cu_2ZnSn(S,Se)_4$	[146]
1.11	13.1	547	34.3	70.0	$Cu_2ZnSn(S,Se)_4$	[3]
1.11	12.8	526	35.3	68.9	$Cu_2ZnSn(S,Se)_4$	[3][a)]
1.11	12.2	472	35.0	73.6	$Cu_2ZnSn(S,Se)_4$	[147]
1.12	12.1	494	36.2	67.5	$Cu_2ZnSn(S,Se)_4$	[4][a)]
1.12	12.3	527	32.3	72.3	$Cu_2Zn(Sn_{0.78}Ge_{0.22})Se_4$	[2]
1.13	12.6	513	35.2	69.8	$Cu_2ZnSn(S,Se)_4$	[2][a)]
1.13	11.1	460	34.5	69.8	$Cu_2ZnSn(S,Se)_4$	[2][a)]
1.14	13.3	531	37.8	66.2	$Cu_2ZnSn(S,Se)_4$	[148]
1.14	12.6	541	35.4	65.9	$Cu_2ZnSn(S,Se)_4$	[2][a)]
1.15	14.1	573	35.1	70.1	$Cu_2ZnSn(S,Se)_4$	[149]
1.15	13.2	531	37.5	66.3	$Cu_2ZnSn(S,Se)_4$	[150]
1.15	10.3	522	28.9	68.5	$Cu_2ZnSn(S,Se)_4$	[4][a)]
1.16	11.2	539	33.1	62.8	$Cu_2ZnSn(S,Se)_4$	[2]
1.16	12.9	494	38.2	68.3	$Cu_2ZnSn(S,Se)_4$	[151]
1.16	12.9	546	35.9	65.8	$Cu_2ZnSn(S,Se)_4$	[4][b)]
1.16	11.8	498	36.3	66.5	$Cu_2ZnSn(S,Se)_4$	[4][b)]
1.18	13.3	546	36.9	66.1	$Cu_2ZnSn(S,Se)_4$	[152]
1.19	9.8	537	32.6	56.3	$Cu_2ZnSn(S,Se)_4$	[4]
1.2	13.7	544	36.7	68.5	$Cu_2ZnSn(S,Se)_4$	[153]
1.20	8.12	432	35.5	57.9	Sb_2Se_3	[154]
1.21	3.7	280	30.9	41.9	$AgBiS_2$	[155]
1.22	7.5	413	28.9	62.4	Sb_2Se_3	[2]
1.23	7.6	410	30.5	60.5	Sb_2Se_3	[156]
1.23	10.6	467	33.5	67.6	Sb_2Se_3	[4][b)]
1.24	9.2	400	32.6	70.6	Sb_2Se_3	[2]
1.27	4.8	370	27.3	47.3	Sb_2Se_3	[2]
1.29	4.0	340	22.9	51.0	Sb_2Se_3	[2]
1.30	10.2	518	27.2	72.4	$AgBiS_2$	[27]
1.30	9.2	0.496	27.1	68.1	$AgBiS_2$	[27][b)]
1.30	8.4	470	31.3	57.3	Sb_2Se_3	[157]
1.31	8.6	440	32.2	60.8	Sb_2Se_3	[158]
1.31	7.3	420	29.2	59.7	Sb_2Se_3	[2]
1.33	8.6	520	27.8	59.8	Sb_2Se_3	[3]
1.35	10.1	551	26.0	70.1	$Sb_2(S,Se)_3$	[4]
1.36	9.2	492	29.5	63.7	Sb_2Se_3	[159][b,c)]
1.37	12.3	668	27.1	67.9	Cu_2ZnSnS_4	[160][c)]
1.37	7.1	480	24.7	60.0	$AgBiS_2$	[3]
1.38	8.1	474	27.7	62.2	Sb_2Se_3	[161]
1.39	8.9	482	26.8	68.5	$AgBiS_2$	[3][a)]
1.39	9.2	495	27.1	68.4	$AgBiS_2$	[3]
1.41	6.3	450	22.1	63.0	$AgBiS_2$	[4]
1.48	10.8	631	25.3	67.4	$Sb_2(S,Se)_3$	[4]
1.45	8.5	625	24.4	55.7	$Cu_2ZnGeSe_4$	[3]
1.50	11.0	731	21.7	69.3	Cu_2ZnSnS_4	[2][a)]

(*Continued*)

Table 6. (Continued)

E_g [eV]	PCE [%]	V_{oc} [mV]	J_{sc} [mA cm^{-2}]	FF [%]	Absorber material/technology	Refs.
1.50	10.0	655	24.1	63.3	$Sb_2(S,Se)_3$	[3][a)]
1.52	12.1	749	23.4	68.9	Cu_2ZnSnS_4	[6][a)]
1.52	8.7	664	20.6	63.9	$(Cu_{0.99}Ag_{0.01})_{1.85}(Zn_{0.8}Cd_{0.2})_{1.1}SnS_4$	[2]
1.53	8.5	670	20.4	62.1	$Sb_2(S,Se)_3$	[4]
1.54	10.7	673	23.7	66.8	$Sb_2(S,Se)_3$	[3]
1.54	9.7	638	23.2	65.5	$Sb_2(S,Se)_3$	[3]
1.55	10.2	736	21.0	65.8	Cu_2ZnSnS_4	[4]
1.55	10.5	664	23.8	66.3	$Sb_2(S,Se)_3$	[3]
1.59	10.7	801	21.0	63.7	Cu_2ZnSnS_4	[162]
1.59	11.4	746	21.8	70.1	Cu_2ZnSnS_4	[4][a)]
1.73	8.0	757	60.5	17.4	Sb_2S_3	[3]
1.80	7.5	711	16.1	65.0	Sb_2S_3	[2]
1.84	4.9	680	13.7	53.0	Sb_2S_3	[4]
1.95	5.8	870	10.8	62.1	Se	[4]
1.97	5.2	991	10.0	52.4	Se	[4]

[a)] Certified power conversion efficiency; [b)] Notable exceptions included missing the illuminated aperture/mask area information; [c)] "Effective" area subtracting that of the busbars and finger electrodes was used for the *PCE* calculation; [d)] large-area cell highlight.

Table 7. Single-junction solar cells with the highest efficiency among established technologies: Performance parameters as a function of device absorber bandgap energy (from the *EQE* spectrum).[12]

E_g [eV]	PCE [%]	V_{oc} [mV]	J_{sc} [mA cm^{-2}]	FF [%]	Absorber material/technology	Refs.
1.09	19.8	716	34.9	79.2	$Cu(In,Ga)Se_2$	[2][a)]
1.10	21.7	718	40.7	74.3	$Cu(In,Ga)Se_2$	[2][a)]
1.11	26.7	751	41.2	86.5	Si	[4][a)]
1.11	26.7	738	42.7	84.9	Si	[2][a)]
1.13	21.4	725	37.3	79.2	Si	[163]
1.13	22.9	744	38.8	79.5	$Cu(In,Ga)Se_2$	[2][a)]
1.13	23.6	767	38.3	80.5	$Cu(In,Ga)Se_2$	[4][a)]
1.14	21.0	757	35.7	77.6	$Cu(In,Ga)Se_2$	[2][a)]
1.15	23.4	734	39.6	80.4	$Cu(In,Ga)Se_2$	[2][a)]
1.17	21.7	727	40.4	73.8	Si	[164]
1.18	20.0	706	40.7	69.7	Si	[3]
1.30	16.3	762	31.4	68.1	$Cu(In,Ga)Se_2$	[2]
1.40	22.3	898	31.7	78.9	CdTe	[4][a)]
1.41	25.0	1045	28.7	83.0	GaAs	[165]
1.42	29.1	1127	29.8	86.7	GaAs	[2][a)]
1.43	22.6	898	31.6	79.6	CdTe	[6]
1.42	21.0	876	30.3	79.4	CdTe	[2][a)]
1.48	18.3	857	27.0	77.0	CdTe	[2][a)]
1.60	15.2	902	23.1	73	$Cu(In,Ga)Se_2$	[2]
1.60	10.2	896	16.4	69.8	Si (amorphous)	[2][a)]
1.69	10.6	896	16.1	75.6	Si (amorphous)	[2]
1.85	10.1	886	16.8	67.0	Si (amorphous)	[2][a)]

[a)] Certified power conversion efficiency.

Table 8. Monolithic multijunction perovskite-based research solar cells with the highest efficiency: Performance parameters as a function of the device photovoltaic bandgap energies (from the *EQE* spectra) of the subcells.

$E_{g,bottom}$ [eV]	$E_{g,middle}$, $E_{g,top}$ [eV]	PCE [%]	V_{oc} [mV]	J_{sc} [mA cm^{-2}]	FF [%]	Bottom absorber material	Middle, top absorber material(s)	Refs.
						Si/perovskite		
1.10	1.68	33.7	1996	21.0	85.3	Si	$Cs_{0.05}FA_{0.8}MA_{0.15}PbBr_{0.75}I_{2.25}$	[37]
1.10	1.69	34.2	1990	20.7	83.2	Si	[a,b]	[6]
1.10	1.69	32.8	1949	20.9	80.5	Si	$Cs_{0.05}FA_{0.8}MA_{0.15}PbBr_{0.75}I_{2.25}$	[166]
1.10	1.69	31.9	1943	22.1	77.6	Si	$Cs_{0.05}FA_{0.8}MA_{0.15}PbBr_{0.75}I_{2.25}$	[166][a]
1.11	1.63	24.1	1786	19.5	69.1	Si	$Cs_xFA_{1-x}Pb(Br,I)_3$	[2]
1.11	1.66	26.0	1820	19.2	75.4	Si	$Cs_{0.1}MA_{0.9}PbBr_{0.3}I_{2.7}$	[2]
1.11	1.67	33.7	1974	21.0	81.3	Si	[b]	[4][a]
1.11	1.67	30.1	1.903	20.1	78.6	Si	$Cs_{0.14}FA_{0.86}PbBr_{0.66}I_{2.34}$	[167]
1.11	1.67	29.8	1920	19.5	79.4	Si	$Cs_{0.209}FA_{0.741}MA_{0.05}PbBr_{0.4275}Cl_{0.15}I_{2.4225}$	[4]
1.11	1.67	26.7	1756	19.2	79.2	Si	$Cs_{0.15}FA_{0.65}MA_{0.2}PbBr_{0.6}I_{2.4}$:$PEA(I_{0.25}SCN_{0.75})$	[2]
1.11	1.68	34.1	1980	20.7	83.2	Si	$Cs_{0.05}FA_{0.8}MA_{0.15}PbBr_{0.72}I_{2.28}$	[30]
1.11	1.68	33.9	1966	20.8	83.0	Si	$Cs_{0.05}FA_{0.8}MA_{0.15}PbBr_{0.72}I_{2.28}$	[30][a]
1.11	1.68	25.7	1781	19.1	75.4	Si	$Cs_{0.05}FA_{0.8}MA_{0.15}PbBr_{0.75}I_{2.25}$	[2][a]
1.11	1.69	29.8	1190	19.5	79.8	Si	[b]	[3][a]
1.11	1.69	29.2	1929	19.5	77.6	Si	$Cs_{0.05}FA_{0.703}MA_{0.247}PbBr_{0.78}I_{2.22}$	[4]
1.12	1.55	22.3	1700	17.5	75.0	Si	$FAMAPbI_3$	[4]
1.12	1.64	26.0	1760	19.2	76.5	Si	$FA_{0.83}MA_{0.17}PbI_3$	[2]
1.12	1.65	26.5	1760	19.4	77.0	Si	$Cs_{0.05}FA_{0.79}MA_{0.16}PbBr_{0.51}I_{2.49}$	[2]
1.12	1.68	28.8 (29.2)[c]	1895	19.2	78.9	Si	$Cs_{0.05}FA_{0.73}MA_{0.22}Pb\ Br_{0.69}I_{2.31}$	[2]
1.12	1.70	32.1	1867	20.7	83.3	Si	$CsFAPb(Br,I)_3$	[168]
1.13	1.65	30.9	1953	19.8	79.9	Si	$Cs_{0.05}FA_{0.855}MA_{0.095}PbBr_{0.6}I_{2.4}$	[169][a]
1.13	1.69	32.5	1980	20.2	81.2	Si	$Cs_{0.209}FA_{0.741}MA_{0.05}PbBr_{0.4275}Cl_{0.15}I_{2.4225}$	[4][a]
1.13	1.69	31.3	1910	20.5	79.8	Si	$Cs_{0.18}FA_{0.82}Pb(Br,I)_3$	[4][a]
1.13	1.67	28.3	1776	20.1	79.6	Si	$FAMAPb(Br,Cl,I)_3$	[3][a]
1.13	1.65	24.9	1735	19.5	73.5	Si	$CsFAPb(Br,I)_3$	[2]
1.13	1.67	27.1	1886	19.1	75.3	Si	$CsFAMAPb(Br,Cl,I)_3$	[2]
1.13	1.68	28.9	1850	19.8	78.9	Si	$CsFAPb(Br,I)_3$:$MA(Cl_{0.5}SCN_{0.5})_{28.9}$	[4]
1.13	1.68	27.9	1833	19.4	77.5	Si	$CsFAPb(Br,I)_3$:$MA(Cl_{0.5}SCN_{0.5})_{28.9}$	[4][a]
1.13	1.69	29.5	1884	20.3	77.3	Si	[b]	[2][a]
1.14	1.68	27.5	1779	19.6	78.9	Si	$Cs_{0.22}FA_{0.78}PbBr_{0.45}Cl_{0.09}I_{2.55}$	[3]
1.14	1.69	26.8	1891	17.8	79.4	Si	[b]	[3][a]
1.14	1.69	26.0	1780	18.2	80.2	Si	$Cs_{0.15}FA_{0.7055}MA_{0.1445}PbBr_{0.6}I_{2.4}$	[3]
1.15	1.62	20.9	1690	15.9	77.6	Si	$MAPbI_3$	[2]
1.15	1.68	25.4	1800	17.8	79.4	Si	$Cs_{0.15}FA_{0.71}MA_{0.14}PbBr_{0.6}I_{2.4}$	[2]

(*Continued*)

Table 8. (Continued)

$E_{g,bottom}$ [eV]	$E_{g,middle}$, $E_{g,top}$ [eV]	PCE [%]	V_{oc} [mV]	J_{sc} [mA cm^{-2}]	FF [%]	Bottom absorber material	Middle, top absorber material(s)	Refs.
1.15	1.68	25.0	1770	18.4	77.0	Si	$Cs_{0.25}FA_{0.75}PbBr_{0.6}I_{2.4}$	[2]
1.16	1.62	19.2	1701	16.1	70.1	Si	$MAPbI_3$	[2]
1.17	1.63	26.4	1804	18.1	80.6	Si	$FA_{0.83}MA_{0.17}PbBr_{0.51}I_{2.49}$	[4]
1.17	1.63	23.7	1770	17.9	74.5	Si	$FA_{0.83}MA_{0.17}PbBr_{0.51}I_{2.49}$	[4][b]
1.17	1.63	19.5	1772	17.7	62.3	Si	$FA_{0.83}MA_{0.17}PbBr_{0.51}I_{2.49}$	[4][b]
						GaAs/perovskite		
1.42	1.85	24.3	2160	14.3	78.8	GaAs	$Cs_{0.16}FA_{0.80}MA_{0.04}PbBr_{1.50}I_{1.50}$	[2]
						CIGS/perovskite		
1.01	1.61	24.3	1570	21.0	73.6	$CuInSe_2$	$Cs_{0.05}FA_{0.85}MA_{0.1}PbI_{2.7}Br_{0.3}$	[3]
1.01	1.61	23.5	1590	19.4	75.5	$CuInSe_2$	$Cs_{0.05}FA_{0.85}MA_{0.1}PbI_{2.7}Br_{0.3}$	[3][a]
1.08	1.64	23.5	1700	19.5	71.0	$Cu(In,Ga)Se_2$	$Cs_{0.05}FA_{0.7885}MA_{0.1615}PbBr_{0.51}I_{2.49}$	[4]
1.10	1.65	22.4	1774	17.3	73.1	$Cu(In,Ga)Se_2$	$Cs_{0.09}FA_{0.77}MA_{0.14}PbBr_{0.42}I_{2.58}$	[2][a]
1.11	1.64	21.6	1580	18.0	76.0	$Cu(In,Ga)Se_2$	$Cs_{0.05}FA_{0.7885}MA_{0.1615}PbBr_{0.51}I_{2.49}$	[2]
1.11	1.65	23.3	1680	19.2	71.9	$Cu(In,Ga)Se_2$	$Cs_{0.05}FA_{0.7885}MA_{0.1615}PbBr_{0.51}I_{2.49}$	[2]
1.11	1.68	24.2	1770	18.8	71.2	$Cu(In,Ga)Se_2$	$Cs_{0.05}FA_{0.7315}MA_{0.2185}PbBr_{0.69}I_{2.31}$	[3]
1.12	1.68	24.2	1768	19.2	72.9	$Cu(In,Ga)Se_2$	[b]	[2][a]
1.13	1.63	18.1	1645	17.7	62.0	$Cu(In,Ga)Se_2$	$FA_{0.83}MA_{0.17}PbBr_{0.51}I_{2.49}$	[35]
						Perovskite/perovskite		
1.25	1.78	27.1	2200	15.3	80.8	$FA_{0.6}MA_{0.4}Pb_{0.4}Sn_{0.6}I_3$	Cs0.3DMA0.1FA0.6PbBr0.9I2.1	[4]
1.25	1.75	27.2	2110	16.1	80.3	$FA_{0.7}MA_{0.3}Pb_{0.5}Sn_{0.5}I_3$	$Cs_{0.3}FA_{0.7}PbBr_{1.2}I_{1.8}$	[170]
1.25	1.79	27.4	2110	15.6	83.8	$FA_{0.6}MA_{0.3}Cs_{0.1}Pb_{0.4}Sn_{0.6}I_3$	$Cs_{0.2}FA_{0.8}PbBr_{1.2}I_{1.8}$	[171]
1.25	1.80	28.4	2111	16.5	81.5	$FA_{0.7}MA_{0.3}Pb_{0.5}Sn_{0.5}I_3$	$Cs_{0.2}FA_{0.8}PbBr_{1.14}I_{1.86}$	[4]
1.25	1.80	28.0	2125	16.4	80.3	$FA_{0.7}MA_{0.3}Pb_{0.5}Sn_{0.5}I_3$	$Cs_{0.2}FA_{0.8}PbBr_{1.14}I_{1.86}$	[4][a]
1.25	1.80	28.2	2159	16.6	78.9	[b]	[b]	[4][a]
1.25	1.80	26.3 (26.4)[c]	2044	16.5	78.1	$FA_{0.7}MA_{0.3}Pb_{0.5}Sn_{0.5}I_3$	$Cs_{0.2}FA_{0.8}Pb\ Br_{1.14}I_{1.86}$	[3][a], [d]
.26	1.78	28.2	2110	16.7	80.2	$FA_{0.7}MA_{0.3}Pb_{0.5}Sn_{0.5}I_3$	$Cs_{0.2}FA_{0.8}PbBr_{1.2}I_{1.8}$	[31]
1.26	1.79	28.1	2135	16.2	81.5	$FAPb_{0.5}Sn_{0.5}I_3$	$Cs_{0.4}DMA_{0.1}FA_{0.5}PbBr_{0.72}Cl_{0.12}I_{2.16}$	[109]
1.26	1.79	27.1	2149	15.9	79.1	$FAPb_{0.5}Sn_{0.5}I_3$	$Cs_{0.4}DMA_{0.1}FA_{0.5}PbBr_{0.72}Cl_{0.12}I_{2.16}$	[109][b]
1.26	1.79	23.1	1950	15.8	75.0	$FA_{0.66}MA_{0.34}Pb_{0.5}Sn_{0.5}I_3$	$Cs_{0.05}(FAMA_{0.95})K_{0.05}Pb(BrI)_3$	[3]
1.26	1.80	29.1	2952	16.5	81.7	[b]	[b]	[4][a]
1.26	1.80	27.1	2132	15.5	82.4	$Cs_{0.1}FA_{0.6}MA_{0.3}Pb_{0.5}Sn_{0.5}I_3$	$Cs_{0.2}FA_{0.8}PbI_{1.8}Br_{1.2}$	[4]
1.26	1.80	26.0	2123	15.3	80.0	$Cs_{0.1}FA_{0.6}MA_{0.3}Pb_{0.5}Sn_{0.5}I_3$	$Cs_{0.2}FA_{0.8}PbI_{1.8}Br_{1.2}$	[4][a]
1.26	1.80	26.2	2040	16	80.1	$FA_{0.7}MA_{0.3}Pb_{0.5}Sn_{0.5}I_3$	$Cs_{0.4}DMA_{0.1}FA_{0.5}PbBr_{0.71}Cl_{0.15}I_{2.14}$	[3]
1.26	1.80	25.6	2000	16.1	79.6	$FA_{0.7}MA_{0.3}Pb_{0.5}Sn_{0.5}I_3$	$CsPbBr_xI_{3-x}$	[4]

(*Continued*)

Table 8. (Continued)

$E_{g,bottom}$ [eV]	$E_{g,middle}$, $E_{g,top}$ [eV]	PCE [%]	V_{oc} [mV]	J_{sc} [mA cm^{-2}]	FF [%]	Bottom absorber material	Middle, top absorber material(s)	Refs.
1.26	1.82	26.3	2130	15.2	81.0	$Cs_{0.05}FA_{0.7}MA_{0.25}Pb_{0.5}Sn_{0.5}I_3$	$Cs_{0.2}FA_{0.8}PbBr_{1.2}I_{1.8}$	[4][a]
1.26	1.82	24.0	1986	15.8	76.6	$FSA:FA_{0.7}MA_{0.3}Pb_{0.5}Sn_{0.5}I_3$	$Cs_{0.2}FA_{0.8}PbBr_{1.2}I_{1.8}$	[2][a]
1.26	1.82	25.5	2009	15.9	79.8	$FSA:FA_{0.7}MA_{0.3}Pb_{0.5}Sn_{0.5}I_3$	$Cs_{0.2}FA_{0.8}PbBr_{1.2}I_{1.8}$	[2]
1.26	1.84	26.6	2119	15.2	82.4	$FA_{0.8}MA_{0.3}Cs_{0.1}Sn_{0.5}Pb_{0.5}I_3$	$FA_{0.8}Cs_{0.2}PbBr_{1.2}I_{1.8}$	[4][a,b]
1.27	1.72	22.9	1915	15.0	79.8	$FA_{0.6}MA_{0.4}Pb_{0.4}Sn_{0.6}I_3$	$Cs_{0.05}FA_{0.8}MA_{0.15}Pb\ Br_{0.45}I_{2.55}$	[2]
1.27	1.81	30.1	2200	16.7	81.8	[b]	[b]	[6][a]
1.27	1.81	25.1	2021	15.6	79.5	$FA_{0.7}MA_{0.3}Pb_{0.5}Sn_{0.5}I_3$	$Cs_{0.2}FA_{0.8}PbBr_{1.2}I_{1.8}$	[4]
1.27	1.81	24.3	2030	15.2	78.8	$Cs_{0.05}FA_{0.5}MA_{0.45}Pb_{0.5}Sn_{0.5}I_3$	$Cs_{0.4}FA_{0.6}PbBr_{1.05}I_{1.95}$	[2]
1.27	1.81	24.5	1927	15.9	80.0	$FA_{0.7}MA_{0.3}Pb_{0.5}Sn_{0.5}I_3$	$Cs_{0.2}FA_{0.8}PbBr_{1.2}I_{1.8}$	[2][a]
1.27	1.82	23.2	1890	15.4	79.8	$Cs_{0.2}FA_{0.8}Pb_{0.5}Sn_{0.5}I_3$	$Cs_{0.2}FA_{0.8}PbBr_{1.2}I_{1.8}$	[3]
1.27	1.85	23.4	2000	15.0	77.8	$Cs_{0.17}FA_{0.83}Pb_{0.5}Sn_{0.5}I_3$	$Cs_{0.05}FA_{0.57}MA_{0.38}PbBr_{1.2}I_{1.8}$	[4]
1.28	1.73	23.1	1880	16.0	77.0	$Cs_{0.25}FA_{0.75}Pb_{0.5}Sn_{0.5}I_3$	$Cs_{0.3}DMA_{0.1}\ FA_{0.6}PbBr_{0.6}I_{2.4}$	[2]
1.28	1.79	24.5	1.8	17.16	79.3	$Cs_{0.025}FA_{0.475}MA_{0.5}Pb_{0.5}Sn_{0.5}Br_{0.075}\ I_{2.925}$	$Cs_{0.2}FA_{0.8}PbBr_{1.2}I_{1.8}$	[4]
1.28	1.82	27.2	2160	15.6	81.0	$Cs_{0.1}FA_{0.7}MA_{0.2}Pb_{0.5}Sn_{0.5}I_3$	$Cs_{0.2}FA_{0.8}Pbr_{0.9}I_{2.1}$	[172]
						OPV/perovskite		
1.21	1.83	21.7	1880	15.7	73.5	PTB7-Th:BTPV-4Cl-eC9	$FA_{0.6}MA_{0.4}PbBr_{1.2}I_{1.8}$	[3]
1.25	1.91	15.0	1710	12.0	73.4	PTB7-Th:COi8DFIC:$PC_{71}BM$	$CsPbBrI_2$	[2]
1.35	1.91	23.2	2150	13.4	80.3	D18-Cl:N3:$PC_{61}BM$	$CsPbBr_{1.1}I_{1.9}$	[4]
1.35	1.91	21.7	2150	13.0	77.5	D18-Cl:N3:$PC_{61}BM$	$CsPbBr_{1.1}I_{1.9}$	[4][b]
1.38	1.91	21.1	1960	13.3	80.9	PM6:Y6-BO	$CsPbBrI_2$	[2]
1.38	1.87	25.9	2120	14.7	83.0	D18-Cl:N3:$PC_{61}BM$	$Cs_{0.2}FA_{0.8}PbBr_{1.4}I_{1.6}$	[33]
1.38	1.87	24.7	2114	14.7	79.5	D18-Cl:N3:$PC_{61}BM$	$Cs_{0.2}FA_{0.8}PbBr_{1.4}I_{1.6}$	[33][a]
1.38	1.88	23.4	2136	14.6	75.2	[b]	[b]	[3][a]
1.38	1.88	21.4	2078	13.2	77.9	PM6:CH1007	$CsPbBr_{1.2}I_{1.8}$	[4][a]
1.38	1.88	22.4	2095	13.9	77.0	PM6:CH1007	$CsPbBr_{1.2}I_{1.8}$	[4]

(*Continued*)

Table 8. (Continued)

$E_{g,bottom}$ [eV]	$E_{g,middle}$, $E_{g,top}$ [eV]	PCE [%]	V_{oc} [mV]	J_{sc} [mA cm^{-2}]	FF [%]	Bottom absorber material	Middle, top absorber material(s)	Refs.
1.40	1.81	23.6	2063	14.8	77.2	PM6:Y6:P_{71}CBM	$Cs_{0.25}FA_{0.75}PbBr_{1.2}I_{1.8}$	[4]
1.40	1.81	22.5	2058	14.9	73.5	PM6:Y6:P_{71}CBM	$Cs_{0.25}FA_{0.75}PbBr_{1.2}I_{1.8}$	[4][a)]
1.40	1.83	15.1	1850	11.5	71.0	PBDB-T:SN6IC-4F	$Cs_{0.1}FA_{0.54}MA_{0.36}PbBr_{1.4}I_{1.8}$	[2]
1.40	1.82	19.5	1925	13.1	77.2	PBDBT-2F:Y6:$PC_{71}BM$	$Cs_{0.18}FA_{0.8}MA_{0.02}PbBr_{1.2}I_{1.8}$	[a)]
1.40	1.82	20.4	1902	13.1	81.5	PBDBT-2F:Y6:$PC_{71}BM$	$Cs_{0.18}FA_{0.8}MA_{0.02}PbBr_{1.2}I_{1.8}$	[2]
1.41	1.86	23.8	2140	14.1	79.0	PM6:Y6:$PC_{61}BM$	$Cs_{0.2}FA_{0.8}PbBr_{1.5}I_{1.5}$	[4]
						DSSC/perovskite		
1.59	1.93	10.5	1170	12.9	70.0	$FA_{0.85}MA_{0.15}PbBr_{0.45}I_{2.49}$	N719	[2]
						Triple-junction		
1.08	1.53, 1.89	22.2	2780	10.2	78.6	Si	$Cs_{0.1}FA_{0.85}MA_{0.05}PbI_3$, $MAPbBr_{1.05}Cl_{0.45}I_{1.5}$	[4]
1.11	1.58, 1.92	27.6	3132	11.6	76.2	Si	$Cs_{0.25}FA_{0.60}MA_{0.15}PbBr_{1.5}I_{1.35}OCN_{0.15}$, $Cs_{0.25}FA_{0.75}PbBr_{1.5}I_{0.5}$	[32]
1.11	1.58, 1.92	27.1	3145	11.1	77.7	Si	$Cs_{0.25}FA_{0.60}MA_{0.15}PbBr_{1.5}I_{1.35}OCN_{0.15}$, $FA_{0.75}Cs_{0.25}PbBr_{1.5}\ I_{0.5}$	[32][a)]
1.12	1.57, 1.88	24.4	2840	11.6	74.0	Si	$FAPbI_3$, $Cs_{0.2}FA_{0.8}PbBr_{1.5}I_{1.5}$	[173]
1.13	1.54, 1.91	20.1	2740	8.5	86.0	Si	$Cs_{0.1}FA_{0.9}PbI_3$, $Cs_{0.2}FA_{0.8}PbBr_{1.65}I_{1.35}$	[3]
1.23	1.57, 1.78	16.8	2780	7.4	81	$FA_{0.66}MA_{0.34}Pb_{0.5}Sn_{0.5}I_3$	$FA_{0.66}MA_{0.34}Pb\ Br_{0.15}I_{2.85}$, $Cs_{0.1}FA_{0.594}MA_{0.306}PbBrI_2$	[3]
1.25	1.61, 1.97	25.1	3330	9.7	78.0	$Cs_{0.05}FA_{0.7}MA_{0.25}Pb_{0.5}Sn_{0.5}I_3$	$Cs_{0.05}FA_{0.9}MA_{0.05}PbBr_{0.45}I_{2.55}$, $Cs_{0.15}FA_{0.85}PbBr_{1.8}I_{1.2}$	[34]
1.25	1.61, 1.97	23.9	3267	9.1	80.3	$Cs_{0.05}FA_{0.7}MA_{0.25}Pb_{0.5}Sn_{0.5}I_3$	$Cs_{0.05}FA_{0.9}MA_{0.05}PbBr_{0.45}I_{2.55}$, $Cs_{0.15}FA_{0.85}PbBr_{1.8}I_{1.2}$	[34][a)]
1.26	1.65, 2.06	19.9	2793	8.8	80.7	$FA_{0.7}MA_{0.3}Pb_{0.5}Sn_{0.5}I_3$	$Cs_{0.05}FA_{0.95}PbBr_{0.45}\ I_{2.55}$, $Cs_{0.2}FA_{0.8}PbBr_{2.1}I_{0.9}$	[3]
1.26	1.6, 1.99	23.3	3181	9.61	76.2	$Cs_{0.05}FA_{0.7}MA_{0.25}Pb_{0.5}Sn_{0.5}I_{3\text{-}0.05}SnF$	$Cs_{0.05}FA_{0.9}MA_{0.05}PbBr_{0.3}I_{2.7}$, $Cs_{0.85}Rb_{0.15}PbBr_{1.25}I_{1.75}$	[4][a)]
1.26	1.6, 1.99	24.3	3215	9.71	77.9	$Cs_{0.05}FA_{0.7}MA_{0.25}Pb_{0.5}Sn_{0.5}I_{3\text{-}0.05}SnF$	$Cs_{0.05}FA_{0.9}MA_{0.05}PbBr_{0.3}I_{2.7}$, $Cs_{0.85}Rb_{0.15}PbBr_{1.25}I_{1.75}$	[4]

[a)] Certified power conversion efficiency; [b)] Notable exception included as a large-area highlight, and/or a *PCE* highlight without the absorber material information; [c)] in parentheses, the certified efficiency from MPP tracking.

Table 9. Monolithic multijunction (non-perovskite) solar cells, including organic and dye-sensitized subcells, with the highest efficiency: Performance parameters as a function of the device bandgap energies (from the *EQE* spectra) of the subcells.

$E_{g,bottom}$ [eV]	$E_{g,top}$ [eV]	PCE [%]	V_{oc} [mV]	J_{sc} [mA cm^{-2}]	FF [%]	Bottom absorber	Top absorber	Refs.
						OPV/OPV		
1.21	1.58	19.0	1690	15.0	74.8	PTB7-Th:BTPSeV-4F	PM6:O1-Br	[4]
1.23	1.66	16.4	1650	14.5	68.5	PTB7-Th:BTPV-4F:$PC_{71}BM$	PM6:m-DTC-2F	[2]
1.24	1.72	17.3	1640	14.4	73.3	PTB7-Th:O6T-4F:$PC_{71}BM$	PBDB-T:F-M	[2]
1.31	1.64	15.9	1660	14.1	68.0	PM6:SFT8-4F	PCE-10:BT-CIC:BEIT-4F	[2]
1.32	1.65	15.0	1600	13.6	69.0	PTB7-Th:PCDTBT:IEICO-4F	PBDB-T-2F:TfIF-4FIC	[2]
1.32	1.74	19.6	1910	14.2	72.4	PBDB-TF:ITCC	PBDB-TF:BTP-eC11	[2]
1.32	1.74	19.5	1912	14.2	72.0	PBDB-TF:ITCC	PBDB-TF:BTP-eC11	[2]
1.36	1.73	18.7	1883	14.0	70.9	PM6:CH1007:$PC_{71}BM$	D18:F-ThBr	[3]
1.37	1.73	15.2	1610	12.9	73.0	PM6:Y6	PV2000:PCBM	[2]
1.37	1.77	20.3	2020	13.2	76.0	BTP-eC9:AITC:PBDB-TCI	AITC:PFBCPZ	[4]
1.37	1.77	20.6	2020	13.3	76.6	BTP-eC9:AITC:PBDB-TCI	AITC:PFBCPZ	[4]
1.38	1.80	20.3	2010	13.1	76.8	PBDB-TF:GS-ISO	PBDM-TF:BTp-eC9	[3]
1.38	1.80	20.3	2010	13.1	76.8	PBDB-TF:GS-ISO	PBDM-TF:BTp-eC9	[3]
1.39	1.78	19.6	2030	13.0	74.2	PBDB-TF:HDO-4Cl:BTP-eC9	PB2:GS-ISO	[4]
1.40	1.71	20.0	1960	13.5	75.9	PB4:FTCC-Br	PBQx-TCl:PBDB-TF:eC9-2Cl	[4]
1.42	1.79	15.0	1590	13.3	71.0	PCE-10:BTCIC	DTDCPB:C_{70}	[2]
1.45	1.76	17.9	2000	11.7	76.3	PM6:PY-IT	PM7:PIDT	[4]
1.48	1.74	14.1	1710	11.7	70.0	PTB7-Th: NOBDT	PBDB-T: F-M	
						OPV/a-Si		
1.33	1.78	15.1	1610	13.2	71.0	PTB7-Th:IEICO-4F	a-Si	[2]
						Si/DSSC		
1.11	1.84	14.7	580	40.9	62.0	Si	N719	[2]
1.24	1.67	17.2	1360	18.1	69.3	Si	SGT-021	[2]
						CIGS/DSSC		
1.21	1.82	13.0	1170	14.6	77.0	Cu(In,Ga)Se_2	N719	[2]
1.22	1.90	12.4	1435	14.1	61.0	Cu(In,Ga)Se_2	N719	[2]
1.22	1.82	15.1	1450	14.1	74.0	Cu(In,Ga)Se_2	N719	[2]
						DSSC/DSSC		
1.40	1.98	11.4	1400	12.2	66.7	DX1	N719	[2]
1.44	1.95	10.4	1450	10.8	67	N719	Black dye	[2]
1.67	1.98	12.3	1825	10.3	65	SGT-121/HC-A1	SGT-021/HC-A4	[3]
1.78	2.37	7.1	1420	7.2	69	N719	D131	[2]

Table 10. Monolithic multijunction (non-perovskite) inorganic absorber-based solar cells with the highest efficiency: Performance parameters as a function of the device bandgap energies (from the *EQE* spectra) of the subcells.

$E_{g,bottom}$ [eV]	$E_{g,middle}$, $E_{g,top}$, [eV]	PCE [%]	V_{oc} [mV]	J_{sc} [mA cm^{-2}]	FF [%]	Bottom absorber	Middle, top absorber(s)	Refs.
					GaAs/GaInP			
1.35	1.90	32.9	2500	15.4	85.7	GaAs	GaInP	[2]
1.41	1.88	32.8	2568	14.66	87.7	GaAs	GaInP	[2]
1.41	1.92	27.4	2400	13.1	88.0	GaAs	GaInP	[2]
1.42	1.85	31.6	2538	14.2	87.7	GaAs	GaInP	[2]
					Si/GaAsP			
1.17	1.90	23.4	1732	17.34	77.7	Si	GaAsP	[2]
					nc-Si/a-Si			
1.36	1.93	11.8	1428	12.27	67.5	nc-Si	a-Si	[2]
					Si/Se			
1.13	1.98	2.7	1403	5.7	34.2	Si	Se	[36]
					Triple-junction cells			
0.92	1.33, 1.88	39.5	3000	15.4	85.3	InGaAs	GaAs, InGaP	[3]
0.98	1.41, 1.89	37.7	3014	14.6	86.0	InGaAs	GaAs, InGaP	[3]
1.09	1.42, 1.92	19.1	2510	9.9	77.0	GaAsBi	GaAs, AlGaAs	[4]
1.13	1.48, 1.93	35.9	3248	13.1	84.3	Si	GaInAsP, InGaP	[3]
1.01	1.50, 1.92	28.1	2952	11.7	81.1	CIGS	AlGaAs/GaInP	[3]
1.30	1.27, 2.03	14.0	1922	9.9	73.4	nc-Si	nc-Si, a-Si	[3]

7.2. Best Performing Flexible Research Solar Cells Tables

Table 11. Flexible perovskite single-junction solar cells with the highest efficiency: Performance parameters as a function of photovoltaic bandgap energy (from the *EQE* spectrum).

E_g [eV]	PCE [%]	V_{oc} [mV]	J_{sc} [mA cm^{-2}]	FF [%]	Absorber perovskite	Refs.
1.44	8.5	650	20.8	62.9	$FAGe_{0.1}Sn_{0.9}I_3$	
1.53	23.1	1130	25.1	81.3	$FA_{0.98}Rb_{0.02}PbCl_{0.4}I_{2.6}$	[174]
1.53	24.9	1170	25.4	83.8	$FAPbI_3$	[46]
1.53	24.5	1150	25.5	83.5	$FAPbI_3$	[46][a)]
1.53	22.1	1140	25.3	76.6	$FAPbI_3$	[46][b)]
1.53	24.5	1200	24.5	83.3	$FAPbI_3$	[45]
1.53	24.0	1170	24.6	83.7	$FAPbI_3$	[45][a)]
1.53	25.1	1180	25.3	84.1	$FAPbI_3$	[44][b)]
1.53	24.9	1180	25.3	83.4	$FAPbI_3$	[44][a)]
1.53	24.6	1170	25.1	83.7	$FAPbI_3$	[175]
1.53	23.5	1150	24.4	83.7	$FAPbI_3$	[175][a)]
1.53	24.8	1190	25.4	82.2	$FAPbI_3$	[176]
1.53	23.2	1145	25.2	80.5	$FAPbI_3$	[4]
1.53	21.0	1140	25.1	73.5	$FAPbI_3$	[4][a)]
1.53	22.1	1130	23.9	81.8	$FAMAPbI_3$	[4]
1.53	20.5	1070	23.6	81.2	$FAMAPbI_3$	[3]
1.53	20.2	1123	24.7	72.9	$FA_{0.87}MA_{0.13}Pb(Cl,I)_3$	[3]
1.54	23.5	1160	24.6	82.4	$FA_{0.93}MA_{0.07}PbI_3$	[177]
1.54	23.0	1160	24.9	79.8	$Cs_{0.05}FA_{0.95}PbI_3$	[178]
1.54	22.4	1160	24.6	78.6	$Cs_{0.05}FA_{0.9}Rb_{0.05}PbBr_{0.09}I_{2.91}$	[179]
1.54	23.9	1160	25.2	81.9	$FA_{0.92}MA_{0.08}PbI_3$	[180]
1.54	23.6	1140	24.6	84.0	$FA_{0.92}MA_{0.08}PbI_3$	[180][a)]

(*Continued*)

Table 11. (Continued)

E_g [eV]	PCE [%]	V_{oc} [mV]	J_{sc} [mA cm^{-2}]	FF [%]	Absorber perovskite	Refs.
1.5	21.9	1120	25.2	77.5	$FA_{0.92}MA_{0.08}PbI_3$	[180][b]
1.54	23.8	1160	25.3	81.2	$Cs_{0.05}FA_{0.931}MA_{0.019}PbBr_{0.06}I_{2.94}$	[181]
1.54	24.1	1140	25.3	83.5	$Cs_{0.05}FA_{0.931}MA_{0.019}PbBr_{0.06}I_{2.94}$	[182]
1.54	25.1	1180	25.4	83.6	$Cs_{0.05}FA_{0.931}MA_{0.019}PbBr_{0.06}I_{2.94}$	[43]
1.54	24.5	1170	25.0	83.7	$Cs_{0.05}FA_{0.84}MA_{0.11}PbBr_{0.12}I_{2.88}$	[47][b]
1.54	22.4	1151	23.4	82.9	$FAMAPbI_3$	[3]
1.54	22.4	1170	24.6	77.8	$Cs_{0.1}FA_{0.9}PbI_3$	[3]
1.55	23.4	1180	24.2	81.9	$FA_{0.3}MA_{0.7}PbI_3$	[183]
1.55	23.4	1164	24.8	80.9	$Cs_{0.05}FA_{0.931}MA_{0.019}PbBr_{0.06}I_{2.94}$	[4][a]
1.55	23.7	1172	24.9	81.3	$Cs_{0.05}FA_{0.931}MA_{0.019}PbBr_{0.06}I_{2.94}$	[4]
1.55	21.3	1160	24.2	76.0	$Cs_{0.05}FA_{0.931}MA_{0.019}PbBr_{0.06}I_{2.94}$	[4][b]
1.56	21.7	1127	24.8	77.7	$Cs_{0.05}FA_{0.931}MA_{0.019}PbBr_{0.06}I_{2.94}$/PM6:CH1007:PCBM	[3]
1.56	20.8	1190	21.9	79.6	$FA_{0.95}MA_{0.05}PbBr_{0.15}I_{2.85}$	[2]
1.56	20.3	1160	23.4	74.8	$FA_{0.95}MA_{0.05}PbBr_{0.15}I_{2.85}$	[2]
1.56	19.9	1109	23.2	77.3	$Cs_{0.05}$ $FA_{0.747}MA_{0.153}Rb_{0.05}PbBr_{0.15}I_{2.85}$	[2][a]
1.56	19.9	1192	21.9	76.3	$FA_{0.95}MA_{0.05}PbBr_{0.15}I_{2.85}$	[2][a]
1.57	19.7	990	24.3	81.9	$MAPbI_3$	[184]
1.57	22.1	1200	22.8	80.9	$Cs_{0.05}FA_{0.90}MA_{0.05}PbBr_{0.15}I_{2.85}$	[4]
1.57	19.5	1110	23.1	76.0	$Cs_{0.03}FA_{0.945}MA_{0.025}PbBr_{0.075}I_{2.925}$	[2]
1.57	19.5	1105	23.1	76.1	$CsFAMAPb(Br,I)_3$	[4]
1.58	19.2	1120	21.7	78.9	$Cs_{0.08}FA_{0.87}MA_{0.05}PbBr_{0.12}I_{2.88}$	[2]
1.59	19.9	1120	23.0	77.5	$FAMAPb(Br,I)_3$	[2]
1.59	19.3	1090	22.7	78.1	$MAPbI_3$–NH_4Cl	[2]
1.59	20.2	1120	22.2	81.1	FAMAPbBrI	[3]
1.60	20.6	1110	23.0	80.7	CsFAMAPbBrI	[3]
1.60	20.5	1140	23.5	76.5	$Cs_{0.04}FA_{0.86}MA_{0.1}PbBr_{0.29}I_{2.71}$	[3]
1.60	17.8	1060	21.8	77.3	CsFAMAPbBrI	[3][b]
1.61	20.1	1150	22.4	78.0	$MAPbI_3$: $Cs_{0.12}MA_{0.88}(MBA)_2Pb_7I_{22}$	[48][b]
1.61	17.3	1062	21.7	74.9	$Cs_{0.05}FA_{0.81}MA_{0.14}PbBr_{0.45}I_{2.55}$	[2][a]
1.61	19.1	1135	21.2	79.2	$Cs_{0.05}FA_{0.75}K_{0.04}MA_{0.15}Rb_{0.01}PbBr_{0.51}I_{2.49}$	[2]
1.62	20.1	1150	22.4	78.0	$Cs_{0.04}FA_{0.8064}MA_{0.1536}PbBr_{0.48}I_{2.52}$	[2]
1.62	18.0	1120	22.3	72.1	$Cs_{0.06}FA_{0.79}MA_{0.15}PbBr_{0.45}I_{2.55}$	[2]
1.63	14.9	1030	21.5	67.3	$MAPbI_3$	[3]
1.63	10.4	1030	19.2	52.8	$FA_{0.85}MA_{0.15}PbBr_{0.45}I_{2.55}$	[2]
1.65	11.2	940	18.4	64.9	$MAPbI_3$	[2]
1.65	7.9	1090	10.8	70.7	$FA_{0.5}MA_{0.5}PbBr_{0.5}I_{2.5}$	[2]
1.66	20.0	1200	20.4	81.9	$Cs_{0.05}FA_{0.732}MA_{0.218}PbBr_{0.69}I_{2.31}$	[185][b]
1.79	14.3	1090	18.5	70.8	$CsPbBr_{0.19}I_{2.81}$	[49][b]
2.27	6.8	1400	7.4	66.1	$FAPbBr_3$	[52][b]

[a] Certified power conversion efficiency; [b] Notable exceptions included as materials and/or large-area highlights.

Table 12. Flexible organic single-junction solar cells with the highest efficiency: Performance parameters as a function of photovoltaic bandgap energy (from the *EQE* spectrum).

E_g [eV]	PCE [%]	V_{oc} [mV]	J_{sc} [mA cm^{-2}]	FF [%]	Absorber blend	Refs.
1.27	7.4	708	15.9	65.2	PTB7-Th:COi 8DFIC:$PC_{71}BM$	[2]
1.32	10.6	690	24.3	63.2	PTB7-Th:IEICO-4F	[2]
1.36	16.6	821	26.8	75.4	PM6:BTP-4Cl-12	[3]

(*Continued*)

Table 12. (Continued)

E_g [eV]	PCE [%]	V_{oc} [mV]	J_{sc} [mA cm^{-2}]	FF [%]	Absorber blend	Refs.
1.37	16.1	840	25.0	76.7	PM6:N3:$PC_{71}BM$	[2]
1.37	15.8	851	25.1	73.9	D18:Y6	[20][a,b]
1.38	16.2	840	25.4	76.0	PM6:BTP-eC9:$PC_{71}BM$	[186]
1.38	12.0	827	21.6	67.4	PM6:BTP-4Cl-12	[3][a]
1.38	17.5	835	27.4	76.7	PM6:BTP-eC9:$PC_{71}BM$	[3]
1.39	16.1	820	25.9	75.8	PM6:BTP-eC9:$PC_{71}BM$	[2]
1.39	15.9	864	25.0	73.5	D-18-Cl:G19:Y6	[3]
1.39	15.7	830	25.4	74.5	PM6:BTP-eC9	[4]
1.39	14.4	830	25.4	68.3	PM6:BTP-eC9	[4][b]
1.39	17.9	768	27.3	85.3	D18:N3:DOY-C4	[187]
1.39	18.2	865	27.4	76.5	PM6:BTP-eC9	[42]
1.39	17.0	874	26.4	73.6	PM6:BTP-eC9	[42]
1.39	13.0	780	24.9	67.2	PM6:BTP-eC9	[42][b]
1.39	17.5	860	27.0	75.4	PM6:BTP-eC9	[42]
1.40	17.2	870	25.5	77.3	PM6:L8-BO	[4][b]
1.40	17.4	869	25.5	78.5	PM6:L8-BO	[4]
1.40	16.1	860	25.9	74.7	PM6:Y6	[2]
1.40	15.2	832	25.1	73.0	PM6:Y6	[2]
1.40	17.1	830	27.4	74.9	PM6:BTP-eC9:$PC_{71}BM$	[3]
1.41	15.2	830	25.0	73.3	PM6:Y6	[3]
1.41	15.1	847	24.9	71.6	PM6:Y6:C6	[2]
1.42	16.6	860	25.9	74.7	PM6:Y6	[3]
1.43	16.5	925	23.6	75.6	PBQx-TF:PBDB-TF:PY-IT	[4]
1.44	10.7	943	17.7	64.3	D18:(40)-b-PYIT	[4]
1.44	10.4	848	17.0	72.2	PM6:Y6	[2]
1.45	16.6	860	25.5	75.8	PM6:L8-BO	[4]
1.45	14.3	920	21.6	71.8	PBQx-TF:DYBT-C4	[188]
1.55	12.0	840	19.5	73.3	PM6:IT-4F	[2]
1.56	11.6	820	19.6	72.2	PM6:IT-4F	[2]
1.56	12.1	826	20.9	70.1	PM6:IT-4F	[2]
1.61	10.9	900	18.7	64.8	PBDB-T:ITIC	[2]
1.63	9.2	770	16.0	74.7	PTB7-Th:$PC_{71}BM$	[2]
1.65	9.3	820	16.5	68.7	J51:ITIC	[2]
1.65	8.2	890	13.4	68.6	PBDB-T:ITIC	[2]
1.82	7.2	925	10.9	71.3	JP02	[2]
2.01	3.7	592	10.4	59.2	P3HT:PCBM	[2]

[a] Certified power conversion efficiency; [b] Notable exceptions included as a material and/or large-area cell highlight.

Table 13. Flexible dye-sensitized single-junction solar cells with the highest efficiency: Performance parameters as a function of device absorber bandgap energy (from the *EQE* spectrum).

E_g [eV]	PCE [%]	V_{oc} [mV]	J_{sc} [mA cm^{-2}]	FF [%]	Sensitizing dye	Refs.
1.65	4.1	770	9.9	53.9	N719	[2]
1.67	12.5	777	21.1	76.5	N719	[41][b]
1.74	4.6	750	10.5	58.0	N719	[2]
1.75	7.6	732	15.0	69.2	N719	[2][a]
1.78	7.5	725	15.4	67.5	N719	[2]
1.79	6.5	729	13.2	68.0	N719	[2]

(*Continued*)

Table 13. (Continued)

E_g [eV]	PCE [%]	V_{oc} [mV]	J_{sc} [mA cm^{-2}]	FF [%]	Sensitizing dye	Refs.
1.80	6.3	732	13.1	66.0	N719	[2]
1.81	6.3	754	12.3	67.9	$(JH\text{-}1)_{0.6}(SQ2)_{0.4}$	[2]
183	5.0	735	10.0	67.8	N719	[2]
1.88	6.0	750	11.2	71.0	N719	[2]
1.90	4.2	680	10.7	57.7	N719	[2]
1.94	4.2	710	10.3	57.2	N719	[2]
1.95	4.9	702	11.2	62.3	N719	[2]
2.02	3.9	720	11.9	45.2	N719	[3]
2.12	5.4	680	10.4	76.3	N719	[2]

[a] Certified power conversion efficiency.

Table 14. Flexible monolithic multijunction solar cells with the highest efficiency: performance parameters as a function of photovoltaic bandgap energies (from the *EQE* spectrum) of each subcell. For triple-junction devices, the middle and top subcell values are listed with a comma separator.

$E_{g,bottom}$ [eV]	$E_{g,top}$ [eV]	PCE [%]	V_{oc} [mV]	J_{sc} [mA cm^{-2}]	FF [%]	Bottom absorber material	Top absorber material (s)	Refs.
						Double junction cells		
1.20	1.68	23.4	1733	17.2	78.9	c-Si	$Cs_{0.05}FA_{0.731}MA_{0.219}PbBr_{0.69}I_{2.31}$	[50]
1.20	1.62	18.1	1645	17.7	62.0	$Cu(In,Ga)Se_2$	$FA_{0.83}MA_{0.17}PbBr_{0.51}I_{2.49}$	[35]
1.25	1.78	24.7	2000	15.8	78.3	$FA_{0.7}MA_{0.3}Pb_{0.5}Sn_{0.5}I_3$	$Cs_{0.2}FA_{0.8}PbBr_{1.05}I_{1.95}$	[3]
1.25	1.78	24.4	2016	15.6	77.3	$FA_{0.7}MA_{0.3}Pb_{0.5}Sn_{0.5}I_3$	$Cs_{0.2}FA_{0.8}PbBr_{1.05}I_{1.95}$	[3][a]
1.26	1.79	23.8	2100	15.1	75.1	$FA_{0.6}MA_{0.4}Pb_{0.4}Sn_{0.6}I_3$	$Cs_{0.12}FA_{0.8}MA_{0.08}PbBr_{1.2}I_{1.8}$	[3]
1.27	1.81	23.8	2012	15.5	76.1	$FA_{0.7}MA_{0.3}Pb_{0.5}Sn_{0.5}I_3$	$Cs_{0.2}FA_{0.8}PbBr_{1.2}I_{1.8}$	[4]
1.28	1.73	21.3	1820	15.6	75.0	$Cs_{0.25}FA_{0.75}Pb_{0.5}Sn_{0.5}I_3$	$Cs_{0.3}DMA_{0.1}FA_{0.6}PbBr_{0.6}I_{2.4}$	[2]
1.40	1.82	13.6	1800	11.1	68.3	PBDB-T:SN6IC-4F	$Cs_{0.1}FA_{0.54}MA_{0.36}PbBr_{1.2}I_{1.8}$	[2]
1.41	1.86	30.4	2547	14.3	84.7	GaAs	InGaP	[2]
1.41	1.92	27.4	2400	13.1	88.0	GaAs	InGaP	[2]
						Triple junction cells		
1.00	1.41, 1.91	30.2	3043	16.1	84.5	$Ga_{0.73}In_{0.27}As$	GaAs, $Ga_{0.51}In_{0.49}P$	[4][b]

[a] Certified power conversion efficiency; [b] *J-V* measured under AM0 136.7 mW cm^{-2}.

Table 15. Flexible emerging inorganic single-junction solar cells with the highest efficiency: Performance parameters as a function of device absorber bandgap energy (from the *EQE* spectrum).

E_g [eV]	PCE [%]	V_{oc} [mV]	J_{sc} [mA cm^{-2}]	FF [%]	Absorber material	Refs.
1.04	4.4	394	23.9	46.4	$Cu_2Cd_xZn_{1-x}Sn(S,Se)_4$	[3]
1.06	12.2	525	36.6	63.5	$Cu_2ZnSn(S,Se)_4$	[39]
1.07	4.9	358	28.7	47.3	$Cu_2ZnSn(S,Se)_4$	[3]
1.09	8.7	401	36.5	59.4	$Cu_2ZnSn(S,Se)_4$	[4]
1.13	10.2	463	35.7	62.0	$Cu_2ZnSn(S,Se)_4$	[3]
1.15	10.1	503	29.6	67.9	$Cu_2ZnSn(S,Se)_4$	[189]
1.16	11.2	539	33.1	62.8	$Cu_2ZnSn(S,Se)_4$	[2]
1.32	8.23	479	26.5	64.9	Sb_2Se_3	[190]
1.32	8.43	452	29.0	64.3	Sb_2Se_3	[40]
1.32	8.42	470	31.3	57.2	Sb_2Se_3	[157]
1.32	8.03	492	26.2	62.3	Sb_2Se_3	[191]
1.52	0.6	204	7.6	35.5	Cu_2ZnSnS_4	[2]
1.59	6.5	601	22.6	48.0	CZTSSe	[3]
1.80	3.8	650	11.6	49.5	Sb_2S_3	[4]

Table 16. Flexible single-junction solar cells with the highest efficiency among established inorganic technologies: Performance parameters as a function of device absorber bandgap energy (from the *EQE* spectrum).

E_g [eV]	PCE [%]	V_{oc} [mV]	J_{sc} [mA cm^{-2}]	FF [%]	Absorber material/technology	Refs.
1.10	26.8	751	41.5	86.1	Si	[38]
1.11	11.5	526	33.8	64.6	$Cu(In,Ga)(S,Se)_2$	[3]
1.14	17.0	656	36.6	70.8	Si	[2]
1.15	18.9	693	35.8	76.3	$Cu(In,Ga)Se_2$	[4]
1.17	18.9	608	39.5[3]	63.0	Si	[2]
1.17	12.0	580	35.8	58.4	$Cu(In,Ga)Se_2$	[2]
1.18	17.6	698	33.9	74.4	$Cu(In,Ga)Se_2$	[4]
1.20	20.4	736	35.1	78.9	$Cu(In,Ga)Se_2$	[2][a)]
1.20	17.6	630	38.9	72.4	$Cu(In,Ga)Se_2$	[185]
1.22	18.7	720	35.0	74.4	$Cu(In,Ga)Se_2$	[2]
1.32	8.4	550	24.3	63.0	Si	[2]
1.42	22.1	980	27.1	83.4	GaAs	[2]
1.45	13.5	786	22.1	77.7	GaAs	[3]
1.45	12.6	829	23.6	64.3	CdTe	[4]
1.46	14.1	821	24.3	70.3	CdTe	[3][a)]
1.46	16.4	831	25.5	77.4	CdTe	[2]
1.49	11.5	821	22.0	63.9	CdTe	[2]
1.79	8.8	888	14.3	70	a-Si:H	[2]
1.88	8.2	820	15.6	64.0	a-Si:H	[2]

[a)] Certified power conversion efficiency.

7.3. Best Performing Transparent and Semitransparent Research Solar Cells Tables

Table 17. (Semi-) Transparent perovskite solar cells with the highest efficiency: Performance parameters as a function of average visible transmittance and photovoltaic bandgap energy (from the *EQE* spectrum). For the tandem cells, the bandgap energies and absorber materials for the bottom and top subcells are separated with a comma in that order.

AVT [%]	E_g [eV]	LUE [%]	PCE [%]	V_{oc} [mV]	J_{sc} [mA cm^{-2}]	FF [%]	Absorber	Refs.
2	1.65	0.40	19.9	1189	20.3	82.0	$Cs_{0.15}FA_{0.8}MA_{0.05}PbBr_{0.54}I_{2.46}$	[4]
3	1.67	0.49	16.3	1099	18.9	78.3	$Cs_{0.25}FA_{0.75}PbBr_{0.6}I_{2.4}$	[3]
3	1.64	0.49	15.7	1070	19.0	77.2	$Cs_{0.175}FA_{0.75}MA_{0.075}PbBr_{0.375}I_{2.625}$	[2]
3	1.53	0.37	12.2	1017	17.5	68.5	$MAPbI_3$	[2]
4	1.63	0.65	18.2	1076	21.1	80.0	$CsFAMAPb(Br,I)_3$	[2]
5	1.60	1.14	19.1	1120	23.2	73.4	$MAPbI_3$	[3]
5	1.60	0.83	16.5	1080	20.6	74.2	$MAPbI_3$	[2]
5	1.61	0.60	12.0	960	19.2	65.3	$MAPb(Cl,I)_3$	[2]
5	1.65	0.56	11.2	940	18.4	64.9	$MAPbI_3$	[2]
6	1.60	0.95	15.8	1100	19.3	74.4	$MAPbI_3$	[2]
7	1.62	1.28	18.3	1100	21.9	75.8	$MAPbBr_{0.12}I_{2.88}$	[4]
7	1.55	0.95	13.6	988	20.4	67.5	$MAPbI_3$	[2]
8	1.52	1.48	19.8	1137	21.9	79.5	$Cs_{0.05}FA_{0.95}PbI_3$	[2]
9	1.63	1.60	17.8	1120	19.3	82.7	$Cs_{0.13}FA_{0.87}PbBr_{0.39}I_{2.61}$	[3]
9	1.64	1.63	17.4	1083	21.5	75.1	$Cs_{0.175}FA_{0.825}PbBr_{0.375}I_{2.625}$	[2]
10	1.78	1.13	11.3	1190	15.0	63.1	$CsPbI_3$	[4]
10	1.59	1.75	17.5	1070	22.4	73.1	$MAPbI_3$	[2]
10	1.65	1.61	16.1	1060	20.4	74.5	$Cs_{0.05}FA_{0.8075}MA_{0.1425}PbBr_{0.45}I_{2.55}$	[2]
12	1.27, 1.80	1.80	15.0	1940	11.4	68.0	$Cs_x(FA_{0.83}MA_{0.17})_{1-x}Pb_{0.5}Sn_{0.5}I_3$, $Cs_{0.2}FA_{0.8}PbBr_{1.2}I_{1.8}$	[4]

(*Continued*)

Table 17. (Continued)

AVT [%]	E_g [eV]	LUE [%]	PCE [%]	V_{oc} [mV]	J_{sc} [mA cm^{-2}]	FF [%]	Absorber	Refs.
12	1.60	1.59	13.2	1000	19.5	67.8	$MAPbI_3$	[2]
13	1.67	1.94	14.9	1100	19.8	68.4	$MAPbBr_{0.5}I_{2.5}$	[2]
13	1.88	1.72	13.2	1298	13.8	74.1	$Cs_{0.25}FA_{0.75}PbBr_{1.5}I_{1.5}$	[3]
14	1.64	1.96	13.6	1048	16.5	78.6	$Cs_{0.175}FA_{0.825}PbBr_{0.375}I_{2.875}$	[2]
14	1.57	1.81	13.0	970	19.1	69.9	$MAPb(Cl,I)_3$	[2]
15	1.64	1.71	11.4	1094	16.8	62.0	$Cs_{0.05}FA_{0.775}MA_{0.1615}PbBr_{0.51}I_{2.49}$	[3]
15	1.61	1.77	11.9	1000	17.8	66.3	$MAPbI_3$	[2]
16	1.76	2.19	13.7	1120	16.7	73.4	$MAPbBrI_2$	[2]
17	1.65	2.18	12.8	1040	16.6	74.1	$Cs_{0.05}FA_{0.8075}MA_{0.1425}PbBr_{0.45}I_{2.55}$	[2]
18	1.73	2.50	14.1	1.230	15.9	72.3	$Cs_{0.1}FA_{0.9}PbI_2Br$	[107]
18	1.77	2.19	12.2	1110	15.1	72.7	$MAPbBrI_2$	[2]
18	1.53	1.64	9.1	1017	14.6	61.5	$MAPbI_3$	[2]
19	1.55	1.67	8.8	941	13.7	68.3	$MAPbI_3$	[2]
20	1.63	2.30	11.7	1080	14.5	74.6	$MAPbI_3$ + BiPy-I	[2]
20	1.63	2.94	14.7	1108	17.6	75.2	$Cs_{0.05}FA_{0.8075}MA_{0.1425}PbBr_{0.45}I_{2.55}$	[2]
21	1.63	2.98	14.2	1117	17.4	73.2	$Cs_{0.05}FA_{0.8075}MA_{0.1425}PbBr_{0.45}I_{2.55}$	[2]
22	1.61	2.90	13.2	1073	17.2	71.7	$Cs_{0.05}FA_{0.8075}MA_{0.1425}PbBr_{0.45}I_{2.55}$	[2]
23	1.61	2.82	12.3	1082	17.1	66.6	$Cs_{0.05}FA_{0.8075}MA_{0.1425}PbBr_{0.45}I_{2.55}$	[2]
23	1.62	2.61	11.3	1040	15.1	72.3	$MAPbI_3$	[2]
23	1.57	2.48	10.8	970	17.3	64.4	$MAPb(Cl,I)_3$	[2]
23	1.88	1.98	8.6	1236	10.0	69.9	$Cs_{0.25}FA_{0.75}PbBr_{1.5}I_{1.5}$	[3]
24	1.87	2.25	9.4	1120	13.6	61.6	$MAPbBr_{1.5}I_{1.5}$	[2]
25	1.55	2.70	10.8	950	16.3	69.7	$MAPbI_3$	[2]
26	1.63	2.65	10.2	1070	12.2	78.1	$MAPbI_3$	[2]
27	1.60	3.26	12.1	1000	18.3	66.2	$MAPbI_3$	[2]
28	1.60	2.37	8.5	964	13.1	66.8	$MAPb(Cl,I)_3$	[2]
28	1.57	2.27	8.1	1030	11.2	70.2	$MAPb(Cl,I)_3$	[2]
30	1.62	3.84	12.8	1030	16.5	74.9	$MAPb(Cl,I)_3$	[2]
30	1.65	2.22	7.4	1010	11.8	62.2	$Cs_{0.05}FA_{0.8075}MA_{0.1425}PbBr_{0.45}I_{2.55}$	[2]
31	1.27, 1.80	2.88	9.3	1940	7.9	61.0	$Cs_x(FA_{0.83}MA_{0.17})_{1-x}Pb_{0.5}Sn_{0.5}I_3$, $Cs_{0.2}FA_{0.}8PbBr1_{.2}I_{1.8}$	[4]
31	1.69	3.69	11.9	1050	16.3	69.4	$MAPbBr_{0.5}I_{2.5}$	[2]
33	1.55	2.41	7.3	1037	13.4	52.5	$MAPbI_3$	[2]
34	1.62	3.98	11.7	990	15.9	74.6	$MAPb(Cl,I)_3$	[2]
35	1.88	4.21	12.0	1289	12.9	72.3	$Cs_{0.25}FA_{0.75}PbBr_{1.5}I_{1.5}$	[3]
36	1.79	3.71	10.3	1080	14.6	65.5	$MAPbBr\ I_2$	[2]
37	1.62	4.00	10.8	1010	14.7	73.1	$MAPb(Cl,I)_3$	[2]
37	1.57	2.89	7.8	970	11.6	69.6	$MAPb(Cl,I)_3$	[2]
38	1.63	4.07	10.7	1060	13.0	77.6	$MAPbI_3$	[2]
41	1.90	3.61	8.8	1110	12.8	62.2	$MAPbBr_{1.5}I_{1.5}$	[2]
42	1.63	4.31	10.3	1000	13.6	75.6	$MAPb(Cl,I)_3$	[2]
45	1.64	3.82	8.5	960	12.6	73.5	$MAPb(Cl,I)_3$	[2]
46	1.57	1.63	3.6	1030	5.4	64.4	$MAPb(Cl,I)_3$	[2]
47	1.63	2.12	4.5	880	8.2	63.0	$MAPbI_3$	[2]
52	1.88	2.13	4.1	1125	5.8	63.0	$Cs_{0.25}FA_{0.75}PbBr_{1.5}I_{1.5}$	[3]
55	2.27	3.76	6.8	1.400	7.4	65.6	$FAPbBr_3$	[52]
66	2.62	0.72	1.1	1000	2.1	52.9	$Cs_2AgBiBr_6$	[2]
68	2.35	5.30	7.8	1550	6.7	72.0	$FAPbBr_{2.43}Cl_{0.57}$	[2]
71	2.28	5.73	8.1	1640	6.7	73.9	$FAPbBr_3$	[51]
72	2.62	1.09	1.5	960	2.1	74.3	$Cs_2AgBiBr_6$	[2]

(*Continued*)

Table 17. (Continued)

AVT [%]	E_g [eV]	LUE [%]	PCE [%]	V_{oc} [mV]	J_{sc} [mA cm^{-2}]	FF [%]	Absorber	Refs.
72	3.03	0.17	0.2	1110	0.6	35.4	$MAPbCl_3$	[2]
73	2.62	1.14	1.6	970	2.2	73.1	$Cs_2AgBiBr_6$	[2]
73	2.84	0.38	0.5	1260	0.9	44.9	$MAPbBr_{0.6}Cl_{2.4}$	[2]
74	2.62	1.10	1.5	970	2.2	71.1	$Cs_2AgBiBr_6$	[2]

Table 18. (Semi-) Transparent organic solar cells with the highest efficiency: Performance parameters as a function of average visible transmittance and photovoltaic bandgap energy (from the *EQE* spectrum).

AVT [%]	E_g [eV]	LUE [%]	PCE [%]	V_{oc} [mV]	J_{sc} [mA cm^{-2}]	FF [%]	Active material	Refs.
1	1.40	0.17	13.3	810	24.6	66.5	PM6:Y6	[2]
2	1.66	0.15	7.6	770	15.6	63.3	PBDTTT-C-T:$PC_{71}BM$	[2]
3	1.40	0.40	12.6	800	24.5	64.5	PM6:Y6	[2]
6	1.47	0.73	12.0	870	19.6	70.4	PM7/PTTtID-Cl/IT-4F	[2]
8	1.41	1.02	12.7	852	21.1	70.4	D18-Cl:Y6:$PC_{71}BM$	[3]
9	1.42	1.28	14.2	854	23.0	72.3	PM6:Y6	[2]
10	1.39	1.41	14.9	847	23.1	75.8	D18: N3	[4]
11	1.66	0.78	7.1	760	14.5	64.4	PBDTTT-C-T:$PC_{71}BM$	[2]
13	1.42	1.73	13.3	853	21.7	71.9	PM6:Y6	[2]
14	1.40	1.86	13.6	850	21.1	75.8	PM6:Y6	[2]
14	1.41	1.71	12.0	844	19.6	72.8	PM6:Y6:C6	[2]
15	1.52	1.34	8.9	772	18.3	63.0	PTB7-Th:FNIC1	[2]
16	1.95	0.45	2.9	540	9.7	55.4	P3HT-PCBM	[2]
17	1.39	2.14	12.6	810	21.2	73.2	PM6:Y6	[2]
18	1.39	2.10	11.7	810	20.7	69.6	PM6:Y6	[2]
19	1.42	2.61	13.6	830	23.4	70.2	PM6:Y7	[3]
19	1.42	2.35	12.4	852	20.4	71.4	PM6:Y6	[2]
20	1.37	2.31	14.0	820	23.0	74.3	PM6:Y6:SN3	[3]
20	1.39	2.80	14.6	860	22.8	74.7	PM6/ICBA:Y6	[3]
20	1.42	2.92	12.3	817	20.6	73.0	PM6:Y6	[2]
20	1.23	2.40	11.6	661	25.6	68.2	PTB7-Th:ATT-9	[3]
21	1.39	3.32	16.1	859	24.6	76.1	PM6-Ir1:BTP-eC9:$PC_{71}BM$	[3]
22	1.41	2.84	12.9	831	20.9	74.3	D18:N3	[4]
25	1.34	2.75	11.0	750	20.9	70.0	PCE-10:A078	[2]
25	1.39	2.65	10.8	830	18.2	71.6	PBT1-C-2Cl: Y6	[4]
25	1.40	2.55	10.2	736	20.3	68.3	PTB7-Th:FOIC	[2]
25	1.43	3.03	12.1	760	23.9	66.6	PM6:Y6	[3]
25	1.45	3.44	13.6	895	19.6	77.1	DA:PM6:L8-BO:Y5	[56]
26	1.40	3.35	12.9	825	21.6	72.4	PM6:Y6	[2]
28	1.39	3.16	11.3	816	19.7	70.3	PM6:Y6-BO	[3]
28	1.66	1.57	5.6	760	11.9	61.9	PBDTTT-C-T:$PC_{71}BM$	[2]
30	1.41	3.24	10.1	880	16.8	67.8	PBOF:eC9:LB-BO	[4]
30	1.35	3.03	10.8	718	21.9	68.7	PTB7-Th:IEICO-4F	[2]
31	1.39	3.66	12.0	758	22.8	69.5	PCE10-BDT2F-0.8:Y6	[3]
32	1.42	3.58	11.2	849	17.0	77.6	PM6:m-BTP-PhC6:BO-Cl	[3]
33	1.39	4.08	12.3	781	22.0	71.3	PM6:PCE 10–2F:Y6	[4]
34	1.40	3.09	9.1	733	18.5	67.1	PTB7-Th:FOIC	[2]
35	1.44	1.47	4.2	860	8.4	58.0	PBOF:eC9:LB-BO	[4]
36	1.37	3.33	8.8	680	18.0	71.9	PCE-10:BT-CIC:TT-FIC	[2]
36	1.86	3.17	6.9	890	11.6	66.5	PSEHTT:ICBA	[2]

(*Continued*)

Table 18. (Continued)

AVT [%]	E_g [eV]	LUE [%]	PCE [%]	V_{oc} [mV]	J_{sc} [mA cm^{-2}]	FF [%]	Active material	Refs.
36	1.24	2.47	9.4	658	20.7	68.7	PTB7-Th:ATT-9	[53]
37	1.86	2.25	6.1	890	10.2	66.8	PSEHTT:ICBA	[2]
38	1.33	2.16	5.7	700	12.4	66.23	PTB7-Th:IEICO-4F	[2]
39	1.41	5.01	13.0	849	19.0	80.3	PBDB-TF:L8-BO:BTP-eC9	[3]
39	1.86	3.78	4.9	880	8.3	67.9	PSEHTT:ICBA	[2]
25	1.43	1.92	9.7	770	20.0	63.0	PM6:Y6	[3]
43	1.34	3.48	8.1	730	16.3	68.1	PCE-10:A078	[2]
43	1.40	3.90	9.0	850	14.0	75.7	PM6:BTP-eC9:L8-BO	[55]
44	1.37	3.52	8.0	680	16.2	72.6	PCE-10:BT-CIC:TT-FIC	[2]
44	1.39	3.65	8.2	806	15.1	67.2	PBT1-C-2Cl:Y6	[4]
44	1.40	5.58	6.7	600	18.6	60.2	PDTTP-TBT:Y6-BO:$PC_{61}BM$	[192]
44	1.39	2.95	12.6	840	19.8	75.8	PM6:BTP-eC9:L8-BO	[57]
46	1.39	5.10	11.2	803	19.3	72.0	DA:PCE10-2F/Y6:Y5	[56]
46	1.34	5.00	10.8	750	20.4	70.6	PCE-10:A078	[2]
47	1.39	5.35	11.4	854	18.0	74.5	PM6:BTP-eC9:L8-BO	[3]
47	1.34	3.34	7.1	730	14.3	68.0	PCE-10:A078	[2]
47	1.86	1.12	2.4	860	4.1	68.2	PSEHTT:ICBA	[2]
49	1.37	3.53	7.2	670	14.8	72.6	PCE-10:BT-CIC:TT-FIC	[2]
49	1.41	2.96	6.0	851	11.1	63.8	FC-S1:PM6:Y6-BO	[4]
50	1.38	4.16	8.3	746	16.7	66.8	PTB7-Th:FOIC:$PC_{71}BM$	[2]
51	1.24	3.73	7.3	645	17.9	63.6	PTB7-Th:ATT-9	[54]
51	1.39	3.75	7.4	749	14.7	66.7	PTB7:FOIC:PC71BM	[2]
53	1.86	0.97	1.8	890	3.8	54.8	PSEHTT:ICBA	[2]
53	1.32	3.04	5.7	750	10.6	69.5	DPP2T:IEICO-4F	[2]
60	1.33	2.32	3.9	749	7.34	70.2	DPP2T:IEICO-4F	[2]
62	1.33	3.66	5.9	690	12.9	66.0	PTB7-Th:6TIC-4F	[2]
71	1.33	2.87	4.1	0.703	9.5	61.0	PTB7-Th:IEICO-4F	[193]
80	1.33	1.91	2.4	0.705	5.7	59.3	PTB7-Th:IEICO-4F	[193]

Table 19. (Semi-) Transparent dye-sensitized solar cells with the highest efficiency: Performance parameters as a function of average visible transmittance and photovoltaic bandgap energy (from the *EQE* spectrum).

AVT [%]	E_g [eV]	LUE [%]	PCE [%]	V_{oc} [mV]	J_{sc} [mA cm^{-2}]	FF [%]	Sensitizing dye	Refs.
1	2.00	0.05	5.2	780	12.4	53.7	N719	[2]
5	1.80	0.55	11.0	871	16.8	75.2	C268+Y1	[3]
9	2.00	0.41	4.5	780	10.3	56.0	N719	[2]
9	1.82	0.39	4.3	720	9.9	60.0	N719+SDA	[2]
10	2.01	0.52	5.2	770	11.9	57.0	N719	[2]
10	2.00	0.49	4.9	765	11.4	56.1	N719	[2]
10	1.81	0.50	5.0	710	11.7	60.7	N719	[3]
13	1.68	1.31	10.1	851	14.9	80.2	SGT-021	[2]
14	1.68	1.39	9.9	850	14.9	78.5	SGT-021	[2]
15	1.68	1.44	9.6	850	14.7	77.2	SGT-021	[2]
17	1.68	1.67	9.8	855	15.1	75.5	SGT-021	[2]
18	2.00	1.58	8.6	750	16.7	68.4	N719 (EtOH)	[2]
23	1.82	0.97	4.2	650	9.9	64.0	N719+SDA	[2]
23	2.01	0.83	3.6	650	8.2	68.0	N719	[2]
24	2.00	1.86	7.8	794	17.4	56.3	N719 (EtOH)	[2]

(*Continued*)

Table 19. (Continued)

AVT [%]	E_g [eV]	LUE [%]	PCE [%]	V_{oc} [mV]	J_{sc} [mA cm^{-2}]	FF [%]	Sensitizing dye	Refs.
25	1.82	0.65	2.6	650	5.6	71.0	N719+SDA	[2]
27	1.77	0.99	3.7	521	10.7	65.8	NPI	[2]
30	2.19	0.45	1.5	640	3.3	70.0	N719	[2]
31	2.23	1.98	6.4	698	13.5	67.9	TPA-1 (EtOH)	[2]
33	2.30	2.02	6.1	711	12.5	68.3	TPA-2 (EtOH)	[2]
36	2.23	2.20	6.1	766	14.5	54.7	TPA-1 (EtOH)	[2]
37	2.46	1.30	3.5	648	8.0	67.5	Cz-2	[2]
38	2.31	2.16	5.7	769	13.6	54.2	TPA-2 (EtOH)	[2]
69	1.39	2.13	3.1	422	11.2	65.6	VG20-C_{16}	[2]
75	1.53	1.88	2.5	408	10.9	56.2	TB207	[3]
76	1.41	1.75	2.3	406	8.6	65.9	VG20-C_{16}	[2]

Table 20. Semitransparent emerging inorganic solar cells with the highest efficiency: Performance parameters as a function of average visible transmittance and photovoltaic bandgap energy (from the *EQE* spectrum).

AVT [%]	E_g [eV]	LUE [%]	PCE [%]	V_{oc} [mV]	J_{sc} [mA cm^{-2}]	FF [%]	Absorber/technology	Refs.
1	1.46	0.03	3.0	475	14.6	42.8	$Cu_2ZnSn(S,Se)_4$	[2]
8	1.83	0.27	3.4	679	12.1	42.0	Sb_2S_3	[2]

Table 21. Semitransparent solar cells among established inorganic technologies with the highest efficiency: Performance parameters as a function of average visible transmittance and photovoltaic bandgap energy (from the *EQE* spectrum).

AVT [%]	E_g [eV]	LUE [%]	PCE [%]	V_{oc} [mV]	J_{sc} [mA cm^{-2}]	FF [%]	Absorber/technology	Refs.
2	1.23	0.20	10.0	640	23.3	66.9	CIGS	[2]
5	1.26	0.49	9.8	630	22.9	67.6	CIGS	[2]
7	1.92	0.50	6.6	881	11.8	63.7	a-Si:H	[2]
9	1.30	0.88	9.8	630	20.9	74.1	CIGS	[2]
9	1.28	0.59	6.5	597	22.9	46.5	CIGS	[2]
11	1.34	0.91	8.4	620	20.4	66.3	CIGS	[2]
16	1.83	1.20	7.5	810	14.2	65.3	a-Si:H	[2]
17	1.83	1.31	7.7	810	14.1	67.3	a-Si:H	[2]
18	2.05	1.07	5.9	720	14.1	58.3	a-SiGe:H	[2]
19	1.87	1.38	7.3	820	13.1	67.6	a-Si:H	[2]
19	1.30	1.28	6.9	640	16.6	64.7	CIGS	[2]
19	1.34	1.24	6.5	580	17.5	63.5	CIGS	[2]
20	1.64	0.34	1.7	495	8.9	40.8	CIGS	[2]
22	2.05	1.20	5.5	760	12.3	58.6	a-Si:H	[2]
23	1.92	1.38	6.0	830	10.6	68.2	a-Si:H	[2]
24	1.68[a)]	1.66	6.9	920	10.7	70.3	a-Si:H	[2]
26	1.50	1.51	5.9	710	14.6	57.4	CIGS	[2]
37	1.54	0.15	0.4	101	14.7	27.2	CdTe	[2]
45	2.16	0.50	1.1	596	3.9	47.3	a-Si:H	[2]

[a)] E_g was taken from the absorbance spectrum.

Table 22. Transparent photovoltaic devices with the highest efficiency including transparent luminescent solar concentrators: Performance parameters (measured under the standard of Yang et al.)[194] as a function of the average visible transmittance and photovoltaic bandgap energy (from the *EQE* spectrum).[12]

AVT [%]	E_g [eV]	LUE [%]	PCE [%]	V_{oc} [mV]	J_{sc} [mA cm^{-2}]	FF [%]	Luminophore(s)/absorber	Refs.
74	1.50	0.92	1.2	990	1.5	81.3	CO_i8DFIC/GaAs	[2]
75	1.64	2.26	3.0	1020	3.8	77.7	$Cs_2Mo_6I_8(CF_3CF_2COO)_6$:BODIPY/GaAs	[3]
84	2.81	0.37	0.4	520	1.3	65.1	$(TBA)_2Mo_6Cl_{14}$/Si	[3]
84	2.60	0.65	0.8	4810	0.2	79.2	Si-QDs/Si	[195]
86	1.52	0.34	0.4	500	1.2	66.7	Cy7-NHS/Si	[3]
89	2.94	1.86	2.1	500	5.7	73.3	Si-CDs/Si	[4]

7.4. Operational Stability Tables of Emerging Research Solar Cells

Table 23. Perovskite solar cells with the highest operational stability test energy yield for 200 and 1000 h under simulated 1 sun illumination as a function of the device photovoltaic bandgap energy (from the *EQE* spectrum).

E_g [eV]	0 h PCE [%]	200 h PCE [%]	1000 h PCE [%]	E_{200h} [Wh cm^{-2}]	E_{1000h} [Wh cm^{-2}]	Absorber	Comments	Refs.
1.40	9.4	9.4	9.2	1.9	9.3	$FASnI_3$+$NaBH_4$+DipI	MPP, AM1.5G, N_2, 70 °C	[3]
1.45	13.8	14.1	13.0	2.8	13.6	$FASnI_3$	MPP, AM1.5G, air	[3]
1.51	22.8	21.9	20.0	4.5	21.2	$Cs_{0.025}FA_{0.90}MA_{0.075}PbI_3$	MPP, AM1.5G, 40 °C, 50% RH, encapsulation	[74]
1.52	25.4	25.1	24.4	5.0	24.8	$Cs_{0.05}FA_{0.95}PbI_3$	MPP, AM1.5G, N_2, 25 °C	[58]
1.53	22.5	22.3	20.9	4.4	21.9	$Cs_{0.04}FA_{0.9}MA_{0.06}PbI_3$	MPP, AM1.5G, 65 °C, 50% RH, encapsulation	[79]
1.53	23.4	22.7	22.3	4.6	22.6	$Cs_{0.05}FA_{0.85}MA_{0.1}PbI_3$	MPP, AM1.5G, 65 °C, 50% RH, encapsulation	[19]
1.53	21.7	22.3	21.3	4.4	22.0	$FAPbI_3$	MPP, AM1.5G, 60 °C, 70% RH, no UV filter	[196]
1.53	24.3	23.8	–	4.8	–	$FAPbI_3$	MPP, AM1.5G, 45 °C	[78]
1.53	19.8	16.0	12.9	3.5	14.7	$FAMAPbI_3$	MPP, AM1.5G, N_2, 45 °C	[4]
1.53	22.9	23.1	23.4	4.6	23.3	$Cs_{0.05}FA_{0.95}PbI_3$	MPP, AM1.5G, N_2, 40 °C	[4]
1.53	23.8	23.1	23.3	4.7	23.2	$Cs_{0.05}$ $FA_{0.9}MA_{0.05}PbI_3$	MPP, AM1.5G	[4]
1.53	23.8	23.2	22.6	4.7	22.8	$Cs_{0.05}FA_{0.9}MA_{0.05}PbI_3$	MPP, AM1.5G, air, 30 °C	[4]
1.53	23.4	20.0	–	4.2	–	$Cs_{0.05}FA_{0.9}MA_{0.05}PbI_3$	MPP, AM1.5G, air, 65 °C	[4]
1.53	23.5	20.9	–	4.3	–	α-$FAPbI_3$	MPP, w-LED, N_2, 35 °C	[3]
1.53	23.1	22.7	20.7	4.6	22.0	$FA_{0.97}MA_{0.03}PbBr_{0.09}I_{2.91}$	MPP, AM1.5G, N_2, 40 °C	[3]
1.54	24.8	24.1	23.0	4.9	23.6	$Cs_{0.05}FA_{0.931}MA_{0.019}PbI_{2.94}Br_{0.06}$	MPP, AM1.5G, N_2, 65 °C	[83]
1.54	24.3	24.6	24.5	5.0	24.5	$Cs_{0.17}FA_{0.83}PbI_3$	MPP, AM1.5G, N_2	[60]
1.54	20.7	20.2	18.1	4.1	19.4	$Cs_{0.05}FA_{0.9}$ $MA_{0.05}PbI_3$	MPP, AM1.5G, 50% RH, 85 °C, encapsulation	[197]
1.54	23.0	20.9	19.4	4.3	20.4	$FAPbI_3$/FGCs	MPP, AM1.5G, N_2, 60 °C	[3]
1.55	25.5	24.2	22.2	4.9	23.7	$FA_{0.97}MA_{0.03}PbBr_{0.09}I_{2.91}$	MPP, AM1.5G, 65 °C, encapsulation	[87]
1.55	25.0	23.8	–	4.8	–	$Cs_{0.1}FA_{0.9}PbI_3$	MPP, w-LED, 30 °C, encapsulation	[90]
1.55	23.4	23.4	22.9	4.7	23.3	$Cs_{0.05}FA_{0.931}MA_{0.019}PbBr_{0.06}I_{2.94}$	w-LED	[4]
1.55	22.0	21.6	20.6	4.4	21.2	$FAPbI_3$	MPP, AM1.5G, air	[4]
1.55	22.9	20.8	–	4.3	–	$FAPbI_3$	MPP, AM1.5G, N_2	[4]

(*Continued*)

Table 23. (Continued)

E_g [eV]	0 h PCE [%]	200 h PCE [%]	1000 h PCE [%]	E_{200h} [Wh cm^{-2}]	E_{1000h} [Wh cm^{-2}]	Absorber	Comments	Refs.
1.56	24.3	23.0	–	4.7	–	$Cs_{0.01}FA_{0.9603}MA_{0.0297}PbBr_{0.09}I_{2.91}$	MPP, w-LED, 40 °C, encapsulation	[96]
1.56	22.0	22.9	–	4.5	–	$FAPbI_3$	MPP, AM1.5G, air, encapsulation	[4]
1.56	21.1	20.9	–	4.2	–	$Cs_{0.05}FA_{0.9025}MA_{0.0475}PbBr_{0.15}I_{2.85}$	MPP, AM1.5G, air, 30–40% RH, 45 °C	[4]
1.57	21.8	22.0	21.8	4.2	22.0	$Cs_{0.05}FA_{0.874}MA_{0.076}PbBr_{0.24}I_{2.76}$	MPP, AM1.5G, N_2, 40 °C, UV-f	[3]
1.57	20.6	20.2	20.2	4.1	20.1	$Cs_{1-x}FA_xPbI_3$	MPP, w-LED, Ar, 55–60 °C	[3]
1.57	19.8	20.6	17.7	4.1	19.1	$FA_{0.95}MA_{0.05}PbBr_{0.15}I_{2.85}$	MPP, w-LED, air, 55 °C	[3]
1.58	23.1	22.9	–	4.6	–	$Cs_{0.05}FA_{0.9}MA_{0.05}Pb\ Br_{0.26}I_{2.74}$	MPP, N_2	[3]
1.58	23.6	20.2	–	4.4	–	$FA_{0.92}MA_{0.08}PbBr_{0.24}I_{2.76}$	MPP, AM1.5G, air, 50% RH	[3]
1.58	19.2	19.3	18.4	3.9	19.0	$Cs_{0.05}FA_{0.7885}MA_{0.1615}PbBr_{0.3}I_{2.7}$	OC, AM1.5G, encapsulation, 70–75 °C	[2]
1.59	17.1	11.6	9.5	2.8	11.1	$Gua_{0.15}MA_{0.85}PbI_3$	MPP, AM1.5G, Ar, 60 °C	[2]
1.60	22.0	22.2	20.2	4.4	21.4	$Cs_{0.05}FA_{0.874}MA_{0.076}PbBr_{0.18}I_{2.76}$	AM1.5G, encapsulation, 55 °C	[4]
1.60	21.8	21.4	19.8	4.3	20.9	$CsMAFAPbI_3$:PPP	MPP, encapsulation, air, AM1.5G, 75 °C	[2]
1.60	21.3	21.1	21.3	4.2	21.2	$CsFAMAPbI_3$:PPP	MPP, encapsulation, air, AM1.5G, 45 °C	[2]
1.60	19.6	19.6	18.8	3.9	19.4	$Cs_{0.05}FA_{0.81}MA_{0.14}PbBr_{0.45}I_{2.55}$	MPP-R_L, AM1.5G, encapsulation, 50–70% RH, 65 °C	[2]
1.61	18.1	11.9	13.6	2.6	13.0	$Gua_{0.25}MA_{0.75}PbI_3$	MPP, AM1.5G, Ar, 60 °C	[2]
1.62	21.1	19.9	18.0	4.0	19.1	$Cs_{0.04}FA_{0.8064}MA_{0.1536}PbBr_{0.48}I_{2.52}$	MPP, AM1.5G, N_2, 40 °C	[2]
1.63	20.0	16.8	11.8 [a]	3.5	15.1	$Cs_{0.05}FA_{0.79}MA_{0.16}PbBr_{0.51}I_{2.49}$	MPP, AM1.5G, N_2, 25 °C	[2]
1.63	21.0	19.7	19.4 [a]	3.9	19.6	$Cs_{0.05}FA_{0.81}MA_{0.14}PbBr_{0.45}I_{2.55}$/FGCs	MPP, AM1.5G, N_2, 60 °C	[2]
1.64	20.1	17.8	–	3.7	–	$Cs_{0.1}\ FA_{0.747}MA_{0.153}PbBr_{0.51}I_{2.49}$	MPP, w-LED, N_2, 25 °C	[2]
1.64[b]	19.7	17.2	–	3.5	–	$Cs_{0.5}FA_{0.7885}MA_{0.1615}PbBr_{0.51}I_{2.49}$	MPP, w-LED, N_2, 20 °C	[2]
1.66	13.0	14.7	13.0	2.8	14.1	$Cs_{0.17}FA_{0.83}PbBr_{0.51}I_{2.49}$	MPP, AM1.5G, 40% RH, 35 °C	[2]
1.69	6.8	6.7	–	1.3	–	$CsGe_{0.5}Sn_{0.5}I_3$	MPP†, AM1.5G, N_2, 45 °C	[2]
1.70	20.1	18.8	–	3.9	–	$CsPbI_3$	MPP, AM1.5G, air, 30% RH	[4]
1.74	12.9	13.4	–	2.7	–	$CsPbI_3$	OC, AM1.5G, N_2, 25 °C, UV-f	[2]
1.78	16.8	17.1	17.1	3.4	17.1	$CsPbBr_xI_{3-x}$	MPP, AM1.5G, air 30–40% RH, 35 °C	[4]
1.79	19.0	18.9	–	3.8	–	$Cs_{0.2}FA_{0.8}PbBr_{1.2}I_{1.8}$	MPP, AM1.5G, encapsulation	[4]

[a] Extrapolated value; [b] E_g was taken from photoluminescence spectrum; abbreviations: MPP, maximum power point (tracking during the test); OC, open-circuit (a condition during the test); UV-f, ultraviolet light filter; w-LED, white-light spectrum light-emitting diode source; RH, relative humidity; MPP-RL, cell is connected to the load resistance that matches the initial MPP.

Table 24. Organic solar cells with the highest operational stability test energy yield for 200 and 1000 h under simulated 1 sun illumination as a function of the device photovoltaic bandgap energy (from the *EQE* spectrum).

E_g [eV]	0 h PCE [%]	200 h PCE [%]	1000 h PCE [%]	E_{200h} [Wh cm^{-2}]	E_{1000h} [Wh cm^{-2}]	Active material	Comments	Refs.
1.40	18.8	16.4	14.6	3.4	15.6	PM6:BTP-eC9	MPP, w-LED, air	[4]
1.43	17.7	16.1	14.7	3.3	7.9	PM6:PY-1S1Se:PY-2Cl	MPP, AM1.5G	[4]
1.56	7.8	7.2	6.8	1.5	7.0	PBDB-T:ITIC-2F	OC, w-LED, N_2, 40 °C, UV-f	[2]

(*Continued*)

Table 24. (Continued)

E_g [eV]	0 h PCE [%]	200 h PCE [%]	1000 h PCE [%]	E_{200h} [Wh cm^{-2}]	E_{1000h} [Wh cm^{-2}]	Active material	Comments	Refs.
1.57	5.0	5.0	4.7	1.0	4.8	P3HT:o-IDTBR	OC, AM1.5G, N_2, UV-f	[2]
1.61	5.1	4.9	4.9	1.1	4.9	Dyad 4	OC, w-LED, N_2, 30 °C	[2]
1.66	8.0	7.4	7.0	1.5	7.3	PBDB-T:ITIC-Th	OC, w-LED, N_2, 40 °C, UV-f	[2]
1.70	8.7	8.1	–	1.6	–	PBDB-T:IDTBR	OC, AM1.5G, N_2, 35–40 °C	[2]
1.84	5.9	5.6	5.4	1.1	5.6	PBDB-T:PCBM	OC, w-LED, N_2, 40 °C, UV-f	[2]
1.94	3.7	3.7	3.7	0.7	3.7	P3HT-PCBM	OC, AM1.5G, air	[2]

Abbreviations: MPP, maximum power point (tracking during the test); OC, open-circuit (condition during test); UV-f, ultraviolet light filter; w-LED, white-light spectrum light-emitting diode source.

Table 25. Dye-sensitized solar cells with the highest operational stability test energy yield for 200 and 1000 h under simulated 1 sun illumination as a function of the device bandgap energy (from the *EQE* spectrum).

E_g [eV]	0 h PCE [%]	200 h PCE [%]	1000 h PCE [%]	E_{200h} [Wh cm^{-2}]	E_{1000h} [Wh cm^{-2}]	Sensitizing dye	Comments	Refs.
1.59	9.0	9.0	8.2	1.8	8.7	TF-tBu_C3F7	OC, AM1.5G, 65 °C	[2]
1.65	11.2	11.0	9.7	2.2	10.4	SGT-021/HC-A6+ThCA	MPP, AM1.5G, 25 °C, 50% RH	[61]
1.75	6.5	6.7	6.3	1.4	6.6	N719	OC, AM1.5G, 35 °C, UV-f	[2]
1.77	6.3	5.8	4.8	1.3	5.5	Z907	OC, w-LED, 20 °C	[2]
1.78	9.3	9.9	7.9	1.9	9.2	N719	OC, AM1.5G, 50 °C	[2]
1.83	8.4	8.3	–	1.7	–	MK2	OC, w-LED	[2]
1.85	8.0	8.3	8.3	1.4	8.1	N719	OC, AM1.5G	[2]
2.07	5.8	6.5	5.9	1.3	6.2	D35	OC, AM1.5G, 60 °C	[2]

Abbreviations: OC, open-circuit (a condition during the test); UV-f, ultraviolet light filter; w-LED, white-light spectrum light-emitting diode source.

Table 26. Multijunction solar cells with the highest stability test energy yield for 200 and 1000 h under simulated/equivalent 1 sun illumination as a function of the device photovoltaic bandgap energies (from the *EQE* spectra).

Bottom E_g [eV]	Top E_g [eV]	0 h PCE [%]	200 h PCE [%]	1000 h PCE [%]	E_{200h} [Wh cm^{-2}]	E_{1000h} [Wh cm^{-2}]	Bottom absorber material	Top absorber material	Comments	Refs.
							Perovskite/perovskite			
1.25	1.80	27.4	28.4	–	5.6	–	$FA_{0.7}MA_{0.3}Pb_{0.5}Sn_{0.5}I_3$	$Cs_{0.2}FA_{0.8}PbBr_{1.14}I_{1.86}$	MPP, AM1.5G, air 30–50% RH, 35 °C	[4]
1.25	1.80	25.6	26.4	17.8	5.2	23.5	$Cs_{0.2}FA_{0.8}PbBr_{01.14}I_{1.86}$	$FA_{0.7}MA_{0.3}Pb_{0.5}Sn_{0.5}I_3$	MPP, AM1.5G, air 30–50% RH, 35 °C	[3]
1.26	1.80	24.1	23.5	23.2	4.8	23.7	$FA_{0.7}MA_{0.3}Pb_{0.5}Sn_{0.5}I_3$	$CsPbBr_xI_{3-x}$	MPP, AM1.5G, air 30–50% RH, 35 °C	[4]
1.26	1.80	26.9	24.6	–	5.1	–	$Cs_{0.1}FA_{0.6}MA_{0.3}Pb_{0.5}Sn_{0.5}I_3$	$Cs_{0.2}FA_{0.8}Pb\ Br_{1.2}I_{1.8}$	MPP, AM1.5G, air 25–35 °C	[4]
1.26	1.82	24.4	24.3	19.3[a)]	4.9	21.8[a)]	FSA: $FA_{0.7}MA_{0.3}Pb_{0.5}Sn_{0.5}I_3$	$FA_{0.8}Cs_{0.2}PbBr_{1.2}I_{1.8}$	MPP, encapsulation, air, 30–50% RH, AM1.5G, no UV-f, 54–60 °C	[2]
1.26	1.82	21.2	20.6	19.8	4.2	20.7	$Cs_{0.05}\ FA_{0.5}MA_{0.45}Pb_{0.5}Sn_{0.5}I_3$	$Cs_{0.4}FA_{0.6}Pb\ Br_{1.05}I_{1.95}$	MPP-R_L, encapsulation, air, AM1.5G, room T	[2]
1.27	1.72	23.1	22.2	20.4	4.7	21.4	$FA_{0.6}MA_{0.4}Pb_{0.4}Sn_{0.6}I_3$	$Cs_{0.05}FA_{0.8}MA_{0.15}PbBr_{0.45}I_{2.55}$	MPP, AM1.5G	[2]
							GaAs/perovskite			
1.42	1.85	24.1	23.9	22.1[a)]	4.76	23.3[a)]	GaAs	$FA_{0.80}MA_{0.04}Cs_{0.16}PbBr_{1.5}I_{1.5}$	MPP, air 20–25% RH, AM1.5G, room T, UV-f	[2]
							CIGS/perovskite			
1.10	1.65	22.0	19.9	18.4[a)]	4.1	19.4[a)]	CIGS	$Cs_{0.09}FA_{0.77}MA_{0.14}PbBr_{0.42}I_{2.58}$	MPP, air 20% RH, 30 °C	[2]
							Si/perovskite			
1.13	1.68	24.0	22.8	21.5	4.6	22.4	Si	$CsFAPb(Br,I)_3$:$MA(Cl_{0.5}SCN_{0.5})$	MPP, w-LED, air, 40% RH, 25 °C	[4]
1.17	1.63	5.4	5.2	–	1.1	–	Si	$FA_{0.83}MA_{0.17}PbBr_{0.51}I_{2.49}$	MPP, AM1.5G, 60 ± 20% RH	[4]

[a)] Extrapolated value; abbreviations: MPP, maximum power point (tracking during the test); UV-f, ultraviolet light filter; RH, relative humidity; MPP-R_L, cell is connected to the load resistance that matches the initial MPP.

Supporting Information

Supporting Information is available from the Wiley Online Library or from the author.

Acknowledgements

O.A. acknowledges the Juan de la Cierva Fellowship grant FJC2021-046887-I funded by MICIU/AEI/10.13039/501100011033 and by the European Union NextGenerationEU/PRTR. C.J.B. gratefully acknowledges financial support through the "Aufbruch Bayern" initiative of the state of Bavaria (EnCN and SFF), the Bavarian Initiative "Solar Technologies go Hybrid" (SolTech), the DFG – SFB953 (project no. 182849149), and DFG – INST 90/917-1 FUGG. R. R. L. gratefully acknowledges support from the National Science Foundation under grant CBET-1702591. C. S. gratefully acknowledges financial support from the Vector Foundation. L.A.C. acknowledges the European Union's Framework Programme for Research and Innovation Horizon Europe (2021-2027) under the Marie Sklodowska-Curie Grant Agreement No. 101068387 "EFESO". Part of this work has been supported by the Helmholtz Association in the framework of the the Solar Technology Acceleration Platform (Solar TAP). The authors also acknowledge Simon Stier for his work as a software developer of the emerging-pv.org website and database, and all the contributions to the database updating; particularly the effort by Wei Yu. The authors also thank Dr. Md Arafat Mahmud, Dr. Guoliang Wang, and Dr. Lulu Sun for their further data contributions.

Open access funding enabled and organized by Projekt DEAL.

Conflict of Interest

Richard R. Lunt is a co-founder, director, and a part-owner of Ubiquitous Energy, Inc., a company working to commercialize transparent photovoltaic technologies. All other authors declare no competing financial interest.

Keywords

bandgap energy, flexible photovoltaics, multijunction solar cells, photovoltaic device operational stability, power conversion efficiency, transparent and semitransparent solar cells

Received: September 23, 2024
Revised: November 6, 2024
Published online:

[1] O. Almora, D. Baran, G. C. Bazan, C. Berger, C. I. Cabrera, K. R. Catchpole, S. Erten-Ela, F. Guo, J. Hauch, A. W. Y. Ho-Baillie, T. J. Jacobsson, R. A. J. Janssen, T. Kirchartz, Y. Li, M. A. Loi, R. R. Lunt, X. Mathew, M. D. McGehee, J. Min, D. B. Mitzi, M. K. Nazeeruddin, J. Nelson, A. F. Nogueira, U. W. Paetzold, N.-G. Park, B. P. Rand, U. Rau, H. J. Snaith, E. Unger, L. Vaillant-Roca, et al., *Adv. Energy Mater.* **2021**, *11*, 2002774.

[2] O. Almora, D. Baran, G. C. Bazan, C. Berger, C. I. Cabrera, K. R. Catchpole, S. Erten-Ela, F. Guo, J. Hauch, A. W. Y. Ho-Baillie, T. J. Jacobsson, R. A. J. Janssen, T. Kirchartz, N. Kopidakis, Y. Li, M. A. Loi, R. R. Lunt, X. Mathew, M. D. McGehee, J. Min, D. B. Mitzi, M. K. Nazeeruddin, J. Nelson, A. F. Nogueira, U. W. Paetzold, N.-G. Park, B. P. Rand, U. Rau, H. J. Snaith, E. Unger, et al., *Adv. Energy Mater.* **2021**, *11*, 2102526.

[3] O. Almora, D. Baran, G. C. Bazan, C. I. Cabrera, S. Erten-Ela, K. Forberich, F. Guo, J. Hauch, A. W. Y. Ho-Baillie, T. J. Jacobsson, R. A. J. Janssen, T. Kirchartz, N. Kopidakis, M. A. Loi, R. R. Lunt, X. Mathew, M. D. McGehee, J. Min, D. B. Mitzi, M. K. Nazeeruddin, J. Nelson, A. F. Nogueira, U. W. Paetzold, B. P. Rand, U. Rau, H. J. Snaith, E. Unger, L. Vaillant-Roca, C. Yang, H.-L. Yip, et al., *Adv. Energy Mater.* **2022**, *13*, 2203313.

[4] O. Almora, C. I. Cabrera, S. Erten-Ela, K. Forberich, K. Fukuda, F. Guo, J. Hauch, A. W. Y. Ho-Baillie, T. J. Jacobsson, R. A. J. Janssen, T. Kirchartz, M. A. Loi, X. Mathew, D. B. Mitzi, M. K. Nazeeruddin, U. W. Paetzold, B. P. Rand, U. Rau, T. Someya, E. Unger, L. Vaillant-Roca, C. J. Brabec, *Adv. Energy Mater.* **2024**, *14*, 2303173.

[5] Emerging PV, https://emerging-pv.org (accessed: August 2024).

[6] M. A. Green, E. D. Dunlop, M. Yoshita, N. Kopidakis, K. Bothe, G. Siefer, D. Hinken, M. Rauer, J. Hohl-Ebinger, X. Hao, *Prog. Photovoltaics* **2024**, *32*, 425.

[7] W. Shockley, H. J. Queisser, *J. Appl. Phys.* **1961**, *32*, 510.

[8] A. S. Brown, M. A. Green, presented at *Conf. Record of the Twenty-Ninth IEEE Photovoltaic Specialists Conf.*, New Orleans, LA, USA, May **2002**.

[9] A. S. Brown, M. A. Green, *Phys. Educ.* **2002**, *14*, 96.

[10] M. Saliba, E. Unger, L. Etgar, J. Luo, T. J. Jacobsson, *Nat. Commun.* **2023**, *14*, 5445.

[11] K. Fukuda, L. Sun, B. Du, M. Takakuwa, J. Wang, T. Someya, L. F. Marsal, Y. Chen, Y. Zhou, H. Chen, S. R. Silva, C. Yang, L. A. Castriotta, W. Li, T. Österberg, A. Ho-Baillie, T. Brown, D. Baran, N. P. Padture, K. Forberich, C. Brabec, O. Almora, *Nat. Energy* **2024**, *9*, 1335.

[12] O. Almora, C. I. Cabrera, J. Garcia-Cerrillo, T. Kirchartz, U. Rau, C. J. Brabec, *Adv. Energy Mater.* **2021**, *11*, 2100022.

[13] L. Krückemeier, U. Rau, M. Stolterfoht, T. Kirchartz, *Adv. Energy Mater.* **2020**, *10*, 1902573.

[14] A. S. Brown, M. A. Green, *Phys. E* **2002**, *14*, 96.

[15] J.-F. Guillemoles, T. Kirchartz, D. Cahen, U. Rau, *Nat. Photon.* **2019**, *13*, 501.

[16] C. Yang, D. Liu, M. Bates, M. C. Barr, R. R. Lunt, *Joule* **2019**, *3*, 1803.

[17] C. J. Traverse, R. Pandey, M. C. Barr, R. R. Lunt, *Nat. Energy* **2017**, *2*, 849.

[18] S. Rühle, *Sol. Energy* **2016**, *130*, 139.

[19] H. Chen, C. Liu, J. Xu, A. Maxwell, W. Zhou, Y. Yang, Q. Zhou, A. S. R. Bati, H. Wan, Z. Wang, L. Zeng, J. Wang, P. Serles, Y. Liu, S. Teale, Y. Liu, M. I. Saidaminov, M. Li, N. Rolston, S. Hoogland, T. Filleter, M. G. Kanatzidis, B. Chen, Z. Ning, E. H. Sargent, *Science* **2024**, *384*, 189.

[20] J. Faisst, E. Jiang, S. Bogati, L. Pap, B. Zimmermann, T. Kroyer, U. Würfel, M. List, *Sol. RRL* **2023**, *7*, 2300663.

[21] S. Guan, Y. Li, C. Xu, N. Yin, C. Xu, C. Wang, M. Wang, Y. Xu, Q. Chen, D. Wang, L. Zuo, H. Chen, *Adv. Mater.* **2024**, *36*, 2400342.

[22] Y. Jiang, S. Sun, R. Xu, F. Liu, X. Miao, G. Ran, K. Liu, Y. Yi, W. Zhang, X. Zhu, *Nat. Energy* **2024**, *9*, 975.

[23] Z. Chen, J. Ge, W. Song, X. Tong, H. Liu, X. Yu, J. Li, J. Shi, L. Xie, C. Han, Q. Liu, Z. Ge, *Adv. Mater.* **2024**, *36*, 2406690.

[24] L. Zhu, M. Zhang, G. Zhou, Z. Wang, W. Zhong, J. Zhuang, Z. Zhou, X. Gao, L. Kan, B. Hao, F. Han, R. Zeng, X. Xue, S. Xu, H. Jing, B. Xiao, H. Zhu, Y. Zhang, F. Liu, *Joule* **2024**, *8*, 3153.

[25] J. Song, Y. Gu, Z. Lin, J. Liu, X. Kang, X. Gong, P. Liu, Y. Yang, H. Jiang, J. Wang, S. Cao, Z. Zhu, H. Peng, *Adv. Mater.* **2024**, *36*, 2312590.

[26] J. Wang, J. Shi, K. Yin, F. Meng, S. Wang, L. Lou, J. Zhou, X. Xu, H. Wu, Y. Luo, D. Li, S. Chen, Q. Meng, *Nat. Commun.* **2024**, *15*, 4344.

[27] X. Li, H. Yu, X. Ma, Z. Liu, J. Huang, Y. Shen, M. Wang, *Chem. Eng. J.* **2024**, *495*, 153328.

[28] U. Rau, B. Blank, T. C. M. Müller, T. Kirchartz, *Phy. Rev. Appl.* **2017**, *7*, 044016.

[29] NREL's Best Research-Cell Efficiency Chart https://www.nrel.gov/pv/cell-efficiency.html (accessed: August 2024).

[30] J. Liu, Y. He, L. Ding, H. Zhang, Q. Li, L. Jia, J. Yu, T. W. Lau, M. Li, Y. Qin, X. Gu, F. Zhang, Q. Li, Y. Yang, S. Zhao, X. Wu, J. Liu, T. Liu, Y. Gao, Y. Wang, X. Dong, H. Chen, P. Li, T. Zhou, M. Yang, X. Ru, F. Peng, S. Yin, M. Qu, D. Zhao, et al., *Nature* **2024**, *5*, 1.
[31] J. Zhou, S. Fu, S. Zhou, L. Huang, C. Wang, H. Guan, D. Pu, H. Cui, C. Wang, T. Wang, W. Meng, G. Fang, W. Ke, *Nat. Commun.* **2024**, *15*, 2324.
[32] S. Liu, Y. Lu, C. Yu, J. Li, R. Luo, R. Guo, H. Liang, X. Jia, X. Guo, Y.-D. Wang, Q. Zhou, X. Wang, S. Yang, M. Sui, P. Müller-Buschbaum, Y. Hou, *Nature* **2024**, *628*, 306.
[33] Z. Zhang, W. Chen, X. Jiang, J. Cao, H. Yang, H. Chen, F. Yang, Y. Shen, H. Yang, Q. Cheng, X. Chen, X. Tang, S. Kang, X.-m. Ou, C. J. Brabec, Y. Li, Y. Li, *Nat. Energy* **2024**, *9*, 592.
[34] J. Wang, L. Zeng, D. Zhang, A. Maxwell, H. Chen, K. Datta, A. Caiazzo, W. H. M. Remmerswaal, N. R. M. Schipper, Z. Chen, K. Ho, A. Dasgupta, G. Kusch, R. Ollearo, L. Bellini, S. Hu, Z. Wang, C. Li, S. Teale, L. Grater, B. Chen, M. M. Wienk, R. A. Oliver, H. J. Snaith, R. A. J. Janssen, E. H. Sargent, *Nat. Energy* **2024**, *9*, 70.
[35] J. Zheng, C. Xue, G. Wang, M. A. Mahmud, Z. Sun, C. Liao, J. Yi, J. Qu, L. Yang, L. Wang, S. Bremner, J. M. Cairney, J. Zhang, A. W. Y. Ho-Baillie, *ACS Energy Lett.* **2024**, *9*, 1545.
[36] R. Nielsen, A. Crovetto, A. Assar, O. Hansen, I. Chorkendorff, P. C. K. Vesborg, *PRX Energy* **2024**, *3*, 013013.
[37] E. Ugur, A. A. Said, P. Dally, S. Zhang, C. E. Petoukhoff, D. Rosas-Villalva, S. Zhumagali, B. K. Yildirim, A. Razzaq, S. Sarwade, A. Yazmaciyan, D. Baran, F. Laquai, C. Deger, I. Yavuz, T. G. Allen, E. Aydin, S. De Wolf, *Science* **2024**, *385*, 533.
[38] Y. Li, X. Ru, M. Yang, Y. Zheng, S. Yin, C. Hong, F. Peng, M. Qu, C. Xue, J. Lu, L. Fang, C. Su, D. Chen, J. Xu, C. Yan, Z. Li, X. Xu, Z. Shao, *Nature* **2024**, *626*, 105.
[39] D.-H. Son, H. K. Park, D.-H. Kim, J.-K. Kang, S.-J. Sung, D.-K. Hwang, J. Lee, D.-H. Jeon, Y. Cho, W. Jo, T. Lee, J. Kim, S.-H. Nam, K.-J. Yang, *Carbon Energy* **2024**, *6*, e434.
[40] X. Liang, Y. Feng, W. Dang, H. Huang, X. Wang, Y. Guo, K. Shen, R. E. I. Schropp, Z. Li, Y. Mai, *ACS Energy Lett.* **2023**, *8*, 213.
[41] Z. Zhu, Z. Lin, Y. Gu, J. Song, X. Kang, H. Jiang, H. Peng, *Adv. Funct. Mater.* **2023**, *33*, 2306742.
[42] J. Zhang, H. Mao, K. Zhou, L. Zhang, D. Luo, P. Wang, L. Ye, Y. Chen, *Adv. Mater.* **2024**, *36*, 2309379.
[43] X. Tong, L. Xie, J. Li, Z. Pu, S. Du, M. Yang, Y. Gao, M. He, S. Wu, Y. Mai, Z. Ge, *Adv. Mater.* **2024**, *36*, 2407032.
[44] N. Ren, L. Tan, M. Li, J. Zhou, Y. Ye, B. Jiao, L. Ding, C. Yi, *iEnergy* **2024**, *3*, 39.
[45] Y. Wang, Y. Meng, C. Liu, R. Cao, B. Han, L. Xie, R. Tian, X. Lu, Z. Song, J. Li, S. Yang, C. Lu, Z. Ge, *Joule* **2024**, *8*, 1120.
[46] Y. Wu, G. Xu, Y. Shen, X. Wu, X. Tang, C. Han, Y. Chen, F. Yang, H. Chen, Y. Li, Y. Li, *Adv. Mater.* **2024**, *36*, 2403531.
[47] C. Gong, C. Wang, X. Meng, B. Fan, Z. Xing, S. Shi, T. Hu, Z. Huang, X. Hu, Y. Chen, *Adv. Mater.* **2024**, *36*, 2405572.
[48] B. Hailegnaw, S. Demchyshyn, C. Putz, L. E. Lehner, F. Mayr, D. Schiller, R. Pruckner, M. Cobet, D. Ziss, T. M. Krieger, A. Rastelli, N. S. Sariciftci, M. C. Scharber, M. Kaltenbrunner, *Nat. Energy* **2024**, *9*, 677.
[49] H. Liu, H. Han, J. Xu, X. Pan, K. Zhao, S. Liu, J. Yao, *Adv. Mater.* **2023**, *35*, 2300302.
[50] X. Wang, J. Zheng, Z. Ying, X. Li, M. Zhang, X. Guo, S. Su, J. Sun, X. Yang, J. Ye, *Sci. Bull.* **2024**, *69*, 1887.
[51] D. Di Girolamo, G. Vidon, J. Barichello, F. Di Giacomo, F. Jafarzadeh, B. Paci, A. Generosi, M. Kim, L. A. Castriotta, M. Frégnaux, J.-F. Guillemoles, F. Brunetti, P. Schulz, D. Ory, S. Cacovich, A. Di Carlo, F. Matteocci, *Adv. Energy Mater.* **2024**, *14*, 2400663.
[52] F. Jafarzadeh, L. A. Castriotta, M. Legrand, D. Ory, S. Cacovich, Z. Skafi, J. Barichello, F. De Rossi, F. Di Giacomo, A. Di Carlo, T. Brown, F. Brunetti, F. Matteocci, *ACS Appl. Mater. Interfaces* **2024**, *16*, 17607.
[53] W. Liu, S. Sun, S. Xu, H. Zhang, Y. Zheng, Z. Wei, X. Zhu, *Adv. Mater.* **2022**, *34*, 2200337.
[54] S. Sun, W. Zha, C. Tian, Z. Wei, Q. Luo, C.-Q. Ma, W. Liu, X. Zhu, *Adv. Mater.* **2023**, *35*, 2305092.
[55] J. Yu, X. Liu, J. Zhou, G. Li, *Adv. Funct. Mater.* **2024**, *34*, 2406070.
[56] X. Huang, X. Ren, Y. Cheng, Y. Zhang, Z. Sun, S. Yang, S. Kim, C. Yang, F. Wu, L. Chen, *Energy Environ. Sci.* **2024**, *17*, 2825.
[57] Y.-F. Zhang, W.-S. Chen, J.-D. Chen, H. Ren, H.-Y. Hou, S. Tian, H.-R. Ge, H.-H. Ling, J.-L. Zhang, H. Mao, J.-X. Tang, Y.-Q. Li, *Adv. Energy Mater.* **2024**, *14*, 2400970.
[58] Z. Liang, Y. Zhang, H. Xu, W. Chen, B. Liu, J. Zhang, H. Zhang, Z. Wang, D.-H. Kang, J. Zeng, X. Gao, Q. Wang, H. Hu, H. Zhou, X. Cai, X. Tian, P. Reiss, B. Xu, T. Kirchartz, Z. Xiao, S. Dai, N.-G. Park, J. Ye, X. Pan, *Nature* **2023**, *624*, 557.
[59] M. V. Khenkin, E. A. Katz, A. Abate, G. Bardizza, J. J. Berry, C. Brabec, F. Brunetti, V. Bulović, Q. Burlingame, A. Di Carlo, R. Cheacharoen, Y.-B. Cheng, A. Colsmann, S. Cros, K. Domanski, M. Dusza, C. J. Fell, S. R. Forrest, Y. Galagan, D. Di Girolamo, M. Grätzel, A. Hagfeldt, E. von Hauff, H. Hoppe, J. Kettle, H. Köbler, M. S. Leite, S. Liu, Y.-L. Loo, J. M. Luther, et al., *Nat. Energy* **2020**, *5*, 35.
[60] H. Xu, Z. Liang, J. Ye, Y. Zhang, Z. Wang, H. Zhang, C. Wan, G. Xu, J. Zeng, B. Xu, Z. Xiao, T. Kirchartz, X. Pan, *Energy Environ. Sci.* **2023**, *16*, 5792.
[61] H. Zhou, H. J. Lee, Masud, M. A, S. H. Kang, C. H. Kim, H. M. Kim, H. K. Kim, *ACS Appl. Mater. Interfaces* **2023**, *15*, 43835.
[62] Q. Sun, Z. Zhang, H. Yu, J. Huang, X. Li, L. Dai, Q. Wang, Y. Shen, M. Wang, *Energy Environ. Sci.* **2024**, *17*, 2512.
[63] W. Zhang, L. Huang, H. Guan, W. Zheng, Z. Li, H. Cui, S. Zhou, J. Liang, G. Li, T. Wang, P. Qin, W. Ke, G. Fang, *Energy Environ. Sci.* **2023**, *16*, 5852.
[64] Y. Zhou, T. Guo, J. Jin, Z. Zhu, Y. Li, S. Wang, S. Zhou, Q. Lin, J. Li, W. Ke, G. Fang, X. Zhang, Q. Tai, *Energy Environ. Sci.* **2024**, *17*, 2845.
[65] J. Chen, J. Luo, E. Hou, P. Song, Y. Li, C. Sun, W. Feng, S. Cheng, H. Zhang, L. Xie, C. Tian, Z. Wei, *Nat. Photon.* **2024**, *18*, 464.
[66] X. Zhou, W. Peng, Z. Liu, Y. Zhang, L. Zhang, M. Zhang, C. Liu, L. Yan, X. Wang, B. Xu, *Energy Environ. Sci.* **2024**, *17*, 2837.
[67] W. Zhang, H. Liu, Y. Qu, J. Cui, W. Zhang, T. Shi, H.-L. Wang, *Adv. Mater.* **2024**, *36*, 2309193.
[68] Y. Shi, Z. Zhu, D. Miao, Y. Ding, Q. Mi, *ACS Energy Lett.* **2024**, *9*, 1895.
[69] B.-B. Yu, Z. Chen, Y. Zhu, Y. Wang, B. Han, G. Chen, X. Zhang, Z. Du, Z. He, *Adv. Mater.* **2021**, *33*, 2102055.
[70] S. Wang, C. Wu, T. Wu, H. Yao, Y. Hua, F. Hao, *ACS Energy Lett.* **2024**, *9*, 1168.
[71] B. Li, C. Zhang, D. Gao, X. Sun, S. Zhang, Z. Li, J. Gong, S. Li, Z. Zhu, *Adv. Mater.* **2024**, *36*, 2309768.
[72] F. Yang, R. Zhu, Z. Zhang, Z. Su, W. Zuo, B. He, M. H. Aldamasy, Y. Jia, G. Li, X. Gao, Z. Li, M. Saliba, A. Abate, M. Li, *Adv. Mater.* **2024**, *36*, 2308655.
[73] X. Li, W. Wang, K. Wei, J. Deng, P. Huang, P. Dong, X. Cai, L. Yang, W. Tang, J. Zhang, *Adv. Mater.* **2024**, *36*, 2308969.
[74] R. Azmi, D. S. Utomo, B. Vishal, S. Zhumagali, P. Dally, A. M. Risqi, A. Prasetio, E. Ugur, F. Cao, I. F. Imran, A. A. Said, A. R. Pininti, A. S. Subbiah, E. Aydin, C. Xiao, S. I. Seok, S. De Wolf, *Nature* **2024**, *628*, 93.
[75] Y. Meng, Y. Wang, C. Liu, P. Yan, K. Sun, Y. Wang, R. Tian, R. Cao, J. Zhu, H. Do, J. Lu, Z. Ge, *Adv. Mater.* **2024**, *36*, 2309208.
[76] J. W. Song, Y. S. Shin, M. Kim, J. Lee, D. Lee, J. Seo, Y. Lee, W. Lee, H.-B. Kim, S.-I. Mo, J.-H. An, J.-E. Hong, J. Y. Kim, I. Jeon, Y. Jo, D. S. Kim, *Adv. Energy Mater.* **2024**, *14*, 2401753.
[77] C. Gong, X. Chen, J. Zeng, H. Wang, H. Li, Q. Qian, C. Zhang, Q. Zhuang, X. Yu, S. Gong, H. Yang, B. Xu, J. Chen, Z. Zang, *Adv. Mater.* **2024**, *36*, 2307422.

[78] L. He, Y. Zhang, B. Zhang, T. Li, Y. Cai, M. Ren, J. Zhang, P. Wang, Y. Yuan, *Energy Environ. Sci.* **2024**, *17*, 3937.
[79] X. Zhu, W. Xiong, C. Hu, K. Mo, M. Yang, Y. Li, R. Li, C. Shen, Y. Liu, X. Liu, S. Wang, Q. Lin, S. Yuan, Z. Liu, Z. Wang, *Adv. Mater.* **2024**, *36*, 2309487.
[80] C. Liu, Y. Yang, H. Chen, J. Xu, A. Liu, A. S. R. Bati, H. Zhu, L. Grater, S. S. Hadke, C. Huang, V. K. Sangwan, T. Cai, D. Shin, L. X. Chen, M. C. Hersam, C. A. Mirkin, B. Chen, M. G. Kanatzidis, E. H. Sargent, *Science* **2023**, *382*, 810.
[81] S. Du, H. Huang, Z. Lan, P. Cui, L. Li, M. Wang, S. Qu, L. Yan, C. Sun, Y. Yang, X. Wang, M. Li, *Nat. Commun.* **2024**, *15*, 5223.
[82] J. Lee, Y. S. Shin, E. Oleiki, J. Seo, J. Roe, D. Lee, Y. Lee, T. Song, H. Jang, J. W. Song, W. Lee, G. Lee, J. Y. Kim, D. S. Kim, *Energy Environ. Sci.* **2024**, *17*, 6003.
[83] A. Sun, C. Tian, R. Zhuang, C. Chen, Y. Zheng, X. Wu, C. Tang, Y. Liu, Z. Li, B. Ouyang, J. Du, Z. Li, J. Cai, J. Chen, X. Wu, Y. Hua, C.-C. Chen, *Adv. Energy Mater.* **2024**, *14*, 2303941.
[84] R. Tian, C. Liu, Y. Meng, Y. Wang, R. Cao, B. Tang, D. Walsh, H. Do, H. Wu, K. Wang, K. Sun, S. Yang, J. Zhu, X. Li, Z. Ge, *Adv. Mater.* **2024**, *36*, 2309998.
[85] X. Wang, H. Huang, M. Wang, Z. Lan, P. Cui, S. Du, Y. Yang, L. Yan, Q. Zhang, S. Qu, M. Li, *Adv. Mater.* **2024**, *36*, 2310710.
[86] Y. Zheng, Y. Li, R. Zhuang, X. Wu, C. Tian, A. Sun, C. Chen, Y. Guo, Y. Hua, K. Meng, K. Wu, C.-C. Chen, *Energy Environ. Sci.* **2024**, *17*, 1153.
[87] K. M. Yeom, C. Cho, E. H. Jung, G. Kim, C. S. Moon, S. Y. Park, S. H. Kim, M. Y. Woo, M. N. T. Khayyat, W. Lee, N. J. Jeon, M. Anaya, S. D. Stranks, R. H. Friend, N. C. Greenham, J. H. Noh, *Nat. Commun.* **2024**, *15*, 4547.
[88] B. Li, Q. Liu, J. Gong, S. Li, C. Zhang, D. Gao, Z. Chen, Z. Li, X. Wu, D. Zhao, Z. Yu, X. Li, Y. Wang, H. Lu, X. C. Zeng, Z. Zhu, *Nat. Commun.* **2024**, *15*, 2753.
[89] K. Zhao, Q. Liu, L. Yao, C. Değer, J. Shen, X. Zhang, P. Shi, Y. Tian, Y. Luo, J. Xu, J. Zhou, D. Jin, S. Wang, W. Fan, S. Zhang, S. Chu, X. Wang, L. Tian, R. Liu, L. Zhang, I. Yavuz, H.-f. Wang, D. Yang, R. Wang, J. Xue, *Nature* **2024**, *632*, 301.
[90] J. Li, H. Liang, C. Xiao, X. Jia, R. Guo, J. Chen, X. Guo, R. Luo, X. Wang, M. Li, M. Rossier, A. Hauser, F. Linardi, E. Alvianto, S. Liu, J. Feng, Y. Hou, *Nat. Energy* **2024**, *9*, 308.
[91] Z. Shen, Q. Han, X. Luo, Y. Shen, Y. Wang, Y. Yuan, Y. Zhang, Y. Yang, L. Han, *Nat. Photon.* **2024**, *18*, 450.
[92] L. Yuan, S. Zou, K. Zhang, P. Huang, Y. Dong, J. Wang, K. Fan, M. Y. Lam, X. Wu, W. Cheng, R. Tang, W. Chen, W. Liu, K. S. Wong, K. Yan, *Adv. Mater.* **2024**, *36*, 2409261.
[93] M. Chen, T. Niu, L. Chao, X. Duan, J. Wang, T. Pan, Y. Li, J. Zhang, C. Wang, B. Ren, L. Guo, M. Hatamvand, J. Zhang, Q. Guo, Y. Xia, X. Gao, Y. Chen, *Energy Environ. Sci.* **2024**, *17*, 3375.
[94] C. Huang, S. Tan, B. Yu, Y. Li, J. Shi, H. Wu, Y. Luo, D. Li, Q. Meng, *Joule* **2024**, *8*, 2539.
[95] Z. Wu, H. Cai, T. Wu, J. Xu, Z. Wang, H. Du, J. Zhao, F. Huang, Y.-B. Cheng, J. Zhong, *Energy Environ. Sci.* **2024**, *17*, 4670.
[96] H. Meng, K. Mao, F. Cai, K. Zhang, S. Yuan, T. Li, F. Cao, Z. Su, Z. Zhu, X. Feng, W. Peng, J. Xu, Y. Gao, W. Chen, C. Xiao, X. Wu, M. D. McGehee, J. Xu, *Nat. Energy* **2024**, *9*, 536.
[97] S. Xiong, F. Tian, F. Wang, A. Cao, Z. Chen, S. Jiang, D. Li, B. Xu, H. Wu, Y. Zhang, H. Qiao, Z. Ma, J. Tang, H. Zhu, Y. Yao, X. Liu, L. Zhang, Z. Sun, M. Fahlman, J. Chu, F. Gao, Q. Bao, *Nat. Commun.* **2024**, *15*, 5607.
[98] D. Zhang, B. Li, P. Hang, J. Xie, Y. Yao, C. Kan, X. Yu, Y. Zhang, D. Yang, *Energy Environ. Sci.* **2024**, *17*, 3848.
[99] P. Zhu, D. Wang, Y. Zhang, Z. Liang, J. Li, J. Zeng, J. Zhang, Y. Xu, S. Wu, Z. Liu, X. Zhou, B. Hu, F. He, L. Zhang, X. Pan, X. Wang, N.-G. Park, B. Xu, *Science* **2024**, *383*, 524.
[100] C. Li, K. Zhang, S. Maiti, Z. Peng, J. Tian, H. Park, J. Byun, Z. Xie, L. Dong, S. Qiu, A. J. Bornschlegl, C. Liu, J. Zhang, A. Osvet, T. Heumueller, S. H. Christiansen, M. Halik, T. Unruh, N. Li, L. Lüer, C. J. Brabec, *ACS Energy Lett.* **2024**, *9*, 779.
[101] H. Zhu, B. Shao, J. Yin, Z. Shen, L. Wang, R.-W. Huang, B. Chen, N. Wehbe, T. Ahmad, M. Abulikemu, A. Jamal, I. Gereige, M. Freitag, O. F. Mohammed, E. H. Sargent, O. M. Bakr, *Adv. Mater.* **2024**, *36*, 2306466.
[102] R. Wang, J. Zhu, J. You, H. Huang, Y. Yang, R. Chen, J. Wang, Y. Xu, Z. Gao, J. Chen, B. Xu, B. Wang, C. Chen, D. Zhao, W.-H. Zhang, *Energy Environ. Sci.* **2024**, *17*, 2662.
[103] G. Wang, J. Zheng, W. Duan, J. Yang, M. A. Mahmud, Q. Lian, S. Tang, C. Liao, J. Bing, J. Yi, T. L. Leung, X. Cui, H. Chen, F. Jiang, Y. Huang, A. Lambertz, M. Jankovec, M. Topič, S. Bremner, Y.-Z. Zhang, C. Cheng, K. Ding, A. Ho-Baillie, *Joule* **2023**, *7*, 2583.
[104] G. Su, R. Yu, Y. Dong, Z. He, Y. Zhang, R. Wang, Q. Dang, S. Sha, Q. Lv, Z. Xu, Z. Liu, M. Li, Z. a. Tan, *Adv. Energy Mater.* **2024**, *14*, 2303344.
[105] Y. An, N. Zhang, Z. Zeng, Y. Cai, W. Jiang, F. Qi, L. Ke, F. R. Lin, S.-W. Tsang, T. Shi, A. K. Y. Jen, H.-L. Yip, *Adv. Mater.* **2024**, *36*, 2306568.
[106] S. Zai, R. Han, W. Zhao, C. Ma, W. Huang, S. Liu, *Adv. Energy Mater.* **2024**, *14*, 2303264.
[107] B. Sharma, R. Garai, M. A. Afroz, T. Sharma, S. Choudhary, R. K. Singh, S. Satapathi, *Adv. Energy Mater.* **2024**, *14*, 2402473.
[108] H. Cui, L. Huang, S. Zhou, C. Wang, X. Hu, H. Guan, S. Wang, W. Shao, D. Pu, K. Dong, J. Zhou, P. Jia, W. Wang, C. Tao, W. Ke, G. Fang, *Energy Environ. Sci.* **2023**, *16*, 5992.
[109] J. Wen, Y. Zhao, P. Wu, Y. Liu, X. Zheng, R. Lin, S. Wan, K. Li, H. Luo, Y. Tian, L. Li, H. Tan, *Nat. Commun.* **2023**, *14*, 7118.
[110] Z. Yi, W. Wang, R. He, J. Zhu, W. Jiao, Y. Luo, Y. Xu, Y. Wang, Z. Zeng, K. Wei, J. Zhang, S.-W. Tsang, C. Chen, W. Tang, D. Zhao, *Energy Environ. Sci.* **2024**, *17*, 202.
[111] X. Huo, J. Lv, K. Wang, W. Sun, W. Liu, R. Yin, Y. Sun, Y. Gao, T. You, P. Yin, *Cell Reports Phys. Sci.* **2024**, *5*, 101976.
[112] W. Zhang, Y. Yue, R. Yang, Y. Zhang, W. Du, G. Lu, J. Zhang, H. Zhou, X. Zhang, Y. Zhang, *Energy Environ. Sci.* **2024**, *17*, 2182.
[113] B. Fan, H. Gao, Y. Li, Y. Wang, C. Zhao, F. R. Lin, A. K. Y. Jen, *Joule* **2024**, *8*, 1443.
[114] C. e. Zhang, R. Zheng, H. Huang, G. Ran, W. Liu, Q. Chen, B. Wu, H. Wang, Z. Luo, W. Zhang, W. Ma, Z. Bo, C. Yang, *Adv. Energy Mater.* **2024**, *14*, 2303756.
[115] C. Xie, X. Zeng, C. Li, X. Sun, S. Liang, H. Huang, B. Deng, X. Wen, G. Zhang, P. You, C. Yang, Y. Han, S. Li, G. Lu, H. Hu, N. Li, Y. Chen, *Energy Environ. Sci.* **2024**, *17*, 2441.
[116] J. Fu, Q. Yang, P. Huang, S. Chung, K. Cho, Z. Kan, H. Liu, X. Lu, Y. Lang, H. Lai, F. He, P. W. K. Fong, S. Lu, Y. Yang, Z. Xiao, G. Li, *Nat. Commun.* **2024**, *15*, 1830.
[117] D. He, J. Zhou, Y. Zhu, Y. Li, K. Wang, J. Li, J. Zhang, B. Li, Y. Lin, Y. He, C. Wang, F. Zhao, *Adv. Mater.* **2024**, *36*, 2308909.
[118] L. Tu, H. Wang, W. Duan, R. Ma, T. Jia, T. A. Dela Peña, Y. Luo, J. Wu, M. Li, X. Xia, S. Wu, K. Chen, Y. Wu, Y. Huang, K. Yang, G. Li, Y. Shi, *Energy Environ. Sci.* **2024**, *17*, 3365.
[119] H. Lu, W. Liu, G. Ran, J. Li, D. Li, Y. Liu, X. Xu, W. Zhang, Z. Bo, *Adv. Mater.* **2024**, *36*, 2307292.
[120] M. Zhang, B. Chang, R. Zhang, S. Li, X. Liu, L. Zeng, Q. Chen, L. Wang, L. Yang, H. Wang, J. Liu, F. Gao, Z.-G. Zhang, *Adv. Mater.* **2024**, *36*, 2308606.
[121] Y. Xie, C. Zhou, X. Ma, S. Y. Jeong, H. Y. Woo, F. Huang, Y. Yang, H. Yu, J. Li, F. Zhang, K. Wang, X. Zhu, *Adv. Energy Mater.* **2024**, *14*, 2400013.
[122] X. He, F. Qi, X. Zou, Y. Li, H. Liu, X. Lu, K. S. Wong, A. K. Y. Jen, W. C. H. Choy, *Nat. Commun.* **2024**, *15*, 2103.

[123] L. Wang, C. Chen, Y. Fu, C. Guo, D. Li, J. Cheng, W. Sun, Z. Gan, Y. Sun, B. Zhou, C. Liu, D. Liu, W. Li, T. Wang, *Nat. Energy* **2024**, *9*, 208.
[124] M. Haris, Z. Ullah, S. Lee, D. H. Ryu, S. U. Ryu, B. J. Kang, N. J. Jeon, B. J. Kim, T. Park, W. S. Shin, C. E. Song, *Adv. Energy Mater.* **2024**, *14*, 2401597.
[125] H. Yu, Y. Wang, C. H. Kwok, R. Zhou, Z. Yao, S. Mukherjee, A. Sergeev, H. Hu, Y. Fu, H. M. Ng, L. Chen, D. Zhang, D. Zhao, Z. Zheng, X. Lu, H. Yin, K. S. Wong, H. Ade, C. Zhang, Z. Zhu, H. Yan, *Joule* **2024**, *8*, 2304.
[126] C. Guo, Y. Sun, L. Wang, C. Liu, C. Chen, J. Cheng, W. Xia, Z. Gan, J. Zhou, Z. Chen, J. Zhou, D. Liu, J. Guo, W. Li, T. Wang, *Energy Environ. Sci.* **2024**, *17*, 2492.
[127] L. Kong, X. Wang, M. Li, Z. Zhang, M. Chen, L. Zhang, L. Ying, D. Ma, J. Chen, *Adv. Energy Mater.* **2024**, *14*, 2402517.
[128] J. Liu, X. Duan, J. Song, C. Liu, J. Gao, M. H. Jee, Z. Tang, H. Y. Woo, Y. Sun, *Energy Environ. Sci.* **2024**, *17*, 3641.
[129] J. Wang, Y. Li, C. Han, L. Chen, F. Bi, Z. Hu, C. Yang, X. Bao, J. Chu, *Energy Environ. Sci.* **2024**, *17*, 4216.
[130] X. He, Z.-X. Liu, H. Chen, C.-Z. Li, *Adv. Mater.* **2024**, *36*, 2306681.
[131] C. Liu, Y. Fu, J. Zhou, L. Wang, C. Guo, J. Cheng, W. Sun, C. Chen, J. Zhou, D. Liu, W. Li, T. Wang, *Adv. Mater.* **2024**, *36*, 2308608.
[132] K. Liu, Y. Jiang, G. Ran, F. Liu, W. Zhang, X. Zhu, *Joule* **2024**, *8*, 835.
[133] X. Chen, M. Chen, J. Liang, H. Liu, X. Xie, L. Zhang, D. Ma, J. Chen, *Adv. Mater.* **2024**, *36*, 2313074.
[134] F. Sun, X. Zheng, T. Hu, J. Wu, M. Wan, Y. Xiao, T. Cong, Y. Li, B. Xiao, J. Shan, E. Wang, X. Wang, R. Yang, *Energy Environ. Sci.* **2024**, *17*, 1916.
[135] J. Huang, T. Chen, L. Mei, M. Wang, Y. Zhu, J. Cui, Y. Ouyang, Y. Pan, Z. Bi, W. Ma, Z. Ma, H. Zhu, C. Zhang, X.-K. Chen, H. Chen, L. Zuo, *Nat. Commun.* **2024**, *15*, 3287.
[136] C.-C. Chen, Y.-H. Chen, V. S. Nguyen, S.-Y. Chen, M.-C. Tsai, J.-S. Chen, S.-Y. Lin, T.-C. Wei, C.-Y. Yeh, *Adv. Energy Mater.* **2023**, *13*, 2300353.
[137] H. Zhou, J.-M. Ji, H. S. Lee, Masud, M. A, D.-N. Lee, C. H. Kim, H. K. Kim, *ACS Appl. Mater. Interfaces* **2023**, *15*, 39426.
[138] L. Cao, L. Wang, Z. Zhou, T. Zhou, R. Li, H. Zhang, Z. Wang, S. Wu, A. Najar, Q. Tian, S. Liu, *Adv. Mater.* **2024**, *36*, 2311918.
[139] W.-C. Huang, C.-C. Chi, C. Lin, C. Ouyang, T.-Y. Lin, C.-H. Lai, *Sol. RRL* **2024**, *8*, 2301039.
[140] Y. Jian, L. Han, X. Kong, T. Xie, D. Kou, W. Zhou, Z. Zhou, S. Yuan, Y. Meng, Y. Qi, G. Liang, X. Zhang, Z. Zheng, S. Wu, *Small Methods* **2024**, https://doi.org/10.1002/smtd.202400041.
[141] M. Wang, H. Geng, J. Zhu, Y. Cui, S. Zhao, J. Fu, D. Kou, J. Sun, C. Zhao, S. Wu, L. Ding, Z. Zheng, *Adv. Funct. Mater.* **2023**, *33*, 2307389.
[142] L. Lou, J. Wang, K. Yin, F. Meng, X. Xu, J. Zhou, H. Wu, J. Shi, Y. Luo, D. Li, Q. Meng, *ACS Energy Lett.* **2023**, *8*, 3775.
[143] H. Wei, C. Cui, Y. Li, Z. Wu, Y. Wei, Y. Han, L. Han, B. Lu, X. Wang, S. Pang, Z. Shao, G. Cui, *Small* **2024**, *20*, 2308266.
[144] N. Otgontamir, T. Enkhbat, E. Enkhbayar, S. Song, S. Y. Kim, T. E. Hong, J. Kim, *Adv. Energy Mater.* **2023**, *13*, 2302941.
[145] X. Xu, J. Zhou, K. Yin, J. Wang, L. Lou, M. Jiao, B. Zhang, D. Li, J. Shi, H. Wu, Y. Luo, Q. Meng, *Nat. Commun.* **2023**, *14*, 6650.
[146] K. Yin, L. Lou, J. Wang, X. Xu, J. Zhou, J. Shi, D. Li, H. Wu, Y. Luo, Q. Meng, *J. Mater. Chem. A* **2023**, *11*, 9646.
[147] Q. Zhou, Y. Sun, H. Li, Y. Sun, W. Zhao, B. Liang, Y. Wang, Y. Ma, L. Zhao, X. Teng, C. Gao, W. Yu, *Adv. Funct. Mater.* **2024**, *34*, 2313301.
[148] Y. Li, Y. Jian, F. Huang, N. Zhou, W. Chai, J. Hu, J. Zhao, Z. Su, S. Chen, G. Liang, *Small* **2024**, *20*, 2401330.
[149] Y. Gong, A. Jimenez-Arguijo, A. G. Medaille, S. Moser, A. Basak, R. Scaffidi, R. Carron, D. Flandre, B. Vermang, S. Giraldo, H. Xin, A. Perez-Rodriguez, E. Saucedo, *Adv. Funct. Mater.* **2024**, *34*, 2404669.
[150] Y. Zhao, J. Zhao, X. Chen, M. Cathelinaud, S. Chen, H. Ma, P. Fan, X. Zhang, Z. Su, G. Liang, *Chem. Eng. J.* **2024**, *479*, 147739.
[151] L. Cao, Z. Zhou, W. Zhou, D. Kou, Y. Meng, S. Yuan, Y. Qi, L. Han, Q. Tian, S. Wu, S. Liu, *Small* **2024**, *20*, 2304866.
[152] X. Chen, Y. Zhao, N. Ahmad, J. Zhao, Z. Zheng, Z. Su, X. Peng, X. Li, X. Zhang, P. Fan, G. Liang, S. Chen, *Nano Energy* **2024**, *124*, 109448.
[153] Y. Zhao, S. Chen, M. Ishaq, M. Cathelinaud, C. Yan, H. Ma, P. Fan, X. Zhang, Z. Su, G. Liang, *Adv. Funct. Mater.* **2024**, *34*, 2311992.
[154] C. H. Don, T. P. Shalvey, D. A. Sindi, B. Lewis, J. E. N. Swallow, L. Bowen, D. F. Fernandes, T. Kubart, D. Biswas, P. K. Thakur, T.-L. Lee, J. D. Major, *Adv. Energy Mater.* **2024**, *14*, 2401077.
[155] Z. Li, G. Zhang, Z. Li, Y. Xie, Y. Xia, Z. Hu, L. Chao, F. Wang, Y. Chen, *Cryst. Eng. Comm.* **2024**, *26*, 3026.
[156] H. Guo, S. Huang, H. Zhu, T. Zhang, K. Geng, S. Jiang, D. Gu, J. Su, X. Lu, H. Zhang, S. Zhang, J. Qiu, N. Yuan, J. Ding, *Adv. Sci.* **2023**, *10*, 2304246.
[157] X. Wen, Z. Lu, X. Yang, C. Chen, M. A. Washington, G.-C. Wang, J. Tang, Q. Zhao, T.-M. Lu, *ACS Appl. Mater. Interfaces* **2023**, *15*, 22251.
[158] S. Chen, Y.-A. Ye, M. Ishaq, D.-L. Ren, P. Luo, K.-W. Wu, Y.-J. Zeng, Z.-H. Zheng, Z.-H. Su, G.-X. Liang, *Adv. Funct. Mater.* **2024**, *34*, 2403934.
[159] G. Chen, Y. Luo, M. Abbas, M. Ishaq, Z. Zheng, S. Chen, Z. Su, X. Zhang, P. Fan, G. Liang, *Adv. Mater.* **2024**, *36*, 2308522.
[160] X. Pan, X. Li, Y. Yang, C. Xiang, A. Xu, H. Liu, W. Yan, W. Huang, H. Xin, *Adv. Energy Mater.* **2023**, *13*, 2301780.
[161] X. Liu, Y. Liu, S. Zhang, X. Sun, Y. Zhuang, J. Liu, G. Wang, K. cheng, Z. Du, *Small Methods* **2024**, *8*, 2300728.
[162] A. Wang, J. Huang, J. Cong, X. Yuan, M. He, J. Li, C. Yan, X. Cui, N. Song, S. Zhou, M. A. Green, K. Sun, X. Hao, *Adv. Mater.* **2024**, *36*, 2307733.
[163] A. Prasetio, R. R. Pradhan, P. Dally, M. Ghadiyali, R. Azmi, U. Schwingenschlögl, T. G. Allen, S. De Wolf, *Adv. Energy Mater.* **2024**, *14*, 2303705.
[164] T. Wu, Z. Liu, H. Lin, P. Gao, W. Shen, *Nat. Commun.* **2024**, *15*, 3843.
[165] A. K. Braun, J. T. Boyer, K. L. Schulte, W. E. McMahon, J. Simon, A. N. Perna, C. E. Packard, A. J. Ptak, *Adv. Energy Mater.* **2024**, *14*, 2302035.
[166] E. Aydin, E. Ugur, B. K. Yildirim, T. G. Allen, P. Dally, A. Razzaq, F. Cao, L. Xu, B. Vishal, A. Yazmaciyan, A. A. Said, S. Zhumagali, R. Azmi, M. Babics, A. Fell, C. Xiao, S. De Wolf, *Nature* **2023**, *623*, 732.
[167] O. Er-raji, M. A. A. Mahmoud, O. Fischer, A. J. Ramadan, D. Bogachuk, A. Reinholdt, A. Schmitt, B. P. Kore, T. W. Gries, A. Musiienko, O. Schultz-Wittmann, M. Bivour, M. Hermle, M. C. Schubert, J. Borchert, S. W. Glunz, P. S. C. Schulze, *Joule* **2024**, *8*, 2811.
[168] Z. Liu, Z. Xiong, S. Yang, K. Fan, L. Jiang, Y. Mao, C. Qin, S. Li, L. Qiu, J. Zhang, F. R. Lin, L. Fei, Y. Hua, J. Yao, C. Yu, J. Zhou, Y. Chen, H. Zhang, H. Huang, A. K. Y. Jen, K. Yao, *Joule* **2024**, *8*, 2834.
[169] D. Turkay, K. Artuk, X.-Y. Chin, D. A. Jacobs, S.-J. Moon, A. Walter, M. Mensi, G. Andreatta, N. Blondiaux, H. Lai, F. Fu, M. Boccard, Q. Jeangros, C. M. Wolff, C. Ballif, *Joule* **2024**, *8*, 1735.
[170] K. Zhang, C. Liu, Z. Peng, C. Li, J. Tian, C. Li, J. G. Cerrillo, L. Dong, F. Streller, A. Späth, A. Musiienko, J. Englhard, N. Li, J. Zhang, T. Du, S. Sathasivam, T. J. Macdonald, A. These, V. M. Le Corre, K. Forberich, W. Meng, R. H. Fink, A. Osvet, L. Lüer, J. Bachmann, J. Tong, C. J. Brabec, *Joule* **2024**, *8*, 2863.
[171] Z. Lin, J. Chen, C. Duan, K. Fan, J. Li, S. Zou, F. Zou, L. Yuan, Z. Zhang, K. Zhang, M. Y. Lam, S. A. Aleksandr, J. Qiu, K. S. Wong, H. Yan, K. Yan, *Energy Environ. Sci.* **2024**, *17*, 6314.
[172] S. Tan, C. Li, C. Peng, W. Yan, H. Bu, H. Jiang, F. Yue, L. Zhang, H. Gao, Z. Zhou, *Nat. Commun.* **2024**, *15*, 4136.
[173] H. Hu, S. X. An, Y. Li, S. Orooji, R. Singh, F. Schackmar, F. Laufer, Q. Jin, T. Feeney, A. Diercks, F. Gota, S. Moghadamzadeh, T. Pan, M. Rienäcker, R. Peibst, B. A. Nejand, U. W. Paetzold, *Energy Environ. Sci.* **2024**, *17*, 2800.

[174] C. Long, E. Feng, J. Chang, Y. Ding, Y. Gao, H. Li, B. Liu, Z. Zheng, L. Ding, J. Yang, *Appl. Phys. Lett.* **2024**, *124*, 123908.
[175] R. Xu, F. Pan, J. Chen, J. Li, Y. Yang, Y. Sun, X. Zhu, P. Li, X. Cao, J. Xi, J. Xu, F. Yuan, J. Dai, C. Zuo, L. Ding, H. Dong, A. K. Y. Jen, Z. Wu, *Adv. Mater.* **2024**, *36*, 2308039.
[176] T. Xue, B. Fan, K.-J. Jiang, Q. Guo, X. Hu, M. Su, E. Zhou, Y. Song, *Energy Environ. Sci.* **2024**, *17*, 2621.
[177] Y. Ma, F. Li, J. Gong, L. Wang, X. Tang, P. Zeng, P. F. Chan, W. Zhu, C. Zhang, M. Liu, *Energy Environ. Sci.* **2024**, *17*, 1570.
[178] P. Liu, H. Wang, T. Niu, L. Yin, Y. Du, L. Lang, Z. Zhang, Y. Tu, X. Liu, X. Chen, S. Wang, N. Wu, R. Qin, L. Wang, S. Yang, C. Zhang, X. Pan, S. Liu, K. Zhao, *Energy Environ. Sci.* **2024**, *14*, 7069.
[179] X. Zhang, Y. Gang, S. Jiang, M. Li, H. Xue, X. Li, *ACS Appl. Mater. Interfaces* **2024**, *16*, 27368.
[180] X. Wu, G. Xu, F. Yang, W. Chen, H. Yang, Y. Shen, Y. Wu, H. Chen, J. Xi, X. Tang, Q. Cheng, Y. Chen, X.-m. Ou, Y. Li, Y. Li, *ACS Energy Lett.* **2023**, *8*, 3750.
[181] J. Chen, X. Fan, J. Wang, J. Wang, J. Zeng, Z. Zhang, J. Li, W. Song, *ACS Nano* **2024**, *18*, 19190.
[182] L. Xie, S. Du, J. Li, C. Liu, Z. Pu, X. Tong, J. Liu, Y. Wang, Y. Meng, M. Yang, W. Li, Z. Ge, *Energy Environ. Sci.* **2023**, *16*, 5423.
[183] W. Xu, B. Chen, Z. Zhang, Y. Liu, Y. Xian, X. Wang, Z. Shi, H. Gu, C. Fei, N. Li, M. A. Uddin, H. Zhang, L. Dou, Y. Yan, J. Huang, *Nat. Photonics* **2024**, *18*, 379.
[184] D. A. Chalkias, A. Nikolakopoulou, L. C. Kontaxis, A. N. Kalarakis, E. Stathatos, *Adv. Funct. Mater.* **2024**, *34*, 2406354.
[185] L. Tang, L. Zeng, J. Luo, W. Wang, Z. Xue, Z. Luo, H. Yan, J. Gong, S. Wang, J. Li, X. Xiao, *Adv. Mater.* **2024**, *36*, 2402480.
[186] X. Lu, C. Xie, Y. Liu, H. Zheng, K. Feng, Z. Xiong, W. Wei, Y. Zhou, *Nat. Energy* **2024**, *9*, 793.
[187] Q. Ye, Z. Chen, D. Yang, W. Song, J. Zhu, S. Yang, J. Ge, F. Chen, Z. Ge, *Adv. Mater.* **2023**, *35*, 2305562.
[188] J.-W. Lee, C. Sun, S. Lee, D. J. Kim, E. S. Oh, T. N.-L. Phan, T. H.-Q. Nguyen, S. Seo, Z. Tan, M. J. Lee, J.-Y. Lee, X. Bao, T.-S. Kim, C. Lee, Y.-H. Kim, B. J. Kim, *Nano Energy* **2024**, *125*, 109541.
[189] Q. Sun, C. Shi, W. Xie, Y. Li, C. Zhang, J. Wu, Q. Zheng, H. Deng, S. Cheng, *Adv. Sci.* **2024**, *11*, 2306740.
[190] J. Yang, M. Chen, G. Chen, Y. Hou, Z. Su, S. Chen, J. Zhao, G. Liang, *Adv. Sci.* **2024**, *11*, 2310193.
[191] M. Chen, M. Ishaq, D. Ren, H. Ma, Z. Su, P. Fan, D. Le Coq, X. Zhang, G. Liang, S. Chen, *J. Energy Chem.* **2024**, *90*, 165.
[192] S. U. Ryu, D. H. Ryu, D. H. Lee, Z. U. Rehman, J.-C. Lee, H. Lim, G. Shin, C. E. Song, T. Park, *Chem. Eng. J.* **2024**, *485*, 149865.
[193] R. Meng, Q. Jiang, D. Liu, *npj Flex. Electron.* **2022**, *6*, 39.
[194] C. Yang, D. Liu, R. R. Lunt, *Joule* **2019**, *3*, 2871.
[195] J. Huang, J. Zhou, E. Jungstedt, A. Samanta, J. Linnros, L. A. Berglund, I. Sychugov, *ACS Photonics* **2022**, *9*, 2499.
[196] S. Sidhik, I. Metcalf, W. Li, T. Kodalle, C. J. Dolan, M. Khalili, J. Hou, F. Mandani, A. Torma, H. Zhang, R. Garai, J. Persaud, A. Marciel, I. A. Muro Puente, G. N. M. Reddy, A. Balvanz, M. A. Alam, C. Katan, E. Tsai, D. Ginger, D. P. Fenning, M. G. Kanatzidis, C. M. Sutter-Fella, J. Even, A. D. Mohite, *Science* **2024**, *384*, 1227.
[197] C. Liu, Y. Yang, H. Chen, I. Spanopoulos, A. S. R. Bati, I. W. Gilley, J. Chen, A. Maxwell, B. Vishal, R. P. Reynolds, T. E. Wiggins, Z. Wang, C. Huang, J. Fletcher, Y. Liu, L. X. Chen, S. De Wolf, B. Chen, D. Zheng, T. J. Marks, A. Facchetti, E. H. Sargent, M. G. Kanatzidis, *Nature* **2024**, *633*, 359.